TECHNICAL REPORT STANDARD TITLE PAGE

1. Report No.	2. Government Accession No.	3. Recipient's Catalog No.
CFHR 3-8-71-156-5F		

4. Title and Subtitle	5. Report Date
A STUDY OF THE RELATIONSHIPS BETWEEN VARIOUS CLASSES OF ROAD-SURFACE ROUGHNESS AND HUMAN RATINGS OF RIDING QUALITY	August 1975
	6. Performing Organization Code
7. Author(s)	8. Performing Organization Report No.
Hugh J. Williamson, W. Ronald Hudson, and C. Dale Zinn	Research Report 156-5F
9. Performing Organization Name and Address	10. Work Unit No.
Center for Highway Research The University of Texas at Austin Austin, Texas 78712	11. Contract or Grant No. Research Study 3-8-71-156
	13. Type of Report and Period Covered
12. Sponsoring Agency Name and Address	Final
Texas State Department of Highways and Public Transportation Transportation Planning Division P. O. Box 5051 Austin, Texas 78763	14. Sponsoring Agency Code

15. Supplementary Notes

Study conducted in cooperation with the U.S. Department of Transportation, Federal Highway Administration.
Research Study Title: "Surface Dynamics Road Profilometer Applications"

16. Abstract

In this study, statistical relationships between each of several classes of road roughness and human panel ratings of riding quality are developed. For this purpose, the roughness is categorized through digital filtering methods on the basis of wavelength. Longitudinal and transverse surface effects are also studied. Multiple regression analysis is used to relate the panel ratings to roughness as a whole and to the individual types of roughness. By using the models so developed, one can obtain for any given road section a measure of riding quality corresponding to each of a set of important aspects of roughness. Use of the models is demonstrated by analyzing the roughness of an illustrative road section just before, just after, and a year after an overlay.

17. Key Words	18. Distribution Statement
present serviceability rating, serviceability index, road roughness, digital filtering, regression analysis, Surface Dynamics Road Profilometer	No restrictions. This document is available to the public through the National Technical Information Service, Springfield, Virginia 22161.

19. Security Classif. (of this report)	20. Security Classif. (of this page)	21. No. of Pages	22. Price
Unclassified	Unclassified	216	

Form DOT F 1700.7 (8-69)

A STUDY OF THE RELATIONSHIPS BETWEEN VARIOUS CLASSES OF ROAD-SURFACE ROUGHNESS AND HUMAN RATINGS OF RIDING QUALITY

by

Hugh J. Williamson
W. Ronald Hudson
C. Dale Zinn

Research Report Number 156-5F

Surface Dynamics Road Profilometer Applications
Research Project 3-8-71-156

conducted for

The Texas Highway Department

in cooperation with the
U. S. Department of Transportation
Federal Highway Administration

by the

CENTER FOR HIGHWAY RESEARCH
THE UNIVERSITY OF TEXAS AT AUSTIN

August 1975

The contents of this report reflect the view of the authors, who are responsible for the facts and the accuracy of the data presented herein. The contents do not necessarily reflect the official views or policies of the Federal Highway Administration. This report does not constitute a standard, specification, or regulation.

PREFACE

This is the fifth report presenting results from Research Project 1-8-71-156, "Surface Dynamics Road Profilometer Applications," which was initiated to carry out the implementation and operation of the Profilometer in field and research applications.

A variety of highway roughness studies have been performed during the project, including the following:

(1) A method was developed for calibrating the Mays Road Meter on a periodic basis. Control procedures were developed for determining when a given Mays Meter needed calibration.

(2) A model was developed to compute a serviceability index, which estimates a human panel rating of riding quality. The serviceability index is calculated in terms of roughness amplitudes and is much less time-consuming than a direct evaluation by a human panel.

(3) A pilot-study analysis of the characteristic roughness patterns on asphalt pavements of different types and ages was performed. The correlations between roughness and other types of distress were also studied.

(4) Another pilot study was performed to demonstrate methods of characterizing the roughness patterns on bridge decks and the adjoining pavement. Three bridge sites were analyzed in detail with respect to specific effects, such as the bump at the end of the bridge and waves coincident with the bridge spans, and with respect to roughness amplitudes on the bridge and on the adjoining pavement.

These studies have all been documented in interim project reports.

Additionally, roughness measurements have been made for use in other research projects and for specific field applications. This service has been provided for the Texas Highway Department and Texas Transportation Institute as well as for the Center for Highway Research.

The purpose of this report is to present the results of a study of the relationships between various types of roughness and human ratings of riding quality. The authors appreciate the suggestions made by the Texas Highway Department representative, Mr. James L. Brown. The programming support by Mr. Randy Wallin and Mr. Jack O'Quin and the engineering consultations and

SDP measurements made by Mr. H. H. Dalrymple and Mr. Noel Wolf are also greatly appreciated.

Hugh J. Williamson
W. Ronald Hudson
C. Dale Zinn

August 1975

LIST OF REPORTS

Report No. 156-1, "Correlation Study of the Mays Road Meter with the Surface Dynamics Profilometer," by Roger S. Walker and W. Ronald Hudson, discusses a study of the correlation between measurements made with the Mays Road Meter and the Surface Dynamics Profilometer and, based on this study, provides a set of calibration, operation, and control procedures for operation of the Mays Road Meter using serviceability index values from the profilometer as a measurement standard.

Report No. 156-2, "The Use of Spectral Estimates for Pavement Characterization," by Roger S. Walker and W. Ronald Hudson, discusses the general uses of road profile spectral estimates for pavement characterization. A model for predicting serviceability index based on road profile amplitude estimates is also described.

Report No. 156-3, "Analysis of Characteristic Roughness Patterns in Pavements and the Relationship Between Roughness and Pavement Distress," by Hugh J. Williamson and W. Ronald Hudson, discusses the characterization and comparison of the roughness on pavements of differing types and ages. The application of digital filtering is treated, and pilot study results are presented.

Report No. 156-4,"The Characterization of Road Roughness on Bridge Decks and the Adjoining Pavement," by David B. Law, Hugh J. Williamson and W. Ronald Hudson, discusses the characterization and comparison of the roughness on bridge decks and the adjoining pavement. Several methods of analysis are presented for analyzing various components of roughness.

Report No. 156-5F, "A Study of the Relationship Between Various Classes of Road Surface Roughness and Human Ratings of Riding Quality," by Hugh J. Williamson, W. Ronald Hudson, and C. Dale Zinn, discusses the development, from road profile data and human panel ratings, a set of regression models for evaluating the severity of several types of roughness. Digital filtering is used to analyze the roughness on a wavelength basis.

ABSTRACT

In this study, statistical relationships between each of several classes of road roughness and human panel ratings of riding quality are developed. For this purpose, the roughness is categorized through digital filtering methods on the basis of wavelength. Longitudinal and transverse surface effects are also studied. Multiple regression analysis is used to relate the panel ratings to roughness as a whole and to the individual types of roughness. By using the models so developed, one can obtain for any given road section a measure of riding quality corresponding to each of a set of important aspects of roughness. Use of the models is demonstrated by analyzing the roughness of an illustrative road section just before, just after, and a year after an overlay.

KEY WORDS: present serviceability rating, serviceability index, road roughness, digital filtering, regression analysis, Surface Dynamics Road Profilometer.

SUMMARY

A detailed study of the relationship between road roughness and human panel serviceability ratings is presented in this report. This type of analysis is necessary to determine what types of roughness road users find most objectionable. Without this knowledge, it would be much more difficult to associate meaning with physical roughness measurements.

Road profile data, obtained by using the General Motors Surface Dynamics Profilometer, were analyzed on the basis of

(1) longitudinal effects, which cause a passing vehicle to accelerate vertically, and transverse effects, which cause a vehicle to rotate slightly, or "roll" about a longitudinal axis (a transverse "wave" occurs when one wheelpath rises and falls relative to the other[1]) and

(2) the lengths of the surface waves. Wavelength bands of 4 to 10, 10 to 25, 25 to 50, and 50 to 100 feet (1.219 to 3.048, 3.048 to 7.620, 7.620 to 15.24, and 15.24 to 30.48 meters) were studied. Because of high-frequency noise produced by the tape recorder which was used at the time of the measurements, but which has since been replaced by a more accurate recorder, roughness waves shorter than 4 feet (1.219 meters) could not be analyzed.

The following results were obtained by determining what proportions of the road-to-road variations in PSR could be "explained" or predicted in terms of all types of roughness combined and in terms of roughness with the specific wavelength bands listed above. Separate studies were performed for concrete and asphalt pavements.

(1) For both the concrete and asphalt cases, multiple correlations of .91 were achieved by predicting PSR in terms of all roughness types combined. Thus, overall roughness and PSR are very closely related.

---

[1] The wavelengths for longitudinal and transverse waves and both measured longitudinally along the roadway.

(2) The characterizing measures of the roughness with 4 to 10-foot (1.219 to 3.048-meter) wavelengths have almost as much predictive value as all the roughness types combined. Correlations of .86 were obtained for both types of pavement for the 4 to 10-foot (1.219 to 3.048-meter) wavelengths.

(3) The strength of the relationship between PSR and roughness within specific wavelength bands decreases steadily as the wavelength increases. The decrease is not drastic, however, since correlations of .75 and .68 for concrete and asphalt pavements, respectively, were obtained for the 50 to 100-foot (15.24 to 30.48-meter) case.

Additional regression studies in which transverse and longitudinal roughness are treated separately and analyses of certain roughness properties of concrete and asphalt pavements are also included in the report. Several applications of the regression models are discussed, and their use in before and after-maintenance studies is demonstrated by the analysis of measured profiles.

IMPLEMENTATION STATEMENT

New capabilities have been developed for analyzing the road roughness measurements obtained by using the General Motors Surface Dynamics Profilometer. These capabilities include

(1) digital computer methods for calculating characterizing measures of various types of roughness and

(2) statistical methods for evaluating the different physical measures on the basis of their relationships to human panel ratings of riding quality.

Several areas of application of these methods are discussed in the report, and their use in before and after-maintenance studies is demonstrated by the analysis of measured profiles.

TABLE OF CONTENTS

CHAPTER 1. INTRODUCTION

Purpose

The objective of this study is to develop methods for quantifying the severity of the important aspects of road roughness; for this purpose, the roughness is categorized on the basis of wavelength and on the basis of longitudinal versus transverse effects. The methods of evaluation are developed by statistically analyzing (through multiple regression techniques) the relationship between human panel ratings of riding quality and road-surface measurements.

The calculation from a road-surface profile of characterizing measures of the various aspects of roughness is a necessary preliminary step to the statistical analysis described above. The relative merits and the pitfalls of a number of mathematical techniques, including power spectral analysis and digital filtering, are discussed from the standpoint of characterizing the important classes of roughness.

Background and Applications

The evaluation of the condition or quality of a road is an essential job of the highway engineer. It is only through this type of evaluation that a number of functions, all of which are required if high-quality roads are to be provided with reasonable expenditure of public money, can be performed. The following list of applications illustrates the importance of an adequate method of evaluating road conditions.

(1) New Pavement Evaluation. It is necessary to have a set of specifications for accepting new pavements. The specifications provide guidelines for use during construction and, thus, prevent many possible misunderstandings between the governmental agency responsible for the construction and the staff performing the field work; without a formal set of acceptance criteria, the supervising agency would have constant difficulties in communicating its criteria for acceptance to the construction contractors. Moreover, it would be difficult without the specifications to accept or reject new constructions on a consistent basis. Clearly, the formulation

of a set of acceptance criteria requires a formally defined method of evaluating the quality or condition of the pavement.

(2) Allocation of maintenance for existing pavements. It is necessary to evaluate existing pavements in order to diagnose problems and prescribe maintenance. The allocation of maintenance resources can be made in a beneficial and efficient way only if the pavement evaluations on which the allocation is based are both meaningful and consistent. An evaluation is meaningful if it reflects or characterizes properties of the pavement which determine the pavement's present or future ability to serve the public.

(3) Pavement research. Through research, improvements can be made to existing methods for pavement design, construction, and rehabilitation practices. Because of the complexity of the pavement system, these objectives cannot be achieved through purely theoretical studies. Thus, evaluations of existing pavements are needed to supply data for research purposes; the network of public roads provides a tremendous laboratory for this purpose.

These comments apply to the special area of rehabilitation. Pavement evaluations immediately before, immediately after, and at successive points in time following rehabilitation of a selected set of pavement projects can be made to answer questions such as the following:

(a) Do the rehabilition methods actually correct the conditions they are designed to correct, or do certain problems, such as surafce roughness with certain ranges of wavelengths, remain after the work is done?

(b) Which rehabilitation practices are most effective for correcting which types of road surface deterioration?

(c) What are the continuing benefits of rehabilitation? What types of problems tend to recur within a reasonably short time after the maintenance is completed?

These three questions, stated above in general terms, relate to all aspects of the rehabilitation process which affect the ultimate quality of the work. The operational procedures, choice of equipment and material, and design parameters, such as thickness of an overlay, are examples of areas for evaluation in a pavement rehabilitation research program.

It is clear that if evaluations made over perhaps a several-year period were to be compared, a consistent means of performing the evaluations would be a critical factor.

An example of an analysis of a pavement's condition before and after an overlay is discussed in the following chapter.

The three areas discussed above are intended to illustrate the extensive practical need for the evaluation of pavements. The research problems involve some very complex physical processes and will continue to be studied in the

future. The operational needs, such as the assessment of road conditions in order to prescribe maintenance, will exist as long as paved roads are in use.

Scope of Report

Perhaps the two most common types of pavement evaluation are the assessments of conditions which relate to (1) probable future deterioration and (2) the present ability of a road to serve the public. Both types of evaluations come into play in all of the three areas discussed above.

The subject of the research reported herein is the development of new methods of the second type. The new methods are designed to give a detailed characterization of the road-surface quality and, thus, to provide the practicing highway engineer with improved capabilities for performing functions in the three areas discussed above.

The methods are based on the prediction of human-panel evaluations of the quality of a road by using descriptors of different aspects of road roughness as predictor variables. Thus, several predictive models are developed, each relating to a certain aspect of riding quality.

In Chapter 2, the current state of the art and basic concepts of present pavement-surface evaluation are discussed by summarizing several published papers and reports which are closely related to this study.

In Chapter 3, the nature and practical advantages over existing approaches of the new models are discussed along with illustrative test cases. The test cases demonstrate the types of physical insights which can be gained about a road's condition by using the models and serve as the basis for discussion of certain applications in the area of maintenance evaluation.

A discussion is given in Chapter 4 on various characteristics of the models and the physical properties on which they are based. The two objectives of this chapter are (1) to provide potential users of the models with background information which will be beneficial in applications and (2) to discuss certain relationships between human riding quality and road-surface deformation which are felt to be of practical significance.

The summary and conclusions of the study are given in Chapter 5. The models themselves are presented in Appendix 1. Appendix 2 includes a discussion of the design of a possible future experiment to assess the effect of

vehicle speed on riding quality. The data from which the models were developed are presented in Appendix 3, and an alternate statistical approach to the one used in this project is discussed in Appendix 4. The mathematical methods used to extract the meaningful information from the large set of measured data required to describe a road surface are discussed in considerable detail in Appendix 5.

CHAPTER 2. LITERATURE SURVEY

The purpose of this chapter is to introduce the basic concepts of the evaluation of the present quality of a road section and to summarize and discuss the state of the art. It is felt that this objective is best achieved by discussing in some detail several published papers and reports which are both important and closely related to this study. A number of other publications are referenced in the following chapters and appendices as their relevancies arise.

The Serviceability Rating

A method for rating the present quality of a road is discussed in Ref 5. The basic term, present serviceability, is given the following definition: "the ability of a specific section of pavement to serve high-speed, high-volume, mixed (truck and automobile) traffic in its existing condition." As the term itself and its definition both indicate, present serviceability relates to present condition only and not to the past or future condition of the pavement.

The Present Serviceability Rating (PSR), then, is defined as the mean of the evaluations of present serviceability made by a human panel. The panel is "intended to represent all highway users." The ratings are made on a scale from 0 to 5 on the basis of the following:

4 - 5	very good
3 - 4	good
2 - 3	fair
1 - 2	poor
0 - 1	very poor.

Serviceability Prediction: SI

The PSR is a meaningful measure in that it is a direct evaluation by road users. The panel ratings, however, are time consuming and, therefore, are expensive. Thus, there was a need for an alternate evaluation method.

The approach which was introduced in Ref 5 and which has subsequently been taken by several other investigators (Refs 11, 16, 19, 20, and 21) is

(1) to obtain (a) panel ratings and (b) physical measurements both for the same set of road sections and then

(2) to use multiple regression to obtain an equation to predict PSR in terms of the physical measurements.

An estimate of a human panel rating of a road can be obtained for any road section by first obtaining the physical measurements necessary for the prediction and then evaluating the predicting equation. The PSR estimate so obtained is called the Serviceability Index (SI).

In Ref 5, equations are given to compute SI in terms of a roughness term, slope variance; the area of cracking or patching per 1000 square feet (92.90 square meters) of pavement surface area; and rut depth, which is the average surface depth in the wheelpath compared to "a line joining two points each two feet [.6 meters] away (transversely) from the center of the wheelpath."

The roughness term, slope variance, was computed as follows: For each wheelpath, "a continuous record of the pavement slope between points 9 in [22.86 centimeters] apart" was obtained. Then the slopes were sampled, "generally at 1-ft [.3048 meter] intervals, over the length of the record" for each wheelpath. Then the variances of both of the two sets of slopes were computed, and the two variances were averaged to obtain the slope variance.

Separate equations were derived for asphaltic concrete and for portland cement concrete[1] pavements. The multiple correlations obtained for the asphalt and concrete cases are .92 and .96, respectively. The standard errors are .38 and .32, respectively.

Prediction of PSR in Terms of Power Spectra

The work reported in Ref 5 shows that PSR can be predicted with high correlation in terms of physical measurements. Because of (1) the efficiency and accuracy with which roughness measurements can be made using modern high-speed equipment and (2) the close relationship demonstrated in Ref 5 and other

---

[1] The terms "concrete" and "asphalt" will, for simplicity, be used henceforth instead of "portland cement concrete" and "asphaltic concrete," respectively.

studies between roughness and PSR, subsequent work in this area has involved primarily PSR prediction in terms of roughness.

Reference 21 presents a study in which an SI model involving only roughness measurements is obtained. The measurements were made using the General Motors Surface Dynamics Profilometer (SDP). The measurements are in the form of a road profile, i.e., a record of road elevation versus distance along the road, for both the right and left wheelpaths. Discussions of the measuring system itself are given in Refs 12, 16, 18, and 22. A brief summary of the system is given at the beginning of Appendix 5.

Although the slope variance is a meaningful characterizing measure[2] of the road roughness, no single number could contain all of the information which is inherent in a measured road profile. Because of the large number of points required to describe a road surface, however, some sort of scheme for computing a small set of summarizing roughness measures is necessary.

In the study presented in Ref 21, power spectral analysis is used to calculate a set of summary measures of the road roughness. The mathematics of power spectra as they are applied to road profile analysis is discussed in some detail in Appendix 5. Spectral analysis can be thought of as a method for decomposing the roughness in the road profile into components by wavelength. A root-mean-square (r.m.s.) amplitude[3] is computed for each of a discrete set of wavelengths. This type of analysis is relevant to ride quality, since road surface irregularities of different wavelengths induce different types of motion in passing vehicles.

A regression model involving roughness amplitudes and a dummy variable to account for visual or auditory differences between concrete and asphalt pavements was developed. The model includes roughness terms representing

---

[2] It will be convenient to use the term "measure" to refer to any quantity which is calculated from a set of measurements, such as a road profile, and which is intended to characterize a certain property, such as the road roughness with wavelengths within a given band.

[3] The calculation of amplitudes from power spectra is discussed in Appendix 5. Also discussed are the meaning and the calculations of cross-amplitude terms for a discrete frequency set.

wavelengths from 8.6[4] to 86 feet (2.6 to 26 meters); although they are significant, amplitudes of shorter waves had to be excluded because of high-frequency tape recorder noise. This point is discussed further in the next chapter. The model has 22 terms, a multiple correlation of .94, and a standard error of .33.

Thus, it was shown that it was possible to predict PSR with high correlation from roughness terms computed from measured road profiles.

Digital Filtering and Amplitude-Frequency Distributions

It is pointed out in Ref 4 that, although the power spectral approach is effective, the calculation of a single overall amplitude corresponding to a given frequency is less than ideal. A more meaningful characterization of the roughness would include information about the amplitude variation as well as the overall average amplitude; any number of combinations of small and large bumps could produce the same overall or average amplitude.

In Ref 4, a method for computing a probability distribution of the roughness amplitudes is given. This is achieved by the following three steps:

(1) obtain a road profile measurement,

(2) filter the measured profile so as to isolate the roughness with wavelengths within a specified band, and

(3) compute the sample distribution function of the peaks in the filtered profile.

The term "filtering" refers to a transformation, which can be performed either by electronic hardware or by digital calculation, through which an artificial profile is computed from the measured road profile. It is possible to design the filter so that certain types of surface irregularities are eliminated, but other types are essentially unaffected, by the filtering operation. In this way, it is possible to isolate for further study the roughness in the

---

[4] Actually, 8.6 feet (2.6 meters) is the center of a band of wavelengths which are included. The band extends from 7.8 to 9.5 feet (2.4 to 2.9 meters). The width of each of the discrete set of frequency intervals is .0116 cycles per foot (.0381 cycles per meter).

measured profile with wavelengths within certain limits. This simplified description of filtering is given here to facilitate the discussion of the characterization of road roughness. A much more extensive treatment of filtering techniques and their application in profile analysis is given in Appendix 5. The figures in the following chapter illustrate the filtering concept by displaying measured and filtered profiles on the same plot.

By performing the three steps listed above, one obtains a detailed description of the roughness with the selected range of wavelengths; the median is an "average" roughness measure, while the points in the upper tail of the distribution characterize the most severe roughness in the road section. If the three steps are performed for a set of contiguous wavelength bands which covers the range of interest, then an extensive description of the longitudinal roughness is obtained. The set of distribution functions is called the "Amplitude-Frequency Distribution."

A technical statistical aspect of the prediction of PSR from a set of roughness measures is discussed in the following section. This discussion is relevant to this study and should be of interest to researchers working in the ride quality field. The reader who is interested primarily in the results of the study, however, may want to skip to the beginning of Chapter 3.

Association of Meaning with the Regression Coefficients in Estimating PSR

A discussion is given in Ref 11 on certain problems which are encountered in the regression of PSR on a set of highly correlated roughness values - specifically, power spectra. The problems arise because of the relationships among the amplitudes of the roughness of different wavelengths; a road which has severe roughness of, say, wavelength 10 feet (3.048 meters) is likely also to have worse-than-average roughness of wavelength 15 feet (4.572 meters). Although exceptions exist, the point is that the power spectral values have high intercorrelations. Thus, the presence of a given variable in the model can have extreme effects on the coefficients of the other variables. It is even possible for a power value to have a positive coefficient, which would seem to indicate that as a particular type of roughness became worse, the serviceability would increase. The explanation, of course, is that other terms, which correlate positively with the roughness term which has a positive coefficient, are present with negative coefficients; thus, the net effect

of an increase in the severity of the roughness is, in all likelihood, a decrease in SI. Nevertheless, it is impossible to infer anything about the relationship between PSR and a particular type of roughness from the coefficient of a term in the SI model.

Stepwise regression (Refs 6 and 7) is a statistical method for selecting the subset of a collection of independent variables which has the greatest combined value for predicting a specific dependent variable. It is pointed out in Ref 11 that, although it may appear that this type of selection would solve the problem by limiting the terms in the model to those with the greatest predictive value, it does not. Random sampling variations play a large role in determining which variables enter the model. From Ref 21, moreover, we know that positive coefficients still appear in the model, even if stepwise procedures are used. The nature of stepwise regression is discussed briefly in Chapter 4.

Thus, certain constraints for controlling the values of the coefficients were investigated in Ref 11. First, the regression model is written

$$SI = \gamma + \sum_{i=1}^{N} \beta_i s_i$$

where the s_i are measures of the roughness at a discrete set of frequencies. Now, define

$$\beta_i = \sum_{k=1}^{n} \alpha_k i^k$$

where

$$i = 1, 2, \ldots N \text{ and } n < N.$$

Thus, the weight β_i associated with the roughness at the i^{th} frequency is a polynomial function of the frequency. The Serviceability Index, then, can obviously be expressed as a function which is linear in the α's and which does not directly involve the β's. Multiple regression analysis is used to determine the α's, which in turn determine the β's. There are several

problems associated with this method, however, including the fact that there is no explicit constraint on the signs of the coefficients. Thus, the following formulation was used:

$$\beta_i = i\, e^{\sum_{k=1}^{K} (\alpha_k)(i^k)}$$

where

$$i = 0, 1, \ldots N .$$

(The coefficient of the exponential function is apparently intended to insure zero weight associated with the zero-frequency component). Thus, the β's are constrained to be positive (the authors of Ref 11 are evidently using a PSR scale which increases with decreasing ride quality; otherwise, the requirement that all the coefficients be positive does not make sense). Nonlinear multiple regression is used, then, to compute the α's , which, as before, determine the β's .

The method discussed in Ref 11 was shown to be successful in that an SI model was developed in which the coefficients

(1) are all positive and

(2) have a single peak corresponding to a wavelength of about 8 feet, suggesting that humans are most sensitive to roughness with wavelengths in this range. This result is intuitively plausible and is consistent with the wavelength study presented herein. Most importantly, no inference whatsoever about the relative importance of the different wavelengths can be drawn from other studies in which regression analysis is applied in a straightforward way.

Additionally, Ref 11 identified and explained a statistical fine point which has important consequences and, therefore, paved the way for further research in relating PSR to individual types of roughness.

Nevertheless, the following points should be taken into account.

(1) When the regression techniques select a model with coefficients which , when taken individually, seem not to make sense, it is because these terms when taken as a whole give the best fit to the data. Any restrictions which are placed on the model are

likely to decrease the extent to which the regression model fits the experimental data on which it is based. Neither the multiple correlation nor any other information is given in Ref 11 which would allow the reader to assess the adequacy of the fit of the model.[5]

If the objective of developing the model were to predict PSR in the most accurate and physically realistic way, then these considerations, not the physical meaningfulness of the individual terms, should be the basis of evaluation of the model.

The relationships between PSR and the individual types of roughness are of interest, however, for numerous practical reasons; for example, some sort of judgement must be made about which types of surface dererioration are undesirable in order to allocate highway maintenance resources. If these relationships are to be examined by means of a single model involving the entire set of roughness measures, then one would require a reasonable agreement between the model and the data; otherwise, there is no empirical justification for use of the model for any purpose.

(2) The method discussed in Ref 11 is dependent on the association of a single variable, wavelength, with the roughness measures; it is on this basis that the polynomials are formulated. If the method were to be applied using an amplitude-frequency distribution instead of a power spectrum as the set of predictor variables, then the two variables, wavelength and another variable associated with the distribution functions, would have to be included. The probability level associated with the various amplitudes in the distribution, for example, could be the second variable. Furthermore, some account should be made of the fact that the importance of the various probability levels might vary with frequency; this could be taken care of by including cross-terms in the polynomial. The polynomial would become even more complex if a set of transverse roughness terms were added to the amplitude-frequency description of the longitudinal waves.

The comments above are not intended as criticism of the polynomial approach as it is used in Ref 11. The point is that the approach might become unwieldy when applied to very detailed roughness characterizations.

In summary, the Serviceability Index, is both (1) a valuable measure of riding quality, since it is closely related to human panel ratings of rideability, and (2) economical to obtain, since it is calculated in terms of physical measurements and does not require a panel rating. Because of

---

[5] A plot of "residuals^2" versus K is given, but "residuals^2" is not defined as a sum of squares, mean square, etc. In any case, additional information would be needed to calculate the multiple correlation.

the close relationship between riding quality and roughness, research emphasis has been placed on the development of SI models in terms of roughness. In the following chapter, a method for extending the SI concept to obtain a more detailed riding-quality evaluation is presented.

CHAPTER 3. THE DETAILED RELATIONSHIP BETWEEN SERVICEABILITY AND SURFACE ROUGHNESS

While the Serviceability Index, which is discussed in the preceding chapter, is a meaningful overall measure of the riding quality of a road, no single number can adequately characterize a complex pattern of surface waves. Sets of summarizing measures, such as the amplitude versus wavelength function and the amplitude-frequency distribution, describe the physical properties of the surface, but are hard to interpret from the standpoint of riding quality. A rise and fall of a given amplitude, say 1 inch (2.54 centimeters), causes a much more severe sensation if it occurs over a 2-foot (.6096-meter)-long interval than if it occurs over 50 feet (15.24 meters) along the roadway.

Thus, there is a need for a <u>set</u> of characterizing measures similar to the overall Serviceability Index which has been used in the past. The collection of profile measurements and accompanying panel serviceability ratings which were used to develop an SI model employing power spectra (Ref 16,and 21) were used to develop such a set of measures. Stated in brief terms, the model development was accomplished by predicting PSR from

(1) an overall set of roughness amplitudes characterizing the road roughness and

(2) subsets of the overall set of roughness measures which characterize, respectively, roughness with the following wavelengths: 4 to 10 feet (1.219 to 3.048 meters), 10 to 25 feet (3.048 to 7.620 meters), 25 to 50 feet (7.620 to 15.24 meters), and 50 to 100 feet (15.24 to 30.48 meters).

The model for the 4 to 10-foot (1.219 to 3.048-meter) wavelengths, for example, is an equation of the form

$$SI = f(M_1, M_2, \ldots M_n)$$

where SI is the Serviceability Index corresponding to this specific type of roughness, and the M_i are the characterizing measures of this class of

roughness. (The additional inclusion of dummy variables is discussed below.)

Because the profile measurements were made in 1968 when the SDP was equipped with an older-style tape recorder, noise prevented the analysis of roughness with wavelengths shorter than 4 feet[1] (1.219 meters). While the noise problem has been mitigated considerably by installing a newer tape recorder with better resolution, it was necessary for the purposes of this study to use the profile measurements that were made at the time of the rating panel evaluations.

At this point, we digress slightly to describe the calculation of the characterizing roughness measures used in this study. Although the highly technical details are deferred to Appendix 5, it is felt that the following brief discussion will aid the reader in associating physical meaning with the roughness terms used in the SI models.

Calculation of Roughness Measures

The roughness measures which describe the longitudinal roughness for either wheelpath for, say, the 4 to 10-foot (1.219 to 3.048-meter) band are calculated by a three-step process:

(1) By using digital filtering, calculate from the measured profile an artificial profile containing only the 4 to 10-foot(1.219 to 3.048-meter)-long waves.[2]

(2) Calculate a moving root-mean-square (r.m.s.) amplitude centered at each point in the section, excluding the values which would be distorted by end effects. Each r.m.s. amplitude describes the roughness along a 10-foot (3.048-meter) interval, which is the longest wavelength of the roughness to be isolated by filtering.

---

[1] It is stated in the preceding chapter that in the original study reported in Ref 21, wavelengths shorter than about 8 feet (2.438 meters) were excluded. In the present study filtering was used to eliminate the noise, which was predominatly in the 2 to 3-foot (.610 to .914-meter)-wavelength range. Visual examination of measured and filtered profile plots was used to verify that the large-amplitude tape recorder noise did not contaminate the information in the 4 to 10-foot (1.219 to 3.048-meter)-wavelength range.

[2] Actually, the cutoff at the edges of the frequency band of interest is not perfect. The characteristics of the sixth-order digital Butterworth filter which was used are discussed in Appendix 5.

(3) Calculate the sample distribution of the local roughness measures.[3] The fiftieth percentile point, the value which is greater than or equal to exactly half the roughness amplitudes, is then an overall or average measure of the section roughness. The ninetieth percentile point, the value greater than or equal to exactly 90 percent of the amplitudes, indicates the severity of the worst roughness in the section.

The three steps are performed for both the right and left wheelpath profiles. Then, since the runs were not consistently made in either the inside or outside lane, no meaning can be associated with the right as opposed to the left wheelpath. For this reason, the corresponding roughness measures for the right and left profiles, e.g., the fiftieth percentile amplitudes, are averaged to obtain a set of longitudinal roughness measures.

Now, the transverse road-surface irregulatities are also of interest, since they cause passing vehicles to "roll" about a lengthwise axis and since this type of motion adversely affects the riding quality of the road.

To study the transverse roughness, we first obtain an artificial profile by computing the pointwise difference between the successive right and left profile elevations. Changes in this profile, then, correspond to changes in elevation of one wheelpath relative to the other and, thus, directly relate to vehicle roll.

The difference profile is also processed by the steps (1), (2), and (3) listed above to obtain transverse roughness measures. The wavelengths have the same meaning as in the longitudinal case; they are measured longitudinally along the road surface. Suppose that the right wheelpath gradually rises by .1 inches (.254 centimeters) relative to the left wheelpath and then gradually returns to its original elevation and that the sinusoidal rise and fall occurs over a distance of 10 feet (3.048 meters) along the roadway. Then this transverse surface irregularity has a wavelength of 10 feet (3.048 meters).

---

[3] Notice that this approach differs from the amplitude-frequency method discussed in the previous chapter in that the distribution of local r.m.s. roughness measures is computed rather than the distribution of peaks in the profile. It is shown in Appendix 5 that the local r.m.s. values are less susceptible to certain filter-induced distortion than the peaks are. For this reason, the local r.m.s. values rather than the peaks were used in this study. This is not a critical point, however; the amplitude-frequency approach is a valid and natural way to characterize road roughness.

The SI models which are discussed in the following sections include as predictor variables both longitudinal and transverse roughness terms and a dummy variable. The dummy variable T is defined as follows:

T = 1 if the pavement is continuously reinforced concrete (CRC)
= 0 otherwise

for concrete pavements and

T = 1 if the pavement is surface-treated (ST)
= 0 otherwise

for asphalt pavements.

The models are given in detail in Appendix 1.

The reason for including the dummy variables is to account for visual or auditory differences experienced in riding over different types of pavements. The sound of the car passing over the joints in some concrete pavements (but not CRC), for example, might influence PSR, but might not be adequately reflected in the roughness terms.

Illustrative Test Case 1

Profile measurements were made on a hot-mix asphalt-concrete road section on IH20 near Odessa, Texas, just before (March, 1974) and just after (April, 1974) an overlay. The pavement which had had a surface treatment, was badly cracked and had severe short-wavelength roughness. A 1 1/4-inch (3.175-centimeter) hot-mix overlay was performed to alleviate this situation.

Before and after-overlay profile plots are shown in Figs 3.1 and 3.2, respectively, for the Odessa section. An artificial profile computed by filtering is shown as an illustration of the isolation of that part of the roughness with a certain range of wavelengths. Additional plots of filtered and unfiltered profiles for these and other sections are presented in Appendix 5.

The SI values obtained from the model which is discussed both in Ref 21 and in the preceding chapter are 3.5 before the overlay and 4.0 after.

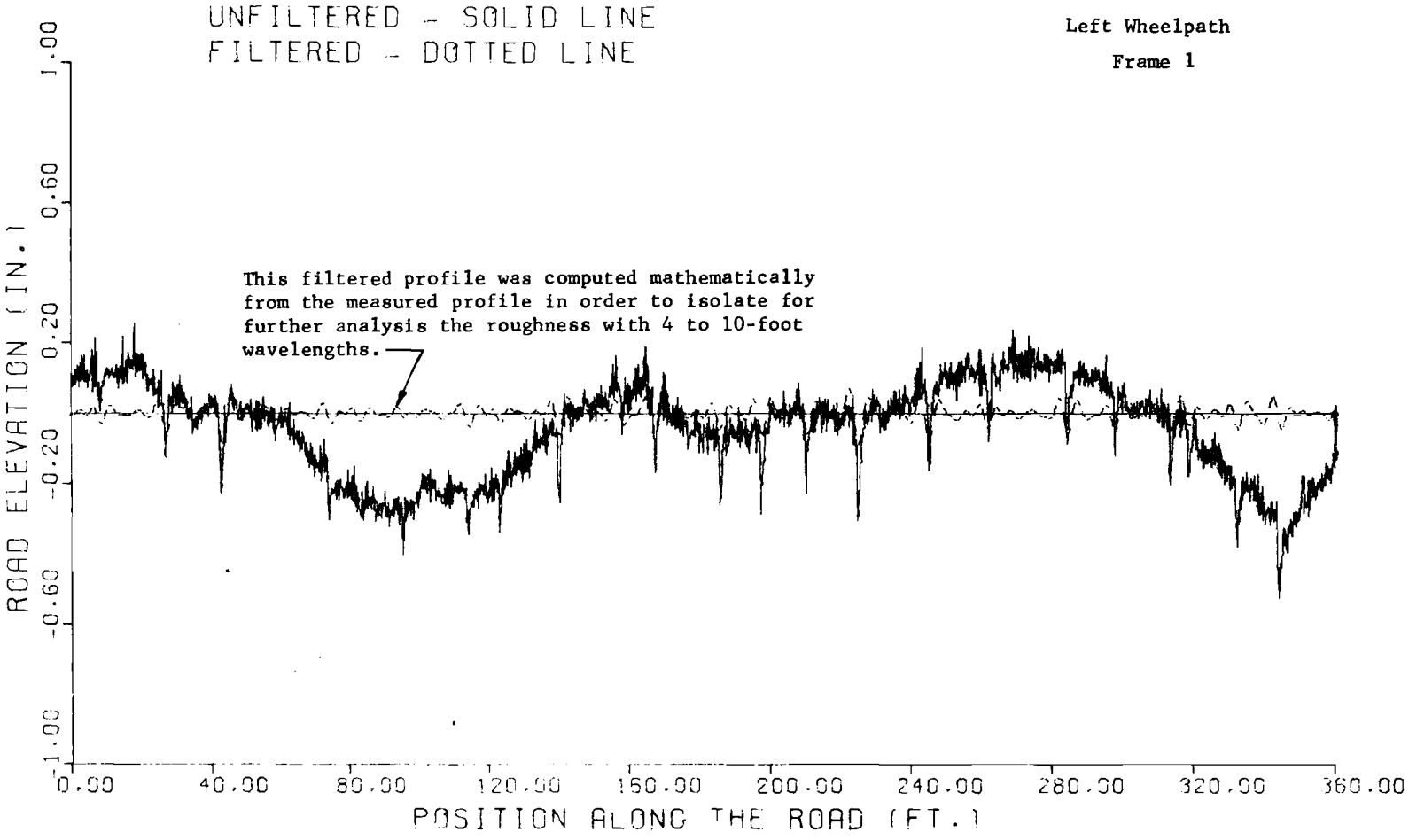

1 foot = .3048 meters
1 inch = 2.540 centimeters

Fig 3.1. Odessa Test Section, March, 1974: Roughness with 4 to 10-foot wavelengths isolated by filter. Before overlay. (continued)

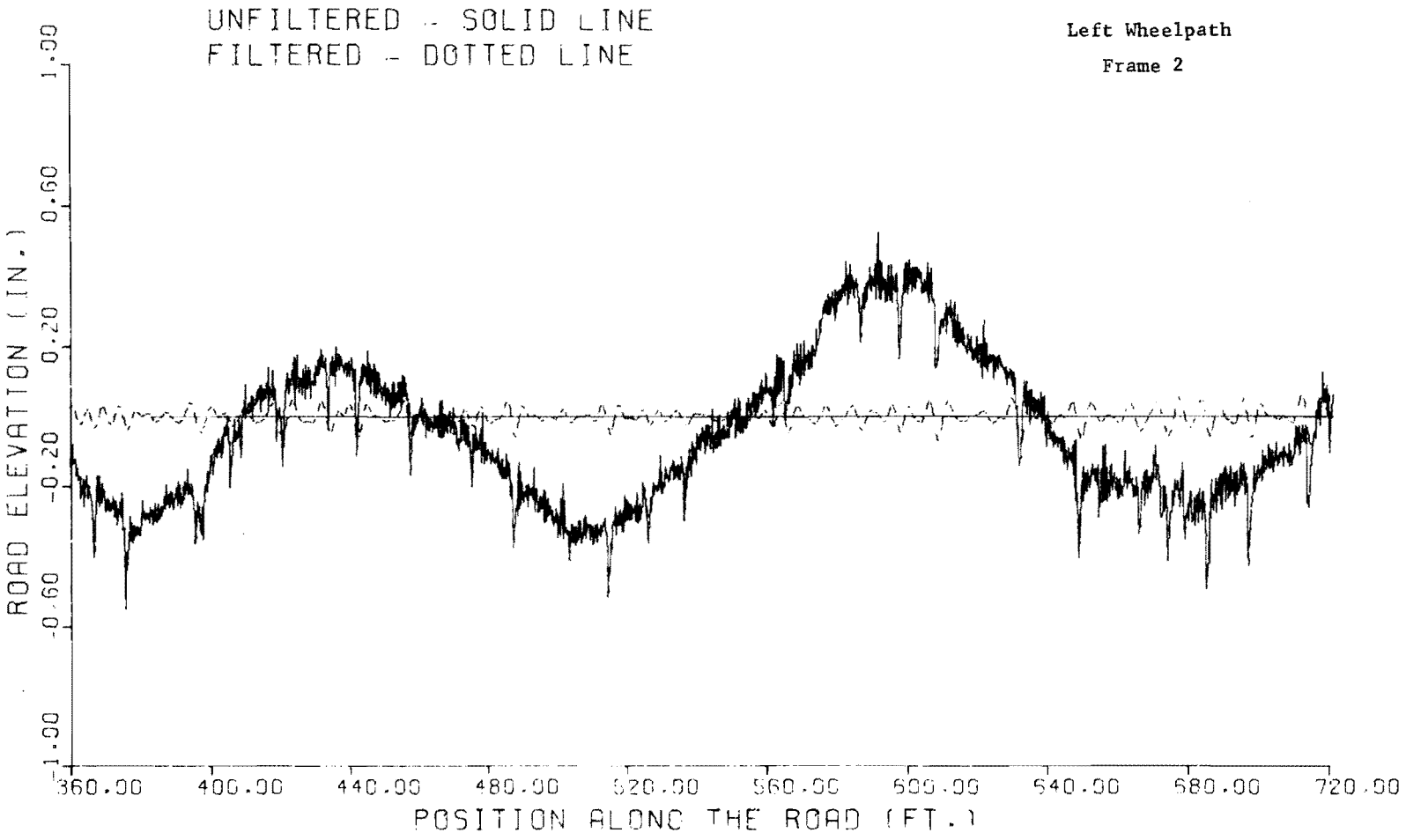

Fig 3.1. (Continued)

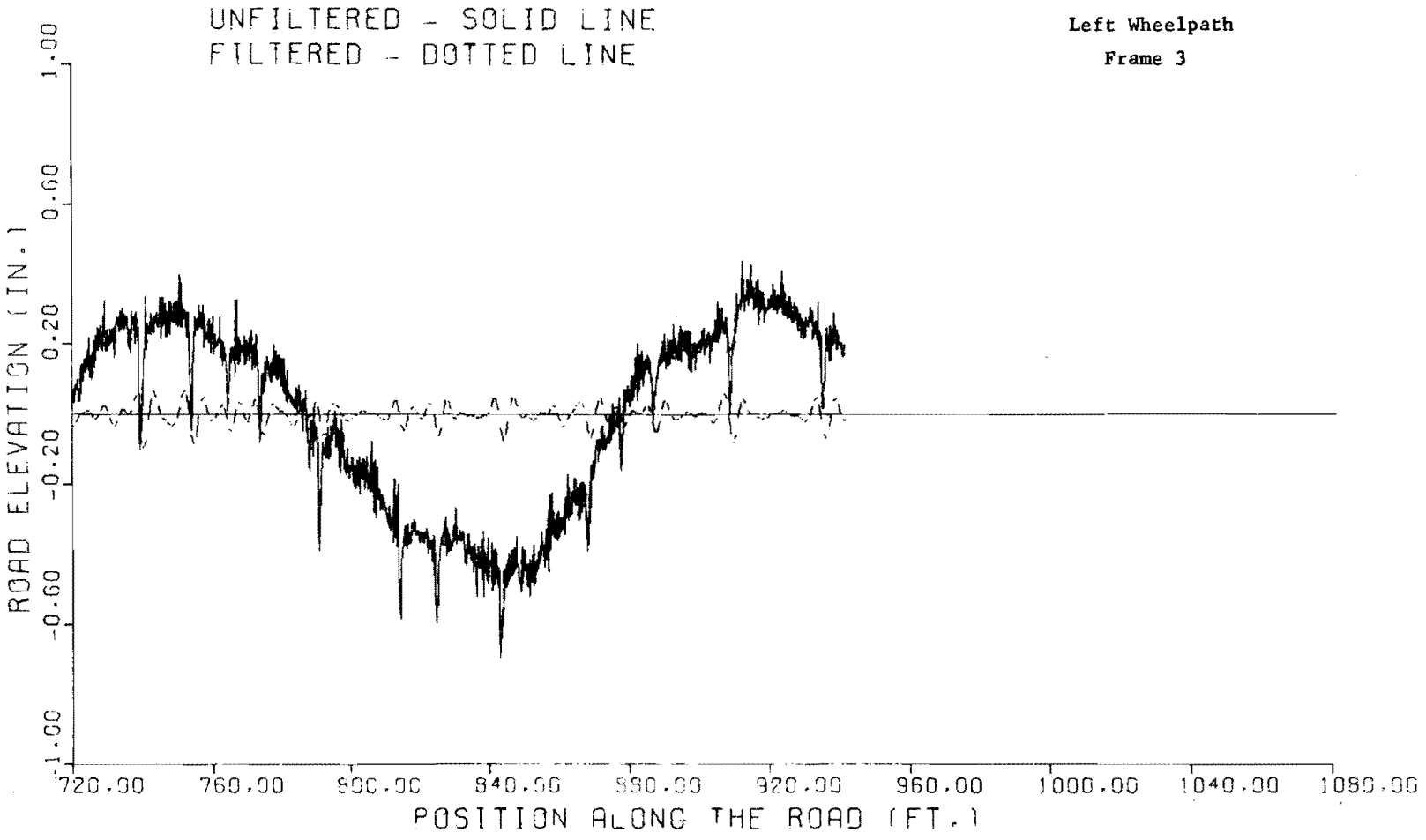

Fig 3.1. (Continued)

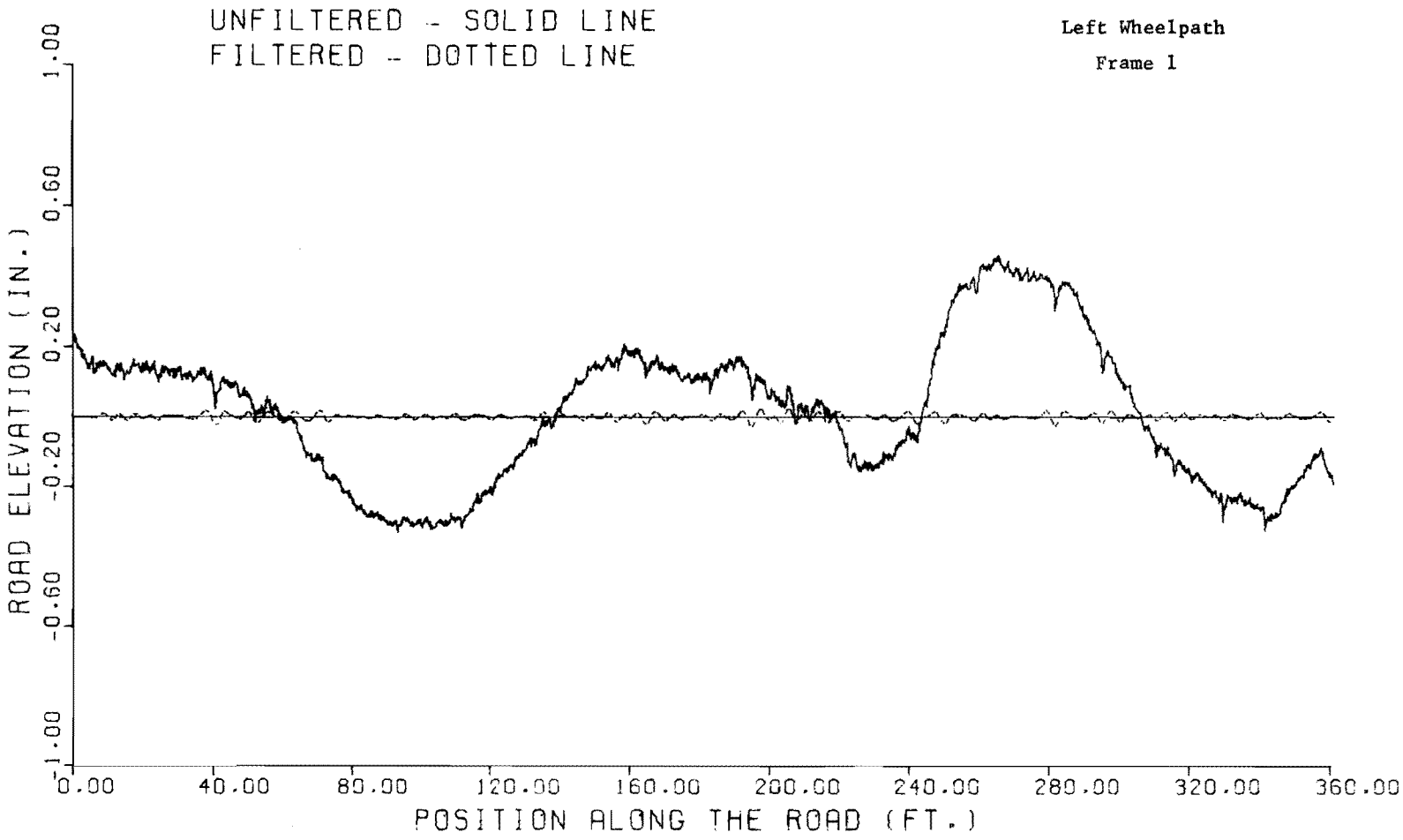

1 foot = .3048 meters
1 inch = 2.540 centimeters

Fig 3.2. Odessa Test Section, April, 1974: Roughness with 4 to 10-foot wavelengths isolated by filter. After overlay.

(continued)

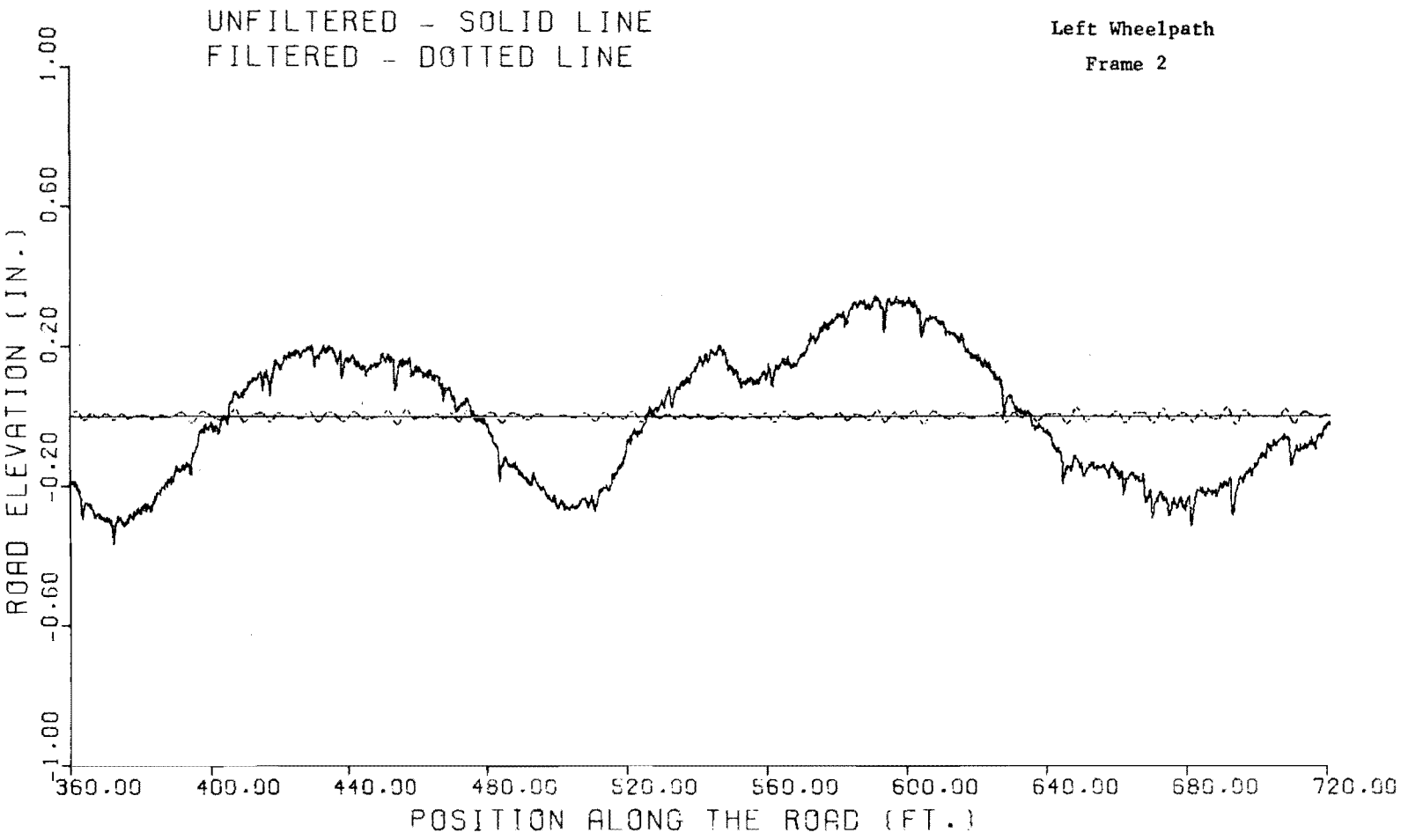

Fig 3.2. (Continued)

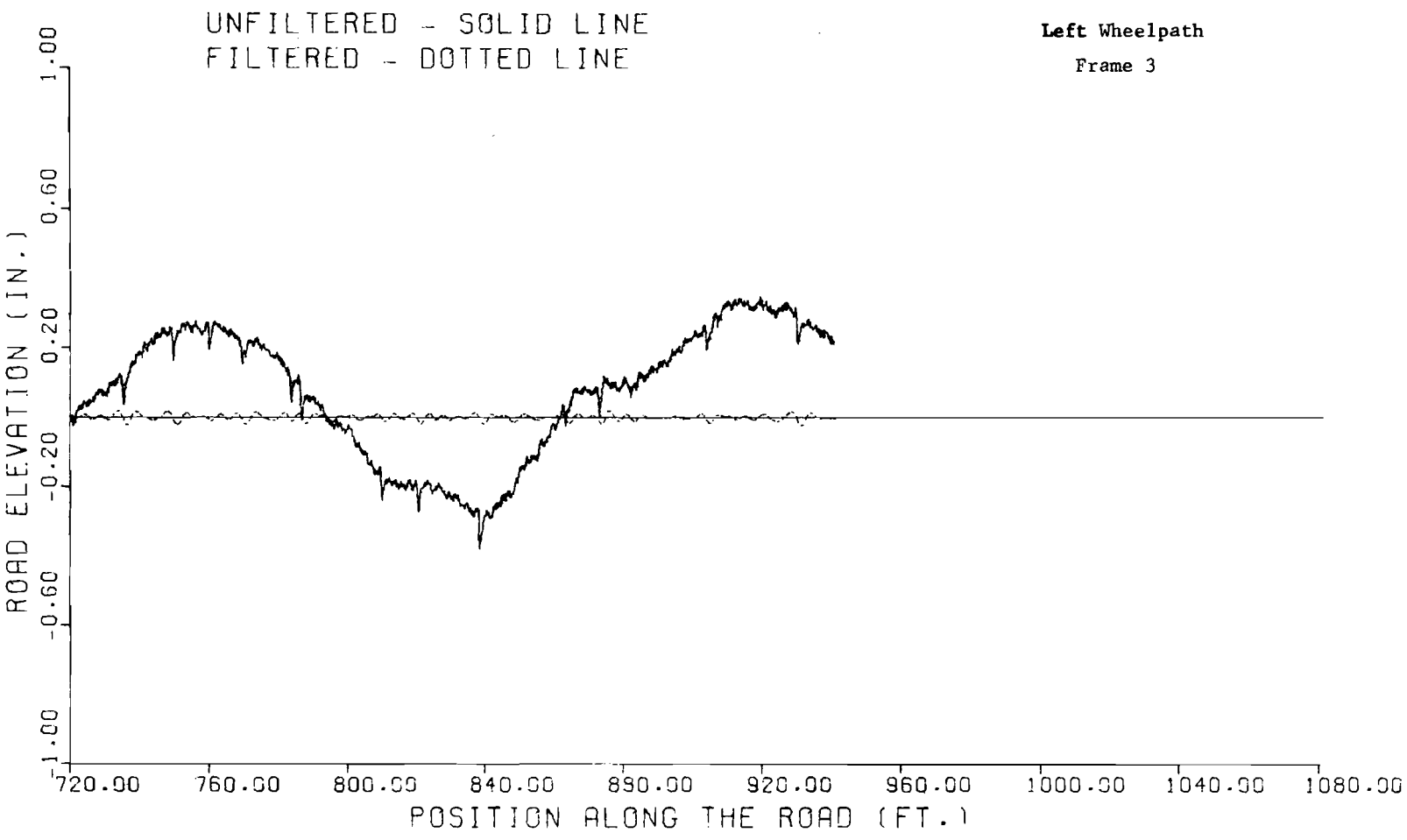

Fig 3.2. (Continued)

The new models were also applied to this section. The SI values which were obtained are given in Table 3.1. The following points should be noted about this test case.

(1) The overall SI value before the overlay is lower than the value for the existing SI model presented in Ref 21 (3.13 versus 3.5). The lower value is considered to be more reasonable because of the severely distressed condition of the pavement.

(2) For conditions just after the overlay, the SI value computed with the new model is higher than the value computed with the existing model (4.0 versus 4.25); more importantly, the SI change is .5 for the existing model and 1.12 for the new model. The larger change is considered to be more reasonable in view of the dramatic improvement of the short waves.

(3) It is evident from the road-profile plots that, although the short-wavelength roughness is improved considerably, there is an increasing similarity between the before and after-profiles as the wavelength increases. For the profile before the overlay, the SI values are very low and increase as the wavelength increases. The SI's are uniformly high after the overlay. The greater improvement of the short waves was expected in view of the construction procedure. A 25-foot (7.618-meter) skid is customarily used to perform this type of overlay, which means that waves shorter than 25 feet (7.618 meters) are controlled, but longer waves are not.

The above test case is given as an illustration of the use of the new SI models. It is felt that the more detailed evaluation of the road roughness gives a much clearer picture of the nature of the improvement achieved by the overlay than a single SI value does. The test case also indicates an important area of application of the SI models: the evaluation of the effectiveness of the different maintenance techniques.

The Odessa section was chosen because the nature of the improvement achieved by the overlay is easy to see from the before and after-maintenance profile plots; thus, it is possible to verify that physically realistic and meaningful results are obtained from the SI models. The very complex nature of a typical road user's subjective evaluation of the present quality of a road section is, in general, not easy to analyze.

If such evaluations were made even by the same set of highway engineers or other raters before and after a maintenance program, random human variations might prevent an accurate evaluation of the benefits of the program. A change in the weather, for example, might bias the results considerably. If it were desired to evaluate the continuing effect of the maintenance by obtaining ratings at say, six-month intervals for several years, then the

TABLE 3.1. SI VALUES BEFORE AND AFTER OVERLAY

		Wavelength (feet)			
	All Roughness	4 to 10	10 to 25	25 to 50	50 to 100
Before	3.13	2.48	2.94	4.01	3.95
After	4.25	4.06	4.06	4.17	4.00
Improvement	1.12	1.58	1.12	0.16	.05

NOTE: 1 foot = .3048 meters

extraneous effects, which would probably be exacerbated by personnel changes, could have seriously deleterious effects on the evaluation program.

The SI values obtained from profile measurements, however, provide a relatively consistent means of performing repeat evaluations at successive points in time. Furthermore, since the models are developed from PSR data, the SI values are closely related to a human rating of ride quality.

The roughness amplitudes on which the serviceability predictions are based are given in Table 3.2. Although the road has a shoulder, there is no curb, and the higher amplitudes for the right wheelpath reflect the more severe deterioration in the outside of the lane. It is interesting that the amplitudes remain larger after the overlay for the outside wheelpath for the 0 to 4, 4 to 10, and 10 to 25-foot (0 to 1.219, 1.219 to 3.048, and 3.048 to 7.620 meter) wavelengths. This is apparently a residual effect of the original roughness.

Another point illustrated by this test case is that all three types of information discussed, road profile plots, SI values, and roughness amplitudes, can help the highway engineer to explain the effects of an overlay on the road-surface condition.

In some areas, the long-wavelength roughness was actually made worse by the overlay; see, for example, position 280 feet (85.34 meters) in frame 1 of Figs 3.1 and 3.2. That this is a real effect, and not a spurious measurement, is evidenced by the fact that the same roughness pattern appears in the profile measured about a year after the overlay (see Fig 3.3). Table 3.2, however, shows that the roughness amplitudes for the right wheelpath and for the transverse profile are decreased by the overlay. Thus, it is reasonable that the SI values for all wavelengths are increased.

While procedural decisions cannot be made on the basis of a single test case, the example discussed above suggests that pavers with sensors and side wires should possibly be used for overlays in order to improve the long, as well as the short, waves. Care would have to be exercised to prevent the introduction of periodic waves into the profile because of a sag in the wires between stakes. Additional test sections, perhaps affected by a swelling subgrade, with more severe long waves would be necessary to verify this suggestion. It is noted in the above test case, however, that the pronounced long (100-foot or 30.48-meter) wave in the profile is virtually unaffected by the overlay. This wave is believed to have been introduced in the grading

TABLE 3.2. ROUGHNESS AMPLITUDES BEFORE AND AFTER OVERLAY OF THE ODESSA ROAD SECTION (inches)

	Before		After	
	Percentile		Percentile	
	50	90	50	90
	0 to 4-Foot Wavelengths			
Right	.03921	.08274	.01904	.02484
Left	.03171	.04987	.00853	.01618
Transverse	.05511	.08997	.01475	.02669
	4 to 10-Foot Wavelengths			
Right	.04556	.07334	.01252	.02064
Left	.02179	.03506	.00791	.01182
Transverse	.04642	.08482	.01392	.02536
	10 to 25-Foot Wavelengths			
Right	.04789	.09637	.01402	.02521
Left	.01871	.02713	.00920	.01602
Transverse	.05008	.09967	.01481	.02959
	25 to 50-Foot Wavelengths			
Right	.02819	.05583	.01574	.02361
Left	.01474	.02497	.01279	.03076
Transverse	.02372	.04941	.00945	.01812
	50 to 100-Foot Wavelengths			
Right	.04848	.07046	.03282	.06039
Left	.02355	.03242	.03709	.06860
Transverse	.02543	.04139	.02085	.03178

NOTE: 1 foot = .3048 meters
1 inch = 2.540 centimeters

The fiftieth and ninetieth percentile values are the amplitudes greater than exactly 50 and 90 percent, respectively, of the local roughness amplitudes in a road section.

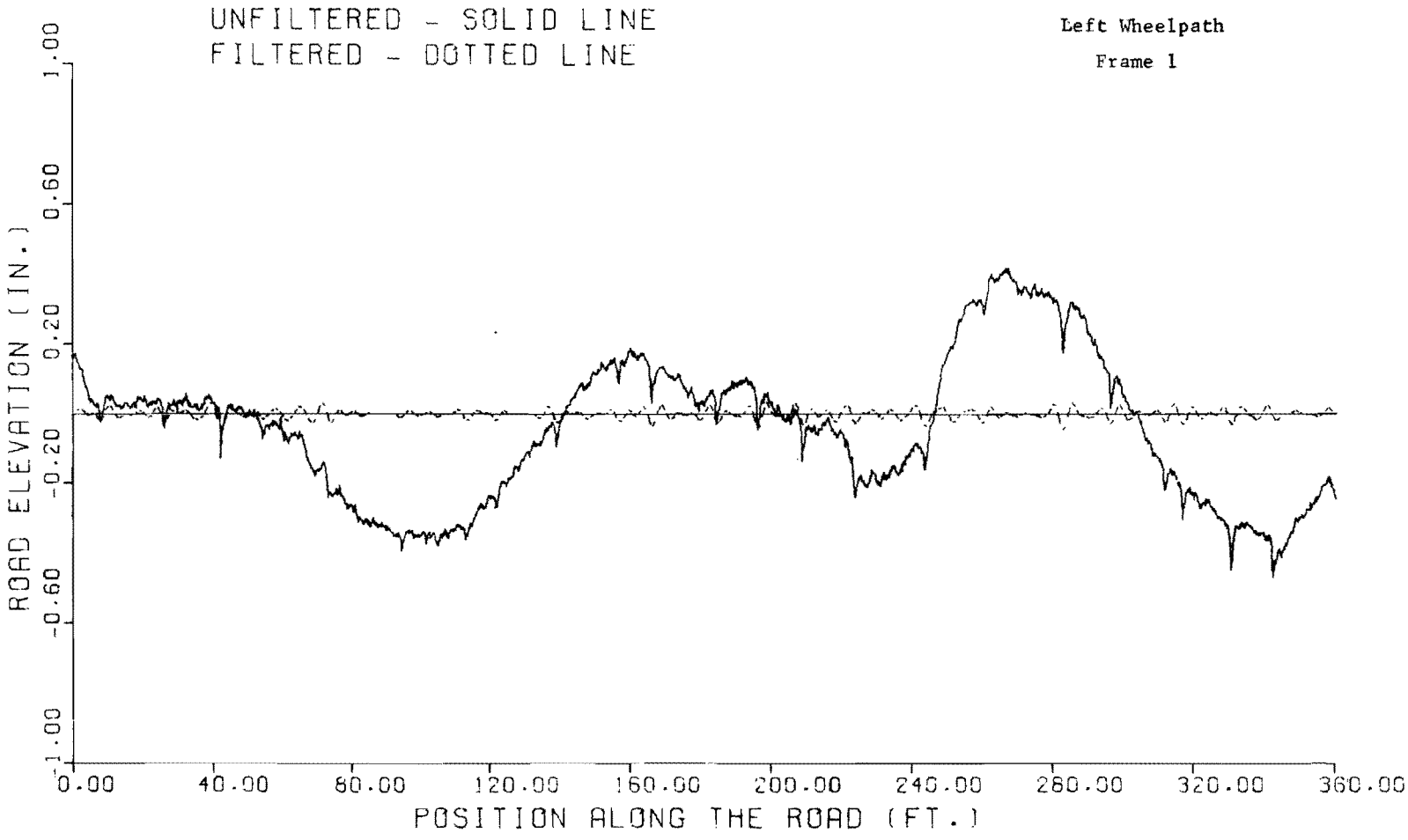

1 foot = .3048 meters
1 inch = 2.540 centimeters

Fig 3.3. Odessa Test Section, March, 1975: Roughness with 4 to 10-foot wavelengths isolated by filter. A year after overlay.

(continued)

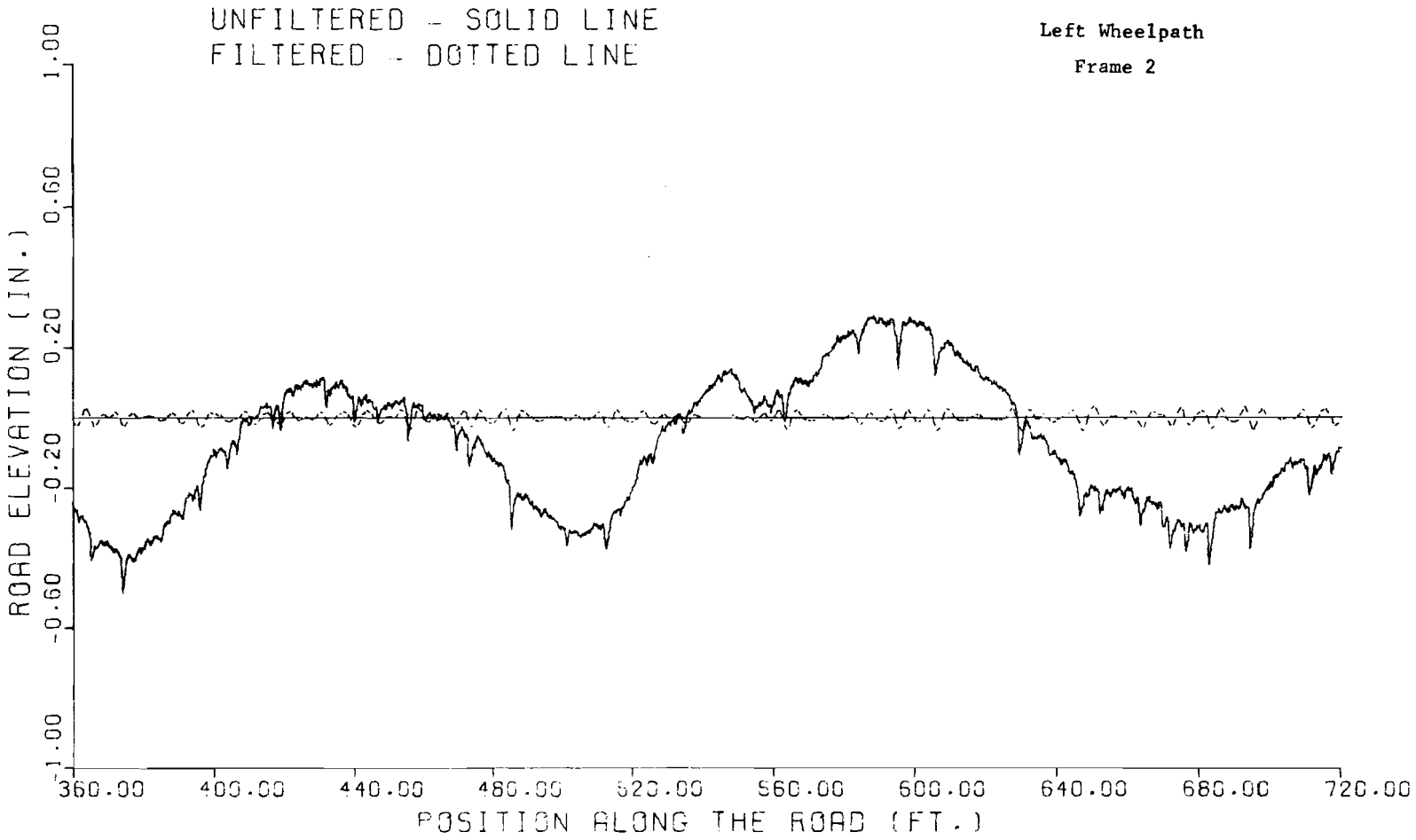

Fig 3.3. (Continued)

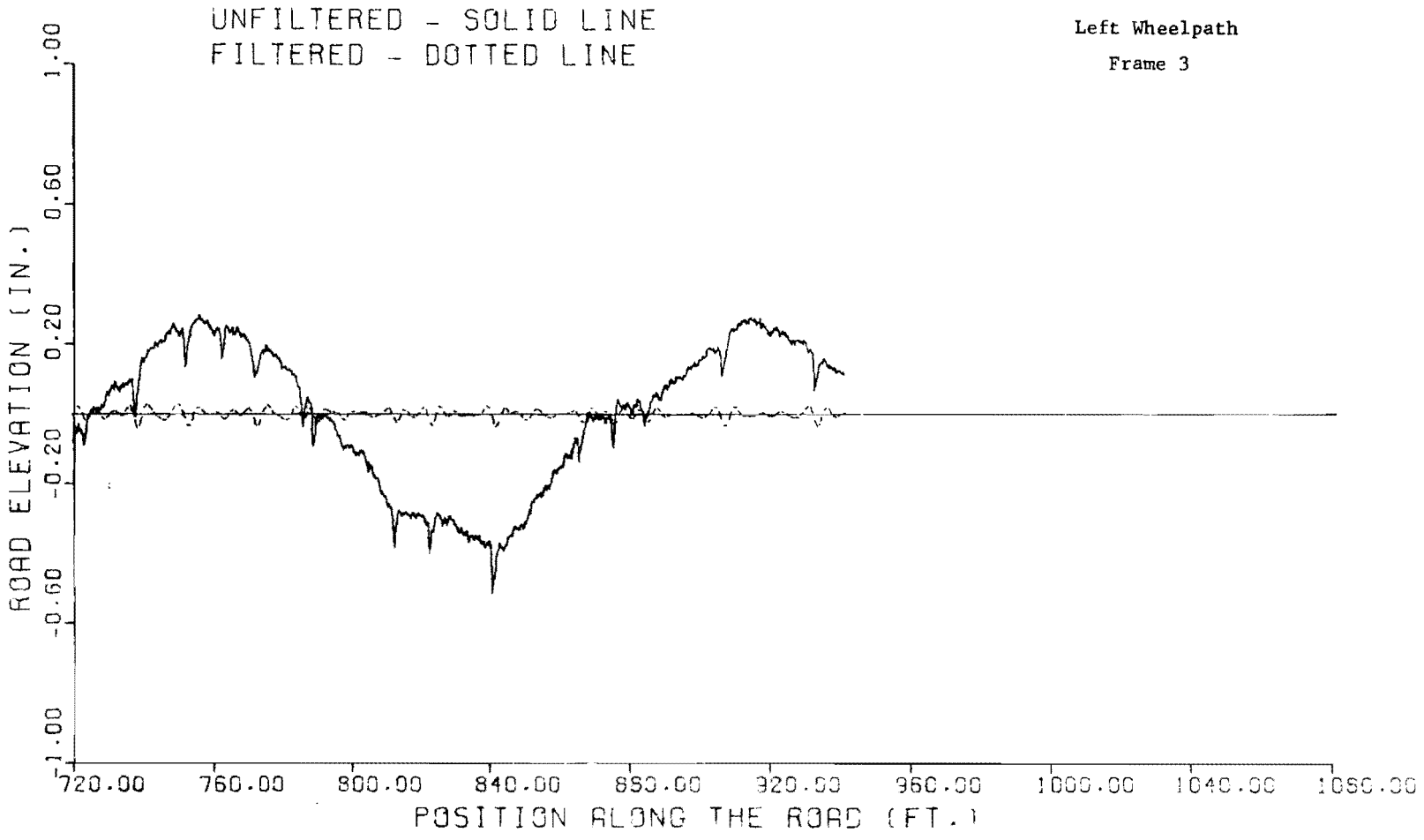

Fig 3.3. (Continued)

process; the profile seems to oscillate between points spaced by about 50 feet (15.24 meters), where the construction stakes may have been placed.

The SI value computed with the existing model for the profile measured a year after the overlay is 4.0. The SI values obtained by using the new models, along with the values just after the overlay, are given in Table 3.3.

It is interesting that the SI loss over the year period decreases monotonically with wavelength; the greatest deterioration in riding quality is in the short wavelengths. A close comparison of the April, 1974, profile plot and the March, 1975, plot, shown in Fig 3.3, reveals that some of the high-frequency waves, which were not fully corrected by the overlay, worsened considerably over the year period. It is also seen that the long waves are not dramatically changed. Thus, we have further evidence that the SI values are consistent with observable profile effects.

The curious SI improvement of .02 for the 50 to 100-foot (15.24 to 30.48-meter) wavelengths is of no significance, since a change of .02 is within the range of measurement error.

The roughness amplitudes are presented in Table 3.4.

Illustrative Test Case 2

In the preceding example, the SI values were discussed from the standpoint of effects which are clearly seen in the accompanying road profile plots. Although this approach is convenient when possible, visual analysis of the roughness components of a road by wavelength is generally extremely difficult; this is part of the reason for the use of methods such as digital filtering.

In this section we discuss two sections on the Old San Antonio Road near Bryan, Texas. The profile plots presented in Appendix 5 are not easily analyzed in detail visually; it will be convenient to made certain comparisons on the basis of the roughness amplitudes presented in Table 3.5.

The Old San Antonio Road is a surface-treated, two-lane road. Since there is neither a shoulder nor a curb, the outside wheelpath has deteriorated more than the inside wheelpath; this explains why in Table 3.5 the amplitudes for the right wheelpath are generally higher than those for the left wheelpath.

TABLE 3.3. SI VALUE JUST AFTER AND A YEAR AFTER MAINTENANCE OF THE ODESSA ROAD SECTION.

		Wavelength (Feet)			
	All Roughness	4 to 10	10 to 25	25 to 50	50 to 100
Just After	4.25	4.06	4.06	4.17	4.00
Year Later	4.18	3.88	3.96	4.15	4.02
Decrease over the year	.07	.18	.10	.02	-.02

NOTE: 1 foot = .3048 meters

TABLE 3.4. ROUGHNESS AMPLITUDES A YEAR AFTER OVERLAY OF THE ODESSA ROAD SECTION (inches)

	Percentile	
	50	90
	0 to 4-Foot Wavelengths	
Right	.01123	.02521
Left	.00816	.01964
Transverse	.01557	.02860
	4 to 10-Foot Wavelengths	
Right	.01625	.02582
Left	.01251	.01837
Transverse	.01821	.03075
	10 to 25-Foot Wavelengths	
Right	.01761	.03028
Left	.01314	.02109
Transverse	.02074	.03770
	25 to 50-Foot Wavelengths	
Right	.01756	.02679
Left	.01389	.02800
Transverse	.01056	.01828
	50 to 100-Foot Wavelengths	
Right	.03678	.05595
Left	.03795	.06762
Transverse	.01820	.03036

NOTE: 1 foot = .3048 meters
1 inch = 2.540 centimeters

The fiftieth and ninetieth percentile values are the amplitudes greater than exactly 50 and 90 percent, respectively, of the local roughness amplitudes in a road section.

TABLE 3.5. ROUGHNESS AMPLITUDES FOR TWO SECTIONS ON THE OLD SAN ANTONIO ROAD (inches)

	Section 2		Section 3	
	Percentile		Percentile	
	50	90	50	90
	0 to 4-Foot Wavelengths			
Right	.02441	.03877	.02102	.03126
Left	.02201	.03443	.02145	.03691
Transverse	.03278	.05091	.03122	.04739
	4 to 10-Foot Wavelengths			
Right	.03566	.07684	.02829	.04619
Left	.02544	.05651	.02680	.04614
Transverse	.04141	.09882	.04073	.06478
	10 to 25-Foot Wavelengths			
Right	.07215	.14931	.04301	.07654
Left	.03326	.07846	.02822	.06280
Transverse	.08038	.16249	.05294	.09172
	25 to 50-Foot Wavelengths			
Right	.16397	.23717	.06100	.10436
Left	.06475	.13005	.02458	.05232
Transverse	.12081	.22340	.05985	.08835
	50 to 100-Foot Wavelengths			
Right	.22984	.42689	.08085	.23014
Left	.20120	.32986	.05884	.11919
Transverse	.12308	.26203	.09336	.16371

NOTE: 1 foot = .3048 meters
1 inch = 2.540 centimeters

The fiftieth and ninetieth percentile values are the amplitudes greater than exactly 50 and 90 percent, respectively, of the local roughness amplitudes in a road section.

Although the road is believed to be affected by a swelling subgrade, there is general deterioration, as evidenced by the low SI values listed in Table 3.6.

The primary purpose of including this test case is to illustrate, as discussed below, the way differential sensitivity of the human ratings to roughness of differing wavelengths is reflected in the SI values. As a general rule, the correlation between PSR and the roughness amplitudes decreases as the wavelength increases; the specific relationships are discussed in the following chapter. The points discussed below indicate that the correlation trend is manifested by a decreasing sensitivity of SI to amplitude changes as the wavelength increases.

Along these lines, the following observations can be made from Table 3.5:

(1) For the 10 to 25-foot (3.048 to 7.620-meter)-long waves, the amplitudes for section 2 are considerably larger than those for section 3, and the SI is significantly lower (1.33 versus 2.46) for section 2.

(2) For the 25 to 50-foot (7.620 to 15.24-meter)-long waves and for the 50 to 100-foot (15.24 to 30.48-meter)-long waves, the amplitudes are again larger for section 2 than for section 3, and it can be seen at a glance that the percentage differences are generally larger here than for the 10 to 25-foot (3.048 to 7.620-meter)-long wavelengths. In spite of this, the SI values are increasingly similar as the wavelength increases.

The practical interpretation is that the SI models explain whatever part of the variation in PSR the roughness terms are capable of explaining. If PSR were perfectly linearly related to a roughness term X_1, then a model $SI = 5\text{-}C_1X_1$, where C_1 is a regression coefficient, could be obtained. The predicted serviceability would be near 5 for small values of X_1 and near 0 for large values. The predicted serviceability would vary significantly as X_1 varied significantly, since the totality of the possible variations in PSR could be explained in terms of X_1.

In the other extreme case, suppose PSR were totally unrelated to another roughness term X_2. Then if PSR were regressed on X_2, the model $SI = C_2$ would be obtained, where C_2 is the sample PSR mean. In this case, the

TABLE 3.6. SI VALUES FOR TWO SECTIONS ON THE OLD SAN ANTONIO ROAD

Type of Roughness (Wavelength in Feet)	Section 2	Section 3
4-10	2.22	2.52
10-25	1.33	2.46
25-50	2.20	2.73
50-100	3.01	3.30
Overall (4-100)	2.16	2.47
Overall (8.6-86: Power Spectrum Model)	1.7	2.4

NOTE: 1 foot = .3048 meters

predicted serviceability would not vary at all, since X_2 would have no predictive value whatsoever.[4]

All the SI models we have discussed are between these two extremes, but the models for long wavelengths are more like the second extreme than are the models for short wavelengths. Thus, the models can be used to assess the significance from the standpoint of riding quality, i.e., from the standpoint of correlation with PSR, of a given roughness amplitude. This significance is obviously not indicated by the roughness measurements alone.

---

[4] An examination of the models given in Appendix 1 shows that the constant terms, which are the SI values if all roughness amplitudes are zero, are near 5 for the overall and 4 to 10-foot (1.219 to 3.048-meter) models. The constant terms decrease with wavelength for the other models. This indicates that the SI models for short wavelengths vary over the entire SI scale as the amount of roughness varies, while the SI values for the long wavelengths vary within a narrower range. Thus, the form of the models supports the points made in the text.

CHAPTER 4. PROPERTIES OF THE SI MODELS

In the preceding chapter, we introduced the basic concept of relating individual components of roughness to PSR, gave illustrative test cases, and discussed certain applications of the SI models. In this chapter, the correlations between the roughness components and PSR are discussed along with certain roughness properties of different types of pavements. There are two reasons for this type of analysis:

(1) to understand the models better in order to use them more intelligently and

(2) to gain insights from the correlations between PSR and the roughness terms about what types of roughness people find most objectionable.

Certain characteristics of the SI models are presented in Table 4.1. Although all of the terms which appear in the table are commonly used, we will briefly discuss the practical meanings of the terms as they apply to the serviceability problem. In the process, we will also interpret Table 4.1.

Correlation with PSR

The correlation (or multiple correlation) coefficient reflects the strength of the relationship between PSR and the combination of terms selected for inclusion in the model. The selection process, called stepwise regression (Refs 6 and 7), successively enters terms into and deletes terms from the predictive model until no further significant improvement can be made. The square of the correlation the proportion of the variation in the dependent variable, PSR, which can be explained or predicted in terms of the independent variables. Thus, if we attempted to regress PSR on a set of variables which were totally unrelated to PSR, then the correlation would be zero. If, on the other hand, we were able to predict the dependent

TABLE 4.1. CHARACTERISTICS OF THE SI MODELS

Type of Roughness (Wavelength in Feet)	Correlation with PSR	Standard Error	Number of Terms in Model*
Concrete Pavements			
4 to 100 (overall)	.91	.32	6
4 to 10	.86	.37	5
10 to 25	.85	.38	4
25 to 50	.77	.46	4
50 to 100	.75	.46	3
Sample size: 22			
Asphalt Pavements			
4 to 100 (overall)	.91	.38	8
4 to 10	.86	.45	6
10 to 25	.82	.49	5
25 to 50	.81	.52	6
50 to 100	.68	.61	2
Sample size: 50			

*Including constant term

NOTE: 1 foot = .3048 meters.

variable perfectly, then the multiple correlation would be one.[1] In essentially all real cases, the correlation is between these two extremes.

It should be noted that the correlations for the models for the individual wavelength bands decrease monotonically as the wavelength increases. The apparent interpretation is that the panel members were less sensitive to the long waves, and, for this reason, a smaller proportion of the variation in PSR is explainable in terms of the long waves than is explainable in terms of the short waves.

It is dangerous, of course, to associate cause-and-effect relationships with correlations in general. Not infrequently, a common factor causes each of two quantities to vary simultaneously. Suppose, for example, that two unrelated products both had increasing sales trends because of an increase in the population. Then the fact that the sales of the two products were correlated would not imply that there was a causative relationship between the two.

Nevertheless, the conclusion that the raters are more sensitive to short than to long waves is believable and seems to be justified in this case, although further experimental work to assess the isolated effect of severe long waves caused by swelling clay would be valuable.

A factor which should be kept in mind, however, is that the various roughness terms are correlated with each other as is evidenced by the data presented in Table 4.2. Although there are exceptions, such as the rapid development of roughness with wavelengths within a narrow band because of a swelling subgrade, the progressing roughness generally spans a wide range of wavelengths. Thus, the correlation between, say, the 4 to 10-foot (1.219 to 3.048-meter)-wavelength roughness terms and PSR is undoubtedly influenced by the fact that the amplitudes of the 10 to 25-foot (3.048 to 7.620-meter)-long waves are correlated with both the 4 to 10-foot (1.219 to 3.048-meter) amplitudes and PSR. Although this effect clouds the relationships between the various types of roughness and PSR, existing roads provide

---

[1] It is meaningful in the univariate case to indicate by positive and negative correlations the cases in which the dependent variable increases and decreases, respectively, as the independent variable increases.

TABLE 4.2. CORRELATIONS BETWEEN MEDIAN AMPLITUDES OF LONGITUDINAL ROUGHNESS

Concrete Pavements

	Wavelength (Feet)			
Wavelength (Feet)	4 to 10	10 to 25	25 to 50	50 to 100
4 to 10	1.0	.886	.682	.307
10 to 25		1.0	.717	.294
25 to 50			1.0	.543
50 to 100				1.0

Asphalt Pavements

	Wavelength (Feet)			
Wavelength (Feet	4 to 10	10 to 25	25 to 50	50 to 100
4 to 10	1.0	.905	.682	.513
10 to 25		1.0	.867	.638
25 to 50			1.0	.842
50 to 100				1.0

NOTE: 1 foot = .3048 centimeters

the most realistic, and probably the best, test cases for highway riding quality.

Quite a bit of work has been done in controlled laboratory settings on human sensitivity to vibrations of different frequencies. In these studies, it is possible to subject the human raters to oscillatory motion of a single frequency, and, thus, the correlation problem can be eliminated. In view of the discrepancies even among laboratory experiments of this type, however, the unconstrained use of their results to draw inferences about highway riding quality is questionable. The extent of the disagreement among these experiments is evidenced by the following statement made by Hanes in Ref 10, page 73: "Sensitivity to vertical (foot-to-head direction) sinusoidal, or approximately sinusoidal, vibration varies with frequency, but the data from various studies show so little agreement that no clearly defined region of maximum sensitivity can be specified."

Standard Error

The standard error is the square root of the mean square of the deviations of the observed PSR values from the regression function; that is,

$$s.e. = \left[\frac{1}{N - K} \sum_{i=1}^{N} \left(Y_i - \hat{Y}_i \right)^2 \right]^{1/2}$$

where

s.e. = standard error,

N = sample size,

K = number of terms (including the constant) in the predicting function,

Y_i = i^{th} observed value of PSR, and

$\hat{Y}_i$ = i^{th} predicted value of PSR.

It is clear that if Y_i and $\hat{Y}_i$ were identical for all i, that is, if the observed and predicted serviceability values agreed perfectly, the standard error would be zero. It is also clear that the larger the discrepancies between the observed and predicted values are, the larger the standard error is. Thus, the standard error is, in a sense, a measure of the accuracy of the prediction, as is the correlation.

Number of Terms in Model

It is easy to develop a predicting function which correlates highly with a measured response by including almost as many terms in the model as there are data points. But if this is done, the correlation is meaningless, since the noise in the data is modeled along with the repeatable trends. Thus, it is significant that each of the SI models contains a small number of terms compared to the size of the sample from which it was developed.

Brief Comments on the Roughness Properties of Asphalt and Concrete

The characteristic roughness of the two types of pavement and, especially, the various causes for roughness is an important area of study in itself. Only a few comments are made on the subject in this section. The purposes are to show that there are some important differences between the predominant roughness characteristics of asphalt and concrete pavements and to demonstrate further the physical meaning of the roughness terms. Particularly, certain advantages of characterizing transverse waves by amplitudes rather than by the more common roll rates will become apparent.

In Table 4.3, the medians and the standard deviations of the medians of the roughness amplitudes are presented. Recall from the preceding chapter that the transverse amplitudes are simply amplitudes of road-surface deflections of one wheelpath relative to the other and that the wavelengths are measured longitudinally along the road exactly as the wavelengths for longitudinal roughness are. The table reveals some differences in the nature

TABLE 4.3. OVERALL SECTION MEDIANS OF ROUGHNESS AMPLITUDES AVERAGED OVER SAMPLES OF ROAD SECTIONS (inches)

Wavelength (feet)	Longitudinal		Transverse	
	Mean	Standard Deviation	Mean	Standard Deviation
Concrete Pavements				
4 to 10	.020	.009	.024	.011
10 to 25	.041	.017	.040	.025
25 to 50	.061	.026	.048	.027
50 to 100	.103	.053	.070	.038
Asphalt Pavements				
4 to 10	.019	.007	.025	.009
10 to 25	.028	.014	.035	.020
25 to 50	.049	.031	.051	.043
50 to 100	.107	.066	.095	.059

NOTE: 1 foot = .3048 meters
1 inch = 2.540 centimeters

of the roughness on the two types of pavement.[2] Notice particularly that the transverse waves are larger relative to the longitudinal waves for asphalt than for concrete. This means that the surface waves in the two wheelpaths are much more similar on concrete pavements than on asphalt. For both types of pavement, the transverse amplitudes decrease relative to the longitudinal amplitudes as the wavelengths increase. This result was expected, since the two wheelpaths may be very dissimilar with respect to short bumps, but it is unlikely that one wheelpath would have, say, a 100-foot (30.48 meter)-long wave unless the other wheelpath had a similar wave.

The fact that the transverse waves are less pronounced on concrete than on asphalt was expected for two reasons. First, concrete is a more rigid material and is not as susceptible to deformations of one wheelpath relative to the other. Second, there are certain construction differences between the two types of pavements. In the construction of a concrete pavement, forms are placed 24 feet (7.315 meters) apart laterally, and the surface is leveled in the transverse dimension over the distance. In the construction of asphalt pavements, the corresponding distance is 12 feet (3.658 meters); the lateral roughness control is performed over half the distance used for concrete pavements. It is evident that this construction difference would tend to produce greater transverse roughness in asphalt than in concrete pavements.

Longitudinal and Transverse Roughness Studied Separately

Since longitudinal and transverse roughness produce very different types of vehicle motion, it is of interest to see how the two types of roughness individually correlate with PSR. In Table 4.4, the correlations are given; the models themselves and additional details are given in Appendix 1.

---

[2] At first glance, the standard deviations presented in the table appear to be so large compared to the means that sampling errors would prevent any inferences from being drawn. This is seen immediately not to be true, however, when one realizes that each standard deviation must be divided by the square root of the sample size (the sample size is ?? for concrete and 50 for asphalt) to obtain the standard deviation of the sample mean. The population standard deviation estimates, which are presented, however, are more meaningful population dispension measures.

TABLE 4.4. CORRELATIONS BETWEEN PSR AND ROUGHNESS, LONGITUDINAL AND TRANSVERSE ROUGHNESS SEPARATED

Wavelength (feet)	Longitudinal	Transverse
Concrete Pavements		
4 to 10	.70	.82
10 to 25	.79	.64*
25 to 50	.77	.64*
50 to 100	.75	.70
Asphalt Pavements		
4 to 10	.65	.75
10 to 25	.74	.75
25 to 50	.74	.74
50 to 100	.63	.68

*These models contain only type variables, no roughness terms.

NOTE: Each model represented in this table has a maximum of four terms.

1 foot = .3048 meters.

In Table 4.5, the correlations are given for a set of models involving roughness terms and no type variables.[3] In this table, we see similar trends of correlation with wavelength for the two types of pavements, and the trends are different for longitudinal and transverse roughness. As the wavelength increases, however, the correlation between the transverse amplitudes and PSR decreases more rapidly for concrete than for asphalt pavements. (Recall Table 4.3.)

Comments on Differing Methods for Relating PSR to the Components of Roughness

The method which has been adopted here for relating PSR to several individual components of roughness is to develop a separate regression model for each component. Applications are discussed in Chapters 1 and 3 and various properties of the models are discussed in this Chapter. The terms included in the models and the coefficients of the terms are given in Appendix 1.

---

[3] Separate models without the type variables were developed because when these variables were included, two of the models contained type variables only and no roughness terms. (See Table 4.4.) Such models involving no roughness measures obviously have no capability for evaluating the roughness of a road section.

When the transverse and longitudinal roughness measures were combined, all models contained roughness measures, and, therefore, a separate set of models without the type variables was not developed for this case.

Another point is that the type variables correlate with all the roughness measures; a hot-mix asphalt-concrete road is likely to have less severe roughness of all types than a surface-treated road. By including the type variable in the prediction of PSR from roughness with wavelengths between λ_1 and λ_2, we are indirectly including part of the information contained by the roughness measures for the other wavelengths. The effect, of course, is to cloud the relationships between individual types of roughness and PSR to some extent.

The reason for including the type variables is to account for visual or auditory effects which are present in the PSR data, but which cannot be explained in terms of roughness. But for the 4 to 10-foot (1.219 to 3.048 meter)-wavelength transverse roughness, the correlations are almost as high without the dummy variables as with them; furthermore, these are the models with the highest multiple correlations. Thus, the visual and auditory effects do not play a very large role.

The models represented in Table 4.5 are, therefore, preferable in some respects to the models represented in Table 4.4.

TABLE 4.5. CORRELATIONS BETWEEN PSR AND ROUGHNESS, LONGITUDINAL AND TRANSVERSE ROUGHNESS SEPARATED: DUMMY TERMS EXCLUDED

Wavelength (feet)	Longitudinal	Transverse
Concrete Pavements		
4 to 10	.53	.75
10 to 25	.71	.63
25 to 50	.57	.59
50 to 100	.56	.42
Asphalt Pavements		
4 to 10	.65	.75
10 to 25	.72	.73
25 to 50	.71	.71
50 to 100	.60	.68

NOTE: Each model represented in this table has a maximum of three terms.

1 foot = .3048 meters.

When standard statistical model-building techniques are used, if the predictor variables are correlated, then the presence of one term in the model affects the coefficients of the other variables. If the predictor variables are highly correlated, as some of the roughness measures are (see Table 4.2), then there is so much interdependence among the coefficients that they do not reflect the true relationships between the roughness terms taken individually and PSR. This very complex problem is treated in Ref 11. That reference is both summarized and discussed in Chapter 2.

In Ref 11, a scheme for imposing constraints which prevent the coefficients from taking on certain ranges of physically nonsensical values is presented. This scheme, which was intended for use in regressing PSR on power spectra, is, for reasons discussed in Chapter 2, not adaptable for regressing PSR on the more detailed set of roughness measures used in this study.

Two other approaches to the problem, however, are discussed in Appendix 4. One of these approaches employs a multivariate statistical method, principal component analysis, for simplifying the set of predictor variables, and the other approach involves constraining the coefficients so that they will be directly related to the correlations between PSR and the roughness terms to which they apply.

It is shown to be clearly possible to constrain the coefficients so that they cannot have certain obviously nonsensical values (e.g., the opposite sign from their correlations with PSR) and so that they at least seem to make physical sense.

Any such constraint, however, limits the ability of the model-building method to fit the predictive model to the data. To the extent that the constraints limit the relationship between the prediction and the quantity which is being predicted, the constraints also limit the usefulness of the model for any purpose - for analysis of individual contributions[4] to SI or for prediction of SI as an overall measure of the roughness of the road. The discussion in Appendix 4 does show, furthermore, that such constraints do limit the correlation.

---

[4] Such inferences would be drawn by using the constrained model for analysis of the sensitivity of PSR to individual roughness terms. This would involve varying the values of the roughness terms one at a time and studying the effects on the SI value.

When a model to evaluate, say, the 4 to 10-foot (1.219 to 3.048-meter)-long roughness is developed by regressing PSR on the roughness measures describing that class of roughness, however, the only limitations on the predictive accuracy are the limits of the relationship between PSR and the class of roughness under investigation; there are no artificial constraints which can possibly distort the prediction.

Although the use of a single constrained model has some interesting possibilities, because of the limitations discussed above, the alternate approach of developing separate regression models for separate types of roughness was adopted for the study.

Comparisons Between the Existing SI Model and the New Models

The primary objective of the study reported herein is to expand the capabilities for evaluating a road by computing a set of SI values, rather than a single SI, as has been done in the past. As a secondary objective, overall SI models were also developed. As shown through test cases in Chapter 3, these new overall models have certain advantages over the SI model which is discussed in Ref 21 and in Chapter 2. The basic differences between the existing and the new models, which were developed from the same data set, are discussed below. For convenience, we will refer to the earlier model as the SI_1 model and to the new models as the SI_2 models.

(1) The SI_1 model includes roughness terms representing wavelengths from 8.6 to 86 feet, (2.6 to 26 meters), while the SI_2 models include the wider range from 4 to 100 feet (1.219 to 30.48 meters). An initial filtering operation was used in the present study to eliminate large-amplitude tape recorder noise in the 2 to 3-foot (.6096 to .9144 meter)-wavelength area which might otherwise have distorted evaluations of the 4 to 8-foot (1.219 to 2.438 meter)-long waves. It is felt that the extra range at the short-wavelength end is significant and probably explains the improved performance in the test cases discussed in Chapter 3.

(2) The single SI_1 model was developed to handle both concrete and asphalt roads, while the SI_2 models include separate equations for the two types of pavement. The development of separate equations is justified by the marked differences discussed in this chapter between the two cases. See especially Tables 4.3 and 4.5.

(3) The SI_1 model has 22 terms, while the SI_2 models have six and eight terms for concrete and asphalt roads, respectively. This is partly because of the separation of the pavements into two more nearly homogeneous classes in developing the SI_2 models.[5]

Another difference may be in the hypothesis testing in the stepwise regression procedure used to develop the SI_2 models. The 75-percent level was used in developing the SI_2 models; that is, a term which is uncorrelated with PSR has one chance in four of erroneously satisfying the statistical criterion for entering the model at a given step. This significance level was selected on the basis of preliminary testing and previous experience; higher levels tend to eliminate terms which probably would make a significant contribution to the model, while using lower levels results in the inclusion of terms which are of questionable value.[6] The significance level used to develop the SI_1 model is not reported in Ref 21. In any case, this is not a particularly significant criticism of the SI_1 model, since the inclusion of a few questionable terms neither helps nor hurts the accuracy of the prediction in general.

(4) The SI_1 model has a multiple correlation of .94, while both the SI_2 models have correlations of .91. The slightly lower correlations could be explained by the smaller number of terms in the SI_2 models.

(5) The predictor variables for the SI_1 model were computed from the measured road profiles by using spectral analysis, while digital filtering was used for the SI_2 models. This point is discussed extensively in Appendix 5.

---

[5] This is not the complete explanation, however, since an eleven-term model with a correlation of .90 for both types of pavements was developed from the filtering data as a preliminary investigation.

[6] This type of investigation is best carried out by studying the behavior of the standard error as successive terms are added to a regression model. The standard error decreases as meaningful terms are added, but oscillates or possibly even increases as meaningless terms are added. The SI_1 models with 22 terms has a standard error of .33, while the SI_2 models with eight and six terms have standard errors of .38 and .32, respectively. The differences of .05 and .01 are small from a practical standpoint. The multiple correlation, on the other hand, cannot decrease as additional terms are added.

(6) Because of end effects, there is distortion in the filtered road profiles near the first and last of the data record. The reasons for the effect are discussed in Appendix 5. The simplest solution is to exclude from further analysis a short interval at either end of the filtered output; one cycle of the longest wavelength to be isolated by filtering, 100 feet (30.48 meters) in this study, has been found to be adequate to remove the distortion.[7] This exclusion of 17.5 percent of the length of the 1140-foot (347.5-meter) section introduces an extra source of error, since the section described by the roughness measures does not coincide exactly with the section rated by the panel. The error which is introduced is random, however, since the first and last parts of the sections are no more or less rough on the average than the center parts; we are not systematically excluding the roughest or smoothest parts of the sections. In view of the very high correlations achieved in the regression analyses, whatever random errors may have been introduced by the data exclusion cannot be large. It is important to realize that exclusion of part of the sections used for the PSR study is not an inherent limitation of the approach used in this study. Although the problem could not have been anticipated at the time the measurements were made in 1968, if an extra 100 feet (30.48 meters) had been measured on either side of each section, then there would have been no problem at all.

The Fourier transform approach used in developing the SI_1 model did not require such an exclusion. Certain preliminary operations (applying a cosine taper window)used in developing the SI_1 model, however, result in weighting the first and last 10 percent of the road profile less heavily than the center part. (See Appendix 5.)

---

[7] Actually, it would have been possible to remove 10 feet (3.048 meters) from either end of the filtered profile including the 4 to 10-foot (1.219 to 3.048-meter) wavelengths, 25 feet (7.620 meters) from the profile including the 10 to 25-foot (3.048 to 7.620-meter) wavelengths, etc., but this scheme would have differentially affected the correlations between PSR and roughness with different ranges of wavelengths and, therefore, would have partially defeated the purpose of the study.

Validation

A set of PSR data which was collected for another current riding-quality project was used to test the predictions of both the SI model presented in Ref 21 and the model presented here.[8]

In Table 4.6, the PSR data and the SI values from the existing model (SI_E) and from the new model (SI_N) are given. The eight asphalt roads which were used are all in the Austin, Texas, area.

The purpose of the other study did not in any way require that the PSR rating sessions be performed consistently with the sessions in which the PSR data for this study were collected. Thus, there are a few differences, including the following.

(1) The original panel included 15 representatives from several professions, including accountants, secretarys, computer programmers, etc. (Ref 16, p 17). The later study included a random sample of 54 undergraduates who were participating in experiments to satisfy lower-division psychology coursework requirements at The University of Texas. Therefore, there is an age difference between the two panels.

(2) In the earlier study, the panel was allowed to redrive the section at any desired speed and "get out and look at or walk over the section" (Ref 16, p 19). Thus, although geometrical factors such as the width of the road were excluded, the ratings do involve the appearance of the pavement. In the later study, the ratings are based solely on the quality of a single ride over the section; the appearance of the pavement is not a factor.

(3) A standard-sized car was used in the earlier study, while a compact car was used in the latter.

The reason for including the points above is neither to provide an exhaustive comparison of the two rating panel studies nor to argue that one procedure is better than the other in any respect; neither of these two objectives is relevant here. The point is simply that the two studies are different, and the existence of certain differences between the PSR data

---

[8] These data were collected for use in a project which is being performed at the Council for Advanced Transportation Studies (CATS), The University of Texas at Austin, under contract to the Department of Transportation. A full investigation of the data will be performed by the CATS research staff. We appreciate very much their making the data available to us for validation purposes.

TABLE 4.6. SI VALUES FROM THE EXISTING MODEL (SI_E) AND FROM THE NEW MODEL (SI_N) AND PSR VALUES

	PSR	SI_E	PSR-SI_E	SI_N	PSR-SI_N
	3.4	3.4	0.0	4.2	-.8
	4.1	4.3	-.2	4.4	-.3
	3.6	4.2	-.6	4.3	-.7
	2.7	2.0	.7	2.7	0.0
	2.4	2.0	.4	2.7	-.3
	2.4	1.9	.5	2.6	-.2
	3.5	3.5	0.0	4.0	-.5
	4.1	4.2	-.1	4.3	-.2
Mean	3.3	3.2	.1	3.7	-.4

obtained in the later study and the SI's based on the PSR data from the earlier study do not invalidate either of the SI models or either PSR study.

Thus, it would not be valid to say that the PSR and the SI averages should be the same, although Table 4.6 shows the averages to be reasonably close. One would, however, expect the PSR and SI data to correlate reasonably well. This condition is certainly satisfied, since the SI_E and SI_N values have correlations of .97 and .95, respectively, with the PSR values.

It is felt that the test described above serves as at least a tentative validation of both the existing and the new SI models which were investigated.

CHAPTER 5. SUMMARY, CONCLUSIONS, AND RECOMMENDATIONS

The essential points of the study reported here are briefly summarized below. A summary of the background, which is discussed in Chapters 1 and 2, is included for completeness and for the convenience of the reader.

Background

(1) There are diverse practical needs for the evaluation of the present condition of a pavement. These needs include the decision to accept or reject a new construction, the allocation of maintenance resources, and the performance of research to improve pavement design, construction, and maintenance practices.

(2) Although subjective judgements by highway engineers are necessary for such functions as identifying probable causes of pavement deterioration, an evaluation method which is consistent, i.e., relatively free from human subjective variations, is also of value.

(3) The Present Serviceability Rating (PSR) is an average of the ratings of a human panel of "the ability of a specific section of pavement to serve high-speed, high-volume, mixed (truck and automobile) traffic in its existing condition" (Ref 5). The PSR is a meaningful evaluation, since it is closely related to the needs of the highway users. If the panel size is sufficiently large[1], then the panel average is quite reliable. The panel rating method, however, is very time consuming and expensive.

(4) For this reason, considerable research effort has been expended to develop methods for predicting PSR in terms of a set of physical measurements which describe the road condition (Refs 5, 11, 16, 19, 20, and 21).

(5) Roughness measurements have been shown to be very closely related to PSR (Ref 21). These measurements are also very conveniently obtained by using modern high-speed profilometer equipment; visual condition surveys are, by comparison, time-consuming and inexact. Thus, roughness data are convenient predictors of PSR.

---

[1] If the panel size is 16, then the panel average has a standard deviation of about .1. This is based on the fact that a single rating has been shown to have a standard deviation of .4 to .5 (Refs 5 and 16).

(6) The roughness data in the form of surface elevation in both wheelpaths versus distance along the road are too numerous for convenient direct use except for visual inspection of plots. The problem of summarizing or characterizing the information is a challenging engineering and mathematical problem in itself. The use of spectral analysis (Refs 2, 3, 8, 11, 13, 19, and 21) to compute a roughness amplitude corresponding to each of a discrete set of roughness wavelengths is a common approach (Ref 21). The use of digital filtering to quantify the distribution of roughness severity in a road section is introduced in Ref 4.

(7) The calculation of an SI value, which is simply a PSR prediction, is a way to convert the roughness amplitudes to a single value which summarizes the overall present riding quality of the road. The SI value is much more easily interpreted than the roughness amplitudes. The development of an SI model using roughness amplitudes computed by means of spectral analysis as predictor variables is discussed in Ref 21.

Summary and Conclusions of this Study

The principal contribution of the research reported herein is the development of SI models which can be used to evaluate, along with overall riding quality, specific aspects of road roughness. For this purpose, the roughness is categorized on the basis of wavelength and on the basis of longitudinal versus transverse effects.

The calculation of characterizing measures of the various aspects of roughness is a necessary preliminary step to the SI model development. The relative merits and the pitfalls of a number of mathematical techniques, including power spectral analysis and digital filtering, are discussed from the standpoint of roughness characterization.

The study is summarized below in further detail.

(1) A properly chosen filter is capable of effectively isolating for further study the roughness in the measured road profile with a given range of wavelengths.[2] By using the filtered output, which is a computed profile containing only the type of roughness isolated by the filter, it is possible to calculate summary measures of the severity of this class of roughness. The following are a few examples of physical effects which are examined through digital filtering in Chapter 3:

---

[2] A sixth-order digitized Butterworth filter was used in this study. The filter and the reasons for its selection are discussed in Appendix 5.

(a) the tendency of the outer wheelpath of the outside lane to deteriorate faster than the inside wheelpath if there is no curb,

(b) the changes in surface roughness after maintenance is performed,

(c) the degree of similarity between the two wheelpaths with respect to roughness of different wavelengths.

(2) While the roughness amplitudes themselves are useful for certain types of analyses such as those discussed above, the interpretation of the importance of the amplitudes is sometimes unclear. This is because of the extreme difficulty of comparing roughness of different wavelengths. The sensation of riding over a 1-inch (2.54-centimeter) rise and fall in the roadway is very different if the bump is 10-feet (3.048-meters)-long than if it is 100-feet (30.48 meters)-long.

(3) Although the SI value is useful, no single number could adequately summarize all the information in the road profile.

(4) One approach to obtaining a more detailed roughness evaluation would be to develop a model which could be used to evaluate the sensitivity of the SI value of a given road to changes in the individual roughness terms. A principal difficulty with this approach is that certain constraints must be imposed in developing the model to insure that the coefficients of the terms are related to the correlations between the terms and PSR. These constraints significantly limit the agreement of the model with the data on which it is based and, thus, also limit the predictive accuracy of the model.

(5) Another approach is to develop, along with an overall model, a separate SI regression model for each type of road roughness which is of interest in itself. In Chapter 3, a set of models for the roughness with 4 to 10, 10 to 25, 25 to 50, and 50 to 100-foot (1.219 to 3.048, 3.048 to 7.620, 7.620 to 15.24, and 15.24 to 30.48-meter) wavelengths is discussed. The use of these models in showing the effects of an overlay on the various types of roughness is demonstrated.

The rationale behind this approach is that the model corresponding to a particular roughness type, say 4 to 10-foot (1.219 to 3.048-meter)-long waves, involves only terms describing that type of roughness[3], and, thus,, the model explains or predicts whatever part of the PSR variation is explainable in terms of the 4 to 10-foot (1.219 to 3.048-meter)-long waves alone.

---

[3] A type variable may also be included to explain whatever visual or auditory differences there may be between the sensations of riding over different types of pavements, such as jointed and continuous concrete pavements.

(6) Another set of models is presented in which distinctions are made between longitudinal and transverse surface irregularities, as well as among effects of different wavelengths. Separate models can be developed for any identifiable set of roughness types for which characterizing measures can be obtained.

(7) The following results were observed from the models describing overall roughness and roughness with the specific wavelength bands listed above.

   (a) For both the concrete and asphalt cases, multiple correlations of .91 were achieved by predicting PSR in terms of all roughness types combined. Thus, a very high proportion of the variation in PSR can be predicted in terms of roughness.

   (b) The characterizing measures of the 4 to 10-foot (1.219 to 3.048-meter)-long waves have almost as much predictive value as all the roughness measures combined. Correlations of .86 were obtained for both types of pavement for the SI models for 4 to 10-foot (1.219 to 3.048-meter) wavelengths.

   (c) The correlations between the roughness measures and PSR decrease steadily as the wavelength increases. The decrease is not drastic, however, since correlations of .75 and .68 for concrete and asphalt pavements, respectively, were obtained for the 50 to 100-foot (15.24 to 30.48-meter) case.

Recommendations

In this section, three important areas are discussed in which the results of this study can be extended or improved.

(1) It would be worthwhile to study the relationship between PSR and roughness with wavelengths less than 4 feet (1.219 meters). While it may be true that, because of the vehicle suspension system, the very short waves are not felt by a passenger, these waves still contribute to road noise.

(2) The single vehicle speed, 50 miles per hour (80.45 kilometers per hour), was used to obtain the PSR data used in this study. The ratings were, therefore, made on a consistent basis so that comparisons can be made among all roads, from farm-to-market roads to interstate highways. The vehicle speed, however, does have an effect on riding quality and would be worth including as an experimental factor in a future study. Appendix 2 includes a discussion of how speed might be treated in such a study.

(3) As discussed in Chapter 4, the correlations among the different types of roughness make it difficult to study the relationships between the individual roughness types and PSR. It might be possible at least partially to overcome this problem by very carefully selecting the sample of pavement sections. Suppose, for

example, that several miles of a roadway were approximately homogeneous with respect to both short and long waves, but that sporadic swelling clay effects caused considerable variation in roughness with wavelengths of 20 to 40 feet (6.096 to 12.19 meters). Then several sections taken from this road could be used to study the isolated effects of this type of roughness.

REFERENCES

1. Anderson, T. W., An Introduction to Multivariate Statistical Methods, John Wiley and Sons, Inc., New York, 1958.

2. Bendat, Julius S. and Allen G. Piersol, Random Data: Analysis and Measurement Procedures, John Wiley and Sons, Inc., New York, 1971.

3. Bergland, G. D., "A Guided Four of the Fast Fourier Transform," IEEE Spectrum, July 1969, pp 41-52.

4. Brickman, Arthur D., James C. Wambold, and John R. Zimmerman, "An Amplitude-Frequency Description of Road Roughness," Highway Research Board Special Report 116, 1971, pp 53-67.

5. Carey, W. N. and P. E. Irick, "The Pavement Serviceability-Performance Concept," Highway Research Board Bulletin 250, 1960, pp 40-58.

6. Dixon, W. J., Editor, Biomedical Computer Programs, University of California Press, 1968.

7. Draper, Norman and Harry Smith, Applied Regression Analysis, John Wiley and Sons, Inc., New York, 1966.

8. Glisson, Tildon H., Charles L. Black, and Andrew P. Sage, "The Digital Computation of Discrete Spectra Using the Fast Fourier Transform," IEEE Transactions on Audio and Electroacoustics, Vol AU-18, No. 3, September 1970, pp 271-287.

9. Goodman, N. R., "Measuring Amplitude and Phase," Journal of the Franklin Institute, Vol 270, No. 6, December 1960, pp 437-450.

10. Hanes, R. M., "Human Sensitivity to Whole-Body Vibrations in Urban Transportation Systems: A Literature Review," APL/JHU-TPR-004, Applied Physics Laboratory, The John Hopkins University, May 1970.

11. Holbrook, L. F. and J. R. Darlington, "Analytical Problems Encountered in the Correlation of Subjective Response and Pavement Power Spectral Density Functions," Highway Research Record No. 471, 1973 pp 83-90.

12. Hudson, W. Ronald, "High-Speed Profile Equipment Evaluation," Research Report 73-1, Center for Highway Research, The University of Texas at Austin, Austin, Texas, January 1966.

13. Jenkins, Gwilyn M. and Donald G. Watts, Spectral Analysis and Its Applications, Holder-Day, 1968.

14. Morrison, Donald F., Multivariate Statistical Methods, McGraw-Hill Book Company, New York, 1967.

15. Rader, Charles M. and Bernard Gold, "Digital Filter Design Techniques in the Frequency Domain," Proceedings of the IEEE, Vol 55, No. 2, February 1967, pp 149-171.

16. Roberts, Freddy L. and W. Ronald Hudson, "Pavement Serviceability Equations Using the Surface Dynamics Profilometer," Research Report 73-3, Center for Highway Research, The University of Texas at Austin, April 1970.

17. Shanks, John L., "Recursion Filters for Digital Processing," Geophysics, Vol XXXII, No. 1, February 1967, pp 33-51.

18. Walker, Roger S., W. Ronald Hudson, and Freddy L. Roberts, "Development of a System for High-Speed Measurement of Pavement," Research Report 73-5F, Center for Highway Research, The University of Texas at Austin, May 1971.

19. Walker, Roger S. and W. Ronald Hudson, "Use of Profile Wave Amplitude Estimates for Pavement Serviceability Measures," Highway Research Record No. 471, 1973, pp 110-117.

20. Walker, Roger S. and W. Ronald Hudson, "A Correlation Study of the Mays Road Meter with the Surface Dynamics Profilometer," Research Report 156-1, Center for Highway Research, The Univeristy of Texas at Austin, February 1973.

21. Walker, Roger S. and W. Ronald Hudson, "The Use of Spectral Estimates for Pavement Characterization," Research Report 156-2, Center for Highway Research, The University of Texas at Austin, August 1973.

22. Walker, Roger S., Freddy L. Roberts, and W. Ronald Hudson, "A Profile Measuring, Recording, and Processing System," Research Report 73-2, Center for Highway Research, The University of Texas at Austin, April 1970.

APPENDIX 1

SI REGRESSION MODELS

APPENDIX 1. SI REGRESSION MODELS

The coefficients and certain other information regarding the SI regression models developed in this study are presented in Tables A1.1 through A1.10. A condensed notation is used to denote the roughness measures. The symbol

AB C

indicates a specific roughness term, as defined below:

A = { L longitudinal roughness; D transverse roughness

B = { 1 4 to 10-foot (1.219 to 3.048-meter) wavelengths; 2 10 to 25-foot (3.048 to 7.620-meter) wavelengths; 3 25 to 50-foot (7.620 to 15.24-meter) wavelengths; 4 50 to 100-foot (15.24 to 30.48-meter) wavelengths

C = { 50 50th percentile roughness measure; 90 90th percentile roughness measure.

The roughness terms are discussed in Chapter 2 and briefly in Appendix 4.

All of the models presented in this appendix are linear except the one for 25 to 50-foot (7.620 to 15.24-meter) wavelengths for asphalt pavements. In this case, a model involving one second degree term is very similar to, but trivially better than, the best linear model, which is also given. (See Table A1.1) A study of the predictive value of all second-degree terms involving the fiftieth percentile longitudinal amplitudes indicated that inclusion of the second degree terms did not improve the prediction except in the case mentioned above. This study involved the models presented in Tables A1.1 and A1.2.

TABLE A1.1. SI MODELS FOR ASPHALT PAVEMENTS

Model for Wavelengths (feet)	Correlation Coefficient	Standard Error	Constant	Variable	Coefficient
Overall SI	.91	.38	4.85	L1 50	110.325
				L1 90	-23.281
				L2 90	-23.460
				D1 50	-108.544
				D1 90	21.210
				D2 50	12.012
				D4 50	-3.256
4 to 10	.86	.45	4.71	L1 50	144.063
				L1 90	-74.001
				D1 50	-112.809
				D1 90	25.508
				ST	.196
10 to 25	.82	.49	4.70	L2 50	32.926
				L2 90	-37.782
				D2 50	-43.899
				D2 90	16.449
25 to 50	.81	.52	4.27	L3 50	13.179
				L3 90	-15.301
				D3 50	-24.327
				D3 90	11.428
				ST	-.388

(Continued)

TABLE A1.1. (Continued)

Model for Wavelength (feet)	Correlation Coefficient	Standard Error	Constant	Variable	Coefficient
25 to 50 (non-linear model)	.81	.51	4.57	$(L3\ 50)^2$	85.188
				L3 90	-14.306
				D3 50	-24.872
				D3 90	11.360
				ST	-.396
50 to 100	.68	.61	4.20	D4 50	-9.665

NOTE: 1 foot = .3048 meters

TABLE A1.2. SI MODELS FOR CONCRETE PAVEMENTS

Model for Wavelengths (feet)	Correlation Coefficient	Standard Error	Constant	Variable	Coefficient
Overall SI	.91	.32	4.91	L1 50	-41.862
				L2 50	-23.130
				L4 50	-2.511
				D1 90	15.720
				CRCP	.460
4 to 10	.86	.37	4.57	L1 50	-76.223
				L1 90	-13.894
				D1 90	22.431
				CRCP	.595
10 to 25	.85	.38	4.52	L2 50	-35.229
				D2 90	6.549
				CRCP	.501
25 to 50	.85	.38	4.52	L3 50	-14.065
				D3 90	2.866
				CRCP	.696
50 to 100	.75	.46	3.92	L4 50	-4.918
				CRCP	.828

NOTE: 1 foot = .3048 meters

TABLE A1.3. SI MODELS FOR ASPHALT PAVEMENTS - LONGITUDINAL - WITH DUMMY TERM

Model for Wavelengths (feet)	Correlation Coefficient	Standard Error	Constant	Variable	Coefficient
4 to 10	.65	.64	4.38	L1 90	-31.235
10 to 25	.74	.57	4.52	L2 50	-40.318
				ST	-0.301
25 to 50	.74	.57	4.18	L3 90	-8.415
				ST	-0.338
50 to 100	.63	.66	4.12	L4 50	-6.995
				ST	-0.294

NOTE: 1 foot = .3048 meters

TABLE A1.4. SI MODELS FOR ASPHALT PAVEMENTS - TRANSVERSE - WITH DUMMY TERM

Model for Wavelengths (feet)	Correlation Coefficient	Standard Error	Constant	Variable	Coefficient
4 to 10	.75	.56	5.13	D1 50	-99.035
				D1 90	-13.535
10 to 25	.75	.57	4.49	D2 50	-53.578
				D2 90	10.654
				ST	-0.260
25 to 50	.74	.57	4.06	D3 50	-12.928
				ST	-0.389
50 to 100	.68	.61	4.20	D4 50	-9.665

NOTE: 1 foot = .3048 meters

TABLE A1.5. SI MODELS FOR ASPHALT PAVEMENTS - LONGITUDINAL - WITHOUT DUMMY TERM

Model for Wavelength (feet)	Correlation Coefficient	Standard Error	Constant	Variable	Coefficient
4 to 10	.65	.64	4.38	L1 90	-31.235
10 to 25	.72	.58	4.49	L2 50	-42.528
25 to 50	.71	.59	4.13	L3 90	-8.872
50 to 100	.61	.67	4.09	L4 50	-7.564

NOTE: 1 foot = .3048 meters

TABLE A1.6. SI MODELS FOR ASPHALT PAVEMENTS - TRANSVERSE - WITHOUT DUMMY TERM

Model for Wavelength (feet)	Correlation Coefficient	Standard Error	Constant	Variable	Coefficient
4 to 10	.75	.56	5.13	D1 50	-99.035
				D1 90	13.535
10 to 25	.73	.58	4.47	D2 50	-57.523
				D2 90	11.780
25 to 50	.71	.59	3.98	D3 50	-13.564
50 to 100	.68	.61	4.20	D4 50	-9.665

NOTE: 1 foot = .3048 meters

TABLE A1.7. SI MODELS FOR CONCRETE PAVEMENTS - LONGITUDINAL - WITH DUMMY TERM

Model for Wavelengths (feet)	Correlation Coefficient	Standard Error	Constant	Variable	Coefficient
4 to 10	.70	.50	3.95	L1 50	-23.323
				CRCP	0.671
10 to 25	.79	.44	4.36	L2 50	-43.523
				L2 90	13.785
				CRCP	0.530
25 to 50	.77	.46	4.01	L3 50	-20.492
				L3 90	6.094
				CRCP	0.707
50 to 100	.75	.46	3.92	L4 50	-4.918
				CRCP	0.828

NOTE: 1 foot = .3048 meters

TABLE A1.8. SI MODELS FOR CONCRETE PAVEMENTS - TRANSVERSE - WITH DUMMY TERM

Model for Wavelengths (feet)	Correlation Coefficient	Standard Error	Constant	Variable	Coefficient
4 to 10	.82	.41	4.64	D1 50	-96.490
				D1 90	26.056
				CRCP	0.505
10 to 25	.64	.53	3.40	CRCP	0.851
25 to 50	.64	.53	3.40	CRCP	0.851
50 to 100	.70	.50	3.80	D4 50	-5.164
				CRCP	0.769

NOTE: 1 foot = .3048 meters

TABLE A1.9. SI MODELS FOR CONCRETE PAVEMENTS - LONGITUDINAL - WITHOUT DUMMY TERM

Model for Wavelengths (feet)	Correlation Coefficient	Standard Error	Constant	Variable	Coefficient
4 to 10	.53	.58	4.55	L1 50	-39.216
10 to 25	.71	.49	4.90	L2 50	-51.142
				L2 90	-13.631
25 to 50	.57	.56	4.65	L3 50	-14.804
50 to 100	.56	.58	4.63	L4 50	-22.091
				L4 90	7.922

NOTE: 1 foot = .3048 meters.

TABLE A1.10. SI MODELS FOR CONCRETE PAVEMENTS - TRANSVERSE - WITHOUT DUMMY TERM

Model for Wavelengths (feet)	Correlation Coefficient	Standard Error	Constant	Variable	Coefficient
4 to 10	.75	.46	5.21	D1 50	-122.483
				D1 90	31.526
10 to 25	.63	.55	4.47	D2 50	-47.454
				D2 90	16.595
25 to 50	.59	.57	4.42	D3 50	-46.514
				D3 90	17.399
50 to 100	.42	.62	4.26	D4 50	-7.268

NOTE: 1 foot = .3048 meters

Numerous plots were made of the regression residuals, $Y_i - \hat{Y}_i$, where Y_i is the ith PSR value in the sample and $\hat{Y}_i$ is the corresponding SI, or PSR estimate, versus a number of roughness measures. The plots indicated that there is no remaining nonlinear trend after the linear prediction is made; in other words, the plots also indicate that the inclusion of nonlinear terms is unnecessary.

The possibility of including in the regression analysis the ninety-fifth and ninety-ninth percentile points in addition to the fiftieth and ninetieth percentile points was excluded on the basis of preliminary analysis. The ninety-fifth percentile points are very highly correlated with the ninetieth percentile points and are slightly lower in correlation with PSR than the ninetieth percentile points are. The ninety-ninth percentile points are correlated with the ninetieth percentile points and are considerably lower in correlation with PSR.

APPENDIX 2

COMMENTS ON A POSSIBLE FUTURE STUDY OF THE RELATIONSHIP BETWEEN PSR AND VEHICLE SPEED

APPENDIX 2. COMMENTS ON A POSSIBLE FUTURE STUDY OF THE RELATIONSHIP BETWEEN PSR AND VEHICLE SPEED

The PSR data used in this report are from a study performed in 1968 (Ref 16). The speed 50 miles per hour (m.p.h.) (80.45 kilometers per hour [km./hr.]) was used for all ratings. Since the speed limit on highways was generally 70 m.p.h. (112.6 km./hr.) in 1968, 50 m.p.h. (80.45 km./hr.) was midway between the highway speed limit and the speed limit of 30 m.p.h. (48.27 km./hr.) on most city streets. The ratings were based not only on the ride, but the raters were also allowed to walk over the road sections and inspect them. Thus, PSR was defined as a common measure of the quality of all roads, regardless of the speed limit. For this purpose the rating speed of 50 m.p.h. (80.45 km./hr.) was reasonable.

In this appendix, a possible future study of human ratings at different speeds is discussed. The objective is <u>not</u> to give a prescription for the execution of such a study, since many of the details, such as the specific sections to be included, are best determined at the time of the study. Instead, certain principles are covered, including applicable statistical approaches and methods for removing bias.

It has been convenient to refer to amplitudes of roughness waves by wavelength in feet (and meters). It does not matter whether wavelength or frequency is the independent variable for the roughness amplitudes.

In a multi-speed study, however, it is suggested that, for the purposes of model-building or any type of comparison among effects at different speeds, frequency in cycles per second (c.p.s.) (as opposed to cycles per unit distance along the roadway) be used.

The rapidity with which the surface irregularities are encountered is closely related to the consequent amount of discomfort experienced. Moreover, the effects at different speeds of the car's suspension system are more nearly constant with frequency in c.p.s. than with frequency in cycles per foot. If frequency in cycles per foot were used as the basis for comparison, differential effects of the suspension system would be confounded with differential effects of vehicle speed.

Wavelength in seconds per cycle would, of course, be equally acceptable to frequency in c.p.s. as an independent variable.

It would be desirable to develop a model of the form

$$SI = f(A\omega_1, \ldots A\omega_n)$$

where $A\omega_i$ is the roughness amplitude corresponding to frequency ω_i in c.p.s. Then this model could be used to calculate SI for <u>any</u> vehicle speed.

It must be realized, however, that PSR may vary with speed due to visual or other psychological effects which are unrelated to roughness. If so, the model as formulated above would not be valid. The addition of one or more terms involving speed to the model would very likely solve the problem, however.

In an ideal experiment to test the effects of speed alone, one would want to obtain PSR values at a set of vehicle speeds while holding all other variables constant. This experiment would show whether a generalized SI model could be developed in terms of the $A\omega_i$ alone or, if not, what terms involving speed were required. It is known, however, that roughness amplitudes generally increase sharply with wavelength; thus, the amplitudes of the vertical deflections for a given frequency in c.p.s. felt by a road user sharply increase as the vehicle speed increases.

Typical power values for roads with PSR values of 2.0 to 2.5 and 4.0 to 4.5 are presented in Ref 21. Values are given, for example, for .081 and .046 cycles per foot (2.6 and 1.5 cycles per meter), both of which correspond to 3.36 c.p.s. at, respectively, 28.4 and 50 m.p.h. (45.70 and 80.45 km./hr.). Table A2.1 illustrates the effect of increasing amplitude trends with wavelength.

The power values are simply roughness amplitudes squared and divided by a constant (the bandwidth of the Fourier transform). The point is that the amplitudes corresponding to 3.36 c.p.s. are considerably higher if the vehicle speed is 50 m.p.h. (80.45 km./hr.) than if the speed is 28.4 m.p.h. (45.70 km./hr.). Note, however, that there is an overlap; that is, the lowest-quality roads have power values at 28.4 m.p.h. (45.70 km./hr) comparable to the powers for the best roads at 50 m.p.h. (80.45 km./hr.).

TABLE A2.1. EFFECT OF VEHICLE SPEED ON TIME-BASED POWER SPECTRUM

For 28.4 m.p.h.		For 50 m.p.h.	
PSR	Power	PSR	Power
2.0-2.5	.0180	2.0-2.5	.0307
4.0-4.5	.0025	4.0-4.5	.0076

Power units: $(\text{inches})^2$/cycle per foot

NOTE: 1 inch = 2.540 centimeters
1 foot = .3048 meters
1 m.p.h. = .6211 km./hr.

By the argument given above, the vehicle speed and the roughness amplitude corresponding to a given frequency are correlated; the correlation between speed and PSR, therefore, yields limited information about the effects of speed alone.

It is possible to develop a regression model from a sample in which the independent variables are highly correlated. Although the results may yield no information about the relationships between the dependent variable and the individual predictor variables, the model may be perfectly valid for predictive purposes. Nevertheless, in this case, it is possible to isolate the effect of speed on PSR; a method for accomplishing this is discussed in the following paragraph.

Although the amplitudes in the sample for a given frequency would generally increase with vehicle speed, if the speeds were, say, 30, 40, and 55 m.p.h. (48.27, 63.36, and 88.50 km./hr.), one would expect that there would be an overlap among the amplitudes for 30 and 40 m.p.h. (48.27 and 63.36 km./hr.) and among the amplitudes for 40 and 55 m.p.h. (63.36 and 88.50 km./hr.). There would probably be some overlap among the amplitudes for 30 and 55 m.p.h. (48.27 and 88.50 km./hr.). Then if models were developed to predict PSR separately for each speed, the predictions could be compared for different speeds but for the same vector of amplitudes. These comparisons would be most meaningful in the ranges of amplitude overlap, since neither of the two models being compared would be evaluated outside the range of values of the sample from which it was developed.

Now that the basic objectives have been presented, we shall discuss the design of an experiment to collect the data necessary for the empirical model development.

A reasonable number and range in quality of each of the following major pavement types should be represented: hot-mix asphalt-concrete, surface-treated, continuously reinforced concrete, and jointed reinforced concrete should be included. It is suggested that about fifteen of each type be included and that separate models be developed for concrete and for asphalt pavements.

It is known from the literature (Ref 5 and 16) that the standard deviation of a PSR rating by a randomly chosen individual is .4 to .5. Then if four panels of four people each were used, and if each panel rated each section, the average of all 16 ratings would have a standard deviation of .1

to .125. Since this is in the range of the replication accuracy of the G.M. Profilometer, and since .125 is only 2.5 percent of the 0 to 5 range for PSR, it is felt that .1 to .125 is acceptable accuracy for the panel mean PSR ratings.

Some caution must be exercised to insure that extraneous factors do not bias the results. The following are possible sources of spurious variations:

(1) miscellaneous factors, such as the weather, surrounding scenery, and personal discomfort of the raters due to headaches or other causes, and

(2) order of running the sections.

The set of factors listed under (1) are largely uncontrollable as far as experimental design is concerned. The raters can be instructed to ignore these effects, however, and questions can be included on the rating forms to obtain parallel evaluations of PSR and of the most likely causes of bias. Then if, for example, it were discovered that there was a high correlation between PSR and the pleasantness of the weather, then the "effect" of weather could be removed. This would be achieved by (1) estimating the trend of PSR with weather by regression analysis and then (2) simply adjusting the PSR data so that PSR and weather became uncorrelated.

The order of running the sections is the second major possible source of bias. If a given section were always rated immediately after a very high-quality interstate highway, then the section might be rated lower than a comparable section which was always rated after a rough farm-to-market road. While it might be argued that this effect would "average out" to a reasonable extent if a large number of test sections were included, further protection would be achieved if half the ratings were made by running the sections in one order and the other half in another order.

There are numerous ways in which the vehicle speed factor could be handled. Assuming that three speeds of, say, 30, 40, and 55 m.p.h. (48.27, 63.36, and 88.50 km./hr.) are included, it is suggested that consideration be given to having each panel rate each section at the three speeds in consecutive runs. If this were done, it is unquestionable that the ratings would be interdependent, but this is not necessarily bad. Since the raters would consciously compare the quality of the consecutive rides over a given section, a highly accurate estimate of PSR <u>differences</u> with vehicle speed

would be obtained. Furthermore, such factors as weather, time of day, and traffic volume would be held as nearly constant as possible for the three runs.

APPENDIX 3

ROUGHNESS DATA USED AS PREDICTOR VARIABLES IN THIS STUDY

APPENDIX 3. ROUGHNESS DATA USED AS PREDICTOR VARIABLES IN THIS STUDY

In Tables A3.1 and A3.2 of this appendix, the roughness measures used in the development of the SI regression models are presented. The terms in the tables are defined as follows:

TYPE - type of pavement.

JRCP - jointed, reinforced concrete pavement.

CRCP - continuously reinforced concrete pavement.

ST - surface-treated pavement.

HMAC - hot-mix asphalt-concrete pavement.

OVLY - overlaid pavement.

PASSBAND - range of wavelengths of the roughness whose amplitudes are being examined.

LONGITUDINAL - roughness measured down the length of the road.

TRANSVERSE - roughness corresponding to road surface changes of one wheelpath relative to the other. The wavelengths are measured along the length of the road, as are the wavelengths of the longitudinal roughness.

PERCENTILES - percentage levels in the roughness amplitude distributions. The value greater than exactly 50 percent of the local roughness amplitudes is an average or overall roughness measure; the value greater than exactly 90 percent of the local amplitudes characterizes the most severe roughness in a given road section.

Eighty-six road sections were used to develop the SI model discussed in Ref 21. The PSR values of 81 of the sections are given in Ref 16, which reports an earlier study employing essentially the same data. Of the 81 listed, two were excluded for reasons given in Appendix A, Ref 16. Of the 79 remaining, six were excluded from this study because of unbelieveable effects seen in the road profile plots, such as violent noise spikes and apparent losses of the vertical reference level resulting in discontinuities in the measured profiles. One other, section number 45, was excluded because

the very large roughness measures which were computed are inconsistent both with the PSR value of 4.02 and with the roughness measures - slope variance and Mays Meter roughness index (Ref 20) - given in Ref 16, Appendix A.

TABLE A3.1. 50th AND 90th PERCENTILE ROAD SURFACE ROUGHNESS AMPLITUDES FOR CONCRETE PAVEMENTS (inches).

SECTION	TYPE	PASSBAND (FT.)	PERCENTILES LONGITUDINAL 50TH	LONGITUDINAL 90TH	TRANSVERSE 50TH	TRANSVERSE 90TH	PSR
3	JRCP	4.0 TO 10.0	.01032	.01978	.01456	.02581	3.76
		10.0 TO 25.0	.02070	.03675	.02959	.04204	
		25.0 TO 50.0	.02813	.08155	.02763	.06475	
		50.0 TO 100.0	.06789	.10372	.04620	.06550	
20	JRCP	4.0 TO 10.0	.01311	.02173	.01554	.02358	3.77
		10.0 TO 25.0	.03225	.05235	.03162	.04635	
		25.0 TO 50.0	.04570	.08457	.04787	.07773	
		50.0 TO 100.0	.06992	.16540	.06398	.09024	
27	JRCP	4.0 TO 10.0	.02390	.03988	.02374	.03976	2.81
		10.0 TO 25.0	.05600	.08922	.03874	.05713	
		25.0 TO 50.0	.04388	.09086	.03862	.07472	
		50.0 TO 100.0	.11210	.16807	.08587	.10619	
31	JRCP	4.0 TO 10.0	.02690	.04273	.02765	.04637	2.26
		10.0 TO 25.0	.06503	.09210	.05386	.08169	
		25.0 TO 50.0	.10236	.15660	.05940	.08821	
		50.0 TO 100.0	.10483	.16772	.08539	.12117	
33	JRCP	4.0 TO 10.0	.03030	.05550	.03769	.05860	2.62
		10.0 TO 25.0	.06502	.09811	.05750	.09022	
		25.0 TO 50.0	.06123	.11681	.06964	.10242	
		50.0 TO 100.0	.10367	.15057	.05945	.08349	
48	JRCP	4.0 TO 10.0	.01308	.02192	.01599	.02490	4.35
		10.0 TO 25.0	.02428	.04038	.02338	.04433	
		25.0 TO 50.0	.04387	.07580	.04239	.05600	
		50.0 TO 100.0	.10340	.15944	.07603	.12476	

(Continued)

TABLE A3.1. (Continued)

SECTION	TYPE	PASSBAND (FT.)	PERCENTILES LONGITUDINAL 50TH	LONGITUDINAL 90TH	TRANSVERSE 50TH	TRANSVERSE 90TH	PSR
65	CRCP	4.0 TO 10.0	.01081	.01610	.01107	.01632	4.42
		10.0 TO 25.0	.01531	.02304	.01375	.02203	
		25.0 TO 50.0	.02413	.03970	.01604	.02791	
		50.0 TO 100.0	.05990	.07665	.03066	.05081	
67	JRCP	4.0 TO 10.0	.02143	.03362	.02437	.03942	3.28
		10.0 TO 25.0	.04352	.07391	.04767	.07043	
		25.0 TO 50.0	.06494	.12169	.04079	.07194	
		50.0 TO 100.0	.07801	.11307	.05728	.08337	
68	JRCP	4.0 TO 10.0	.02403	.03930	.02552	.03991	3.15
		10.0 TO 25.0	.03616	.07143	.03814	.05797	
		25.0 TO 50.0	.10257	.15845	.03862	.06509	
		50.0 TO 100.0	.17567	.26358	.08297	.14339	
69	CRCP	4.0 TO 10.0	.02148	.07140	.02265	.03628	3.37
		10.0 TO 25.0	.03956	.08597	.02942	.04607	
		25.0 TO 50.0	.07714	.15327	.04413	.08424	
		50.0 TO 100.0	.29990	.63672	.16525	.31330	
76	CRCP	4.0 TO 10.0	.01280	.02018	.01459	.02277	4.36
		10.0 TO 25.0	.03468	.04822	.02714	.04841	
		25.0 TO 50.0	.04078	.07337	.04414	.07231	
		50.0 TO 100.0	.10318	.18813	.06652	.12097	
77	CRCP	4.0 TO 10.0	.01608	.02659	.02139	.03172	4.35
		10.0 TO 25.0	.03196	.04779	.03245	.04553	
		25.0 TO 50.0	.06607	.10412	.04623	.07779	
		50.0 TO 100.0	.06673	.11508	.03891	.06051	

(Continued)

TABLE A3.1. (Continued)

SECTION	TYPE	PASSBAND (FT.)	PERCENTILES LONGITUDINAL 50TH	LONGITUDINAL 90TH	TRANSVERSE 50TH	TRANSVERSE 90TH	PSR
78	CRCP	4.0 TO 10.0	.01771	.03045	.02232	.03811	3.66
		10.0 TO 25.0	.04129	.06609	.03419	.05563	
		25.0 TO 50.0	.09037	.15436	.06395	.11449	
		50.0 TO 100.0	.12702	.23678	.09019	.13790	
79	CRCP	4.0 TO 10.0	.00990	.01692	.01111	.01945	4.45
		10.0 TO 25.0	.02160	.03724	.01561	.03345	
		25.0 TO 50.0	.04104	.06605	.02222	.04112	
		50.0 TO 100.0	.07545	.16862	.04116	.08277	
80	CRCP	4.0 TO 10.0	.00839	.01432	.00801	.01315	4.63
		10.0 TO 25.0	.01937	.02698	.01425	.02210	
		25.0 TO 50.0	.03256	.06539	.01655	.03728	
		50.0 TO 100.0	.06396	.09369	.03058	.05024	
91	JRCP	4.0 TO 10.0	.02204	.03821	.02643	.04854	3.40
		10.0 TO 25.0	.05383	.08780	.04551	.07182	
		25.0 TO 50.0	.06504	.11059	.05104	.09318	
		50.0 TO 100.0	.11613	.18734	.06442	.11459	
92	JRCP	4.0 TO 10.0	.04053	.06947	.04898	.13256	3.48
		10.0 TO 25.0	.05812	.11370	.08901	.23065	
		25.0 TO 50.0	.07846	.15995	.11191	.24392	
		50.0 TO 100.0	.11465	.17339	.11273	.24221	
98	CRCP	4.0 TO 10.0	.03147	.05888	.03504	.08958	4.37
		10.0 TO 25.0	.04602	.07794	.04509	.12479	
		25.0 TO 50.0	.04966	.09873	.05164	.13797	
		50.0 TO 100.0	.06387	.08603	.06196	.09538	

(Continued)

TABLE A3.1. (Continued)

SECTION	TYPE	PASSBAND (FT.)	PERCENTILES LONGITUDINAL 50TH	LONGITUDINAL 90TH	TRANSVERSE 50TH	TRANSVERSE 90TH	PSR
99	JRCP	4.0 TO 10.0	.03835	.10231	.05138	.16090	3.80
		10.0 TO 25.0	.07960	.16431	.12004	.23357	
		25.0 TO 50.0	.11061	.27145	.11986	.26635	
		50.0 TO 100.0	.12941	.28870	.16549	.22846	
102	JRCP	4.0 TO 10.0	.02494	.04135	.02788	.04066	3.72
		10.0 TO 25.0	.05285	.08221	.04990	.06871	
		25.0 TO 50.0	.08392	.13429	.06510	.11097	
		50.0 TO 100.0	.10938	.15016	.05723	.12159	
107	JRCP	4.0 TO 10.0	.01781	.02659	.01809	.02710	3.85
		10.0 TO 25.0	.03563	.06285	.02656	.04207	
		25.0 TO 50.0	.05445	.12451	.02903	.05278	
		50.0 TO 100.0	.07992	.13136	.03633	.05635	
113	CRCP	4.0 TO 10.0	.01417	.02379	.01581	.02463	4.68
		10.0 TO 25.0	.02516	.03994	.01767	.02803	
		25.0 TO 50.0	.02700	.07391	.01572	.03385	
		50.0 TO 100.0	.04284	.06186	.01968	.03524	

NOTE: 1 foot = .3048 meters
1 inch = 2.540 centimeters

TABLE A3.2. 50th AND 90th PERCENTILE ROAD SURFACE ROUGHNESS AMPLITUDES FOR ASPHALT PAVEMENTS (inches).

SECTION	TYPE	PASSBAND (FT.)	PERCENTILES LONGITUDINAL 50TH	LONGITUDINAL 90TH	TRANSVERSE 50TH	TRANSVERSE 90TH	PSR
1	HMAC	4.0 TO 10.0	.00932	.01489	.01331	.02200	4.30
		10.0 TO 25.0	.01044	.01808	.01357	.02245	
		25.0 TO 50.0	.01981	.03051	.02252	.04227	
		50.0 TO 100.0	.05560	.08990	.04951	.07496	
2	HMAC	4.0 TO 10.0	.02197	.03584	.02637	.04221	3.21
		10.0 TO 25.0	.02996	.04790	.02739	.04672	
		25.0 TO 50.0	.03272	.06526	.02359	.06008	
		50.0 TO 100.0	.04502	.09213	.05752	.10139	
4	HMAC	4.0 TO 10.0	.00997	.01486	.01314	.02104	3.98
		10.0 TO 25.0	.01188	.01951	.01346	.02121	
		25.0 TO 50.0	.01590	.02628	.01959	.03305	
		50.0 TO 100.0	.05529	.07162	.04207	.05733	
5	ST	4.0 TO 10.0	.02384	.05027	.03501	.05961	2.08
		10.0 TO 25.0	.02859	.06093	.03937	.06555	
		25.0 TO 50.0	.02777	.06114	.04166	.06325	
		50.0 TO 100.0	.05087	.06887	.05606	.07734	
6	HMAC	4.0 TO 10.0	.01239	.02278	.01931	.03047	3.35
		10.0 TO 25.0	.01948	.04039	.02424	.03968	
		25.0 TO 50.0	.02955	.04630	.02591	.04929	
		50.0 TO 100.0	.06396	.13678	.05346	.08066	
11	OVLY	4.0 TO 10.0	.01543	.02372	.02356	.03716	3.28
		10.0 TO 25.0	.01979	.03937	.02764	.04962	
		25.0 TO 50.0	.02133	.03591	.02573	.03701	
		50.0 TO 100.0	.04848	.07667	.05510	.09474	

(Continued)

TABLE A3.2. (Continued)

SECTION	TYPE	PASSBAND (FT.)	PERCENTILES LONGITUDINAL 50TH	LONGITUDINAL 90TH	TRANSVERSE 50TH	TRANSVERSE 90TH	PSR
15	ST	4.0 TO 10.0	.02075	.03395	.03253	.05181	3.11
		10.0 TO 25.0	.03221	.05485	.05243	.08907	
		25.0 TO 50.0	.06932	.14992	.08799	.21760	
		50.0 TO 100.0	.15534	.27217	.16372	.37224	
17	OVLY	4.0 TO 10.0	.02035	.03152	.03139	.04679	3.83
		10.0 TO 25.0	.02958	.04571	.04099	.06260	
		25.0 TO 50.0	.03743	.07321	.03550	.08666	
		50.0 TO 100.0	.05173	.09648	.05227	.10757	
18	OVLY	4.0 TO 10.0	.01510	.02133	.02259	.03170	4.34
		10.0 TO 25.0	.01703	.02961	.01922	.02763	
		25.0 TO 50.0	.02420	.04692	.02022	.03219	
		50.0 TO 100.0	.03700	.05341	.03273	.05935	
24	ST	4.0 TO 10.0	.01889	.03153	.02556	.03972	3.29
		10.0 TO 25.0	.02434	.04178	.02774	.06234	
		25.0 TO 50.0	.02417	.03915	.02679	.04344	
		50.0 TO 100.0	.07570	.15038	.09166	.12828	
25	HMAC	4.0 TO 10.0	.01517	.02254	.02281	.03480	3.96
		10.0 TO 25.0	.02069	.03037	.03598	.05369	
		25.0 TO 50.0	.02361	.05031	.02269	.03139	
		50.0 TO 100.0	.04092	.06536	.04289	.07914	
28	ST	4.0 TO 10.0	.01811	.02849	.02250	.03471	3.89
		10.0 TO 25.0	.01639	.02751	.02316	.03860	
		25.0 TO 50.0	.01834	.02873	.02283	.03529	
		50.0 TO 100.0	.07127	.10207	.07621	.10401	

(Continued)

TABLE A3.2. (Continued)

SECTION	TYPE	PASSBAND (FT.)	PERCENTILES LONGITUDINAL 50TH	LONGITUDINAL 90TH	TRANSVERSE 50TH	TRANSVERSE 90TH	PSR
30	ST	4.0 TO 10.0	.01941	.04559	.03075	.06561	2.43
		10.0 TO 25.0	.02921	.07045	.04407	.10930	
		25.0 TO 50.0	.06519	.11926	.08329	.15324	
		50.0 TO 100.0	.11416	.18069	.16916	.27363	
32	HMAC	4.0 TO 10.0	.00793	.01322	.01122	.01709	4.07
		10.0 TO 25.0	.00913	.01443	.01300	.02012	
		25.0 TO 50.0	.01892	.03220	.01775	.03114	
		50.0 TO 100.0	.04015	.06610	.04763	.07871	
34	HMAC	4.0 TO 10.0	.00964	.02136	.01190	.01922	4.40
		10.0 TO 25.0	.01034	.01867	.01098	.02096	
		25.0 TO 50.0	.01881	.03114	.01992	.03460	
		50.0 TO 100.0	.05631	.13429	.05344	.07807	
35	HMAC	4.0 TO 10.0	.01290	.02314	.01873	.03096	2.86
		10.0 TO 25.0	.01893	.04677	.02662	.06499	
		25.0 TO 50.0	.04308	.08521	.04543	.06709	
		50.0 TO 100.0	.07008	.18653	.07645	.18341	
36	ST	4.0 TO 10.0	.03361	.07231	.05052	.10125	1.10
		10.0 TO 25.0	.07146	.13182	.09086	.20270	
		25.0 TO 50.0	.13422	.31090	.20644	.46977	
		50.0 TO 100.0	.17388	.26601	.19015	.33663	
37	OVLY	4.0 TO 10.0	.02483	.03928	.03419	.05353	3.37
		10.0 TO 25.0	.03606	.05947	.05142	.08117	
		25.0 TO 50.0	.04179	.08116	.06596	.10010	
		50.0 TO 100.0	.05991	.12099	.08206	.15340	

(Continued)

TABLE A3.2. (Continued)

SECTION	TYPE	PASSBAND (FT.)	PERCENTILES LONGITUDINAL 50TH	LONGITUDINAL 90TH	TRANSVERSE 50TH	TRANSVERSE 90TH	PSR
38	HMAC	4.0 TO 10.0	.02285	.04781	.02705	.06386	2.14
		10.0 TO 25.0	.03733	.08454	.04354	.12339	
		25.0 TO 50.0	.05114	.11566	.07274	.16475	
		50.0 TO 100.0	.20185	.44451	.21194	.50673	
39	OVLY	4.0 TO 10.0	.02765	.04657	.04432	.07208	1.75
		10.0 TO 25.0	.04815	.08239	.07368	.14677	
		25.0 TO 50.0	.09578	.15924	.12237	.19013	
		50.0 TO 100.0	.15297	.23402	.11604	.16052	
40	HMAC	4.0 TO 10.0	.02549	.05077	.03378	.06585	2.11
		10.0 TO 25.0	.04288	.08162	.05064	.10443	
		25.0 TO 50.0	.09005	.16944	.08949	.16408	
		50.0 TO 100.0	.28352	.42670	.14509	.33271	
44	ST	4.0 TO 10.0	.02060	.03498	.02712	.04618	3.20
		10.0 TO 25.0	.02472	.04186	.03786	.05988	
		25.0 TO 50.0	.02893	.06820	.04463	.08987	
		50.0 TO 100.0	.10333	.19852	.08720	.12849	
46	HMAC	4.0 TO 10.0	.01264	.02144	.01706	.02768	3.63
		10.0 TO 25.0	.01614	.03849	.01828	.03798	
		25.0 TO 50.0	.02862	.07266	.02900	.07633	
		50.0 TO 100.0	.09065	.18689	.05725	.09779	
49	OVLY	4.0 TO 10.0	.01395	.02062	.02104	.03415	4.23
		10.0 TO 25.0	.01528	.02564	.02075	.02838	
		25.0 TO 50.0	.02948	.05586	.02628	.03710	
		50.0 TO 100.0	.06872	.11063	.08720	.12361	

(Continued)

TABLE A3.2. (Continued)

SECTION	TYPE	PASSBAND (FT.)	PERCENTILES LONGITUDINAL 50TH	LONGITUDINAL 90TH	TRANSVERSE 50TH	TRANSVERSE 90TH	PSR
64	OVLY	4.0 TO 10.0	.01603	.02506	.02159	.03314	3.70
		10.0 TO 25.0	.02121	.03246	.02705	.03923	
		25.0 TO 50.0	.04600	.07848	.04216	.07053	
		50.0 TO 100.0	.13396	.20288	.08458	.14656	
66	HMAC	4.0 TO 10.0	.01309	.02240	.01576	.02425	3.35
		10.0 TO 25.0	.02447	.06176	.02470	.06350	
		25.0 TO 50.0	.06103	.18747	.03424	.17608	
		50.0 TO 100.0	.11088	.47753	.12582	.32618	
70	OVLY	4.0 TO 10.0	.01948	.03699	.02445	.04211	2.93
		10.0 TO 25.0	.03955	.06440	.03636	.06252	
		25.0 TO 50.0	.11702	.18559	.07424	.12938	
		50.0 TO 100.0	.23330	.47488	.18722	.26534	
71	HMAC	4.0 TO 10.0	.01818	.02983	.01592	.02731	3.88
		10.0 TO 25.0	.02185	.04279	.01758	.03782	
		25.0 TO 50.0	.01873	.04742	.01308	.02520	
		50.0 TO 100.0	.04134	.14403	.02304	.08088	
72	OVLY	4.0 TO 10.0	.01457	.02604	.02041	.03498	3.21
		10.0 TO 25.0	.02395	.04426	.02558	.05640	
		25.0 TO 50.0	.05981	.09810	.04318	.10269	
		50.0 TO 100.0	.14382	.21123	.12148	.19463	
73	OVLY	4.0 TO 10.0	.01124	.01822	.01173	.02096	3.85
		10.0 TO 25.0	.02457	.03919	.02771	.04223	
		25.0 TO 50.0	.03981	.05519	.02426	.03715	
		50.0 TO 100.0	.07167	.19505	.06088	.12393	

(Continued)

TABLE A3.2. (Continued)

SECTION	TYPE	PASSBAND (FT.)	PERCENTILES LONGITUDINAL 50TH	LONGITUDINAL 90TH	TRANSVERSE 50TH	TRANSVERSE 90TH	PSR
74	OVLY	4.0 TO 10.0	.01493	.02632	.01618	.02814	3.70
		10.0 TO 25.0	.02206	.03664	.01948	.03301	
		25.0 TO 50.0	.03093	.04640	.02625	.04035	
		50.0 TO 100.0	.04292	.06762	.03592	.04768	
75	OVLY	4.0 TO 10.0	.01486	.02580	.01696	.02782	2.98
		10.0 TO 25.0	.02369	.04405	.02304	.05260	
		25.0 TO 50.0	.04797	.16431	.04006	.17261	
		50.0 TO 100.0	.09461	.19904	.03612	.17642	
81	HMAC	4.0 TO 10.0	.01798	.02783	.01933	.03168	3.80
		10.0 TO 25.0	.02217	.04068	.02732	.05449	
		25.0 TO 50.0	.03180	.04699	.03322	.06133	
		50.0 TO 100.0	.07589	.20826	.05051	.14582	
82	ST	4.0 TO 10.0	.01614	.02811	.02196	.03243	4.08
		10.0 TO 25.0	.01824	.03256	.02364	.03743	
		25.0 TO 50.0	.02412	.03975	.02028	.04314	
		50.0 TO 100.0	.07985	.11468	.06519	.09044	
83	ST	4.0 TO 10.0	.02345	.04074	.03141	.05417	2.32
		10.0 TO 25.0	.02632	.04684	.03510	.05468	
		25.0 TO 50.0	.03974	.05779	.04566	.07272	
		50.0 TO 100.0	.11781	.22407	.14547	.20931	
84	ST	4.0 TO 10.0	.02570	.06048	.03021	.04864	2.50
		10.0 TO 25.0	.04530	.07169	.04905	.07360	
		25.0 TO 50.0	.13094	.21932	.08930	.20055	
		50.0 TO 100.0	.36858	.50881	.19869	.38493	

(Continued)

TABLE A3.2. (Continued)

SECTION	TYPE	PASSBAND (FT.)	PERCENTILES LONGITUDINAL 50TH	LONGITUDINAL 90TH	TRANSVERSE 50TH	TRANSVERSE 90TH	PSR
85	HMAC	4.0 TO 10.0	.01549	.03154	.02723	.05304	2.63
		10.0 TO 25.0	.02779	.05605	.03742	.06345	
		25.0 TO 50.0	.03714	.08936	.04671	.08571	
		50.0 TO 100.0	.11841	.20247	.09339	.17036	
86	ST	4.0 TO 10.0	.03249	.07591	.03379	.05910	2.48
		10.0 TO 25.0	.04900	.10534	.04136	.07083	
		25.0 TO 50.0	.07629	.10582	.02764	.05903	
		50.0 TO 100.0	.13206	.39536	.09351	.20118	
87	HMAC	4.0 TO 10.0	.01686	.02904	.02806	.04715	2.85
		10.0 TO 25.0	.01894	.03313	.02950	.04759	
		25.0 TO 50.0	.02772	.04897	.02942	.05047	
		50.0 TO 100.0	.09417	.13997	.08037	.14137	
93	HMAC	4.0 TO 10.0	.03340	.08185	.04239	.20941	4.15
		10.0 TO 25.0	.05503	.12853	.09963	.38613	
		25.0 TO 50.0	.06886	.16550	.13342	.34499	
		50.0 TO 100.0	.11748	.25335	.17462	.26721	
97	HMAC	4.0 TO 10.0	.03428	.06929	.04047	.11269	3.50
		10.0 TO 25.0	.04969	.09970	.06609	.16914	
		25.0 TO 50.0	.06788	.10467	.08772	.15816	
		50.0 TO 100.0	.11195	.19991	.09282	.21560	
100	HMAC	4.0 TO 10.0	.01576	.02533	.02076	.03289	4.02
		10.0 TO 25.0	.02391	.04475	.03081	.04883	
		25.0 TO 50.0	.03458	.06480	.04486	.05909	
		50.0 TO 100.0	.07094	.17370	.04975	.09366	

(Continued)

TABLE A3.2. (Continued)

SECTION	TYPE	PASSBAND (FT.)	PERCENTILES LONGITUDINAL 50TH	LONGITUDINAL 90TH	TRANSVERSE 50TH	TRANSVERSE 90TH	PSR
101	ST	4.0 TO 10.0	.01711	.02960	.02368	.03708	3.55
		10.0 TO 25.0	.02029	.03225	.02291	.04422	
		25.0 TO 50.0	.03734	.07947	.04821	.11660	
		50.0 TO 100.0	.13230	.21937	.14570	.22991	
103	HMAC	4.0 TO 10.0	.02127	.03159	.02361	.03734	3.93
		10.0 TO 25.0	.02881	.04520	.03180	.05032	
		25.0 TO 50.0	.03483	.05685	.03523	.06207	
		50.0 TO 100.0	.08001	.12122	.06419	.08448	
104	ST	4.0 TO 10.0	.03108	.06226	.03152	.05616	2.47
		10.0 TO 25.0	.04946	.09683	.06227	.10033	
		25.0 TO 50.0	.10290	.19337	.10763	.18929	
		50.0 TO 100.0	.18743	.33727	.21977	.29446	
105	HMAC	4.0 TO 10.0	.02861	.06948	.03617	.07243	1.13
		10.0 TO 25.0	.06485	.11788	.08719	.18033	
		25.0 TO 50.0	.12532	.28068	.21025	.39075	
		50.0 TO 100.0	.19906	.31057	.27313	.37940	
108	ST	4.0 TO 10.0	.02565	.04258	.02782	.04479	2.73
		10.0 TO 25.0	.04017	.06880	.02830	.05410	
		25.0 TO 50.0	.08272	.18900	.04580	.11698	
		50.0 TO 100.0	.16250	.20145	.08132	.10764	
110	HMAC	4.0 TO 10.0	.01096	.01652	.01235	.01914	4.33
		10.0 TO 25.0	.01085	.01579	.00925	.01333	
		25.0 TO 50.0	.03061	.05315	.01579	.02809	
		50.0 TO 100.0	.05264	.09917	.02540	.05227	

(Continued)

TABLE A3.2. (Continued)

SECTION	TYPE	PASSBAND (FT.)	PERCENTILES LONGITUDINAL 50TH	LONGITUDINAL 90TH	TRANSVERSE 50TH	TRANSVERSE 90TH	PSR
111	ST	4.0 TO 10.0	.01886	.03100	.02168	.03582	4.00
		10.0 TO 25.0	.02027	.03117	.01473	.02289	
		25.0 TO 50.0	.03807	.05584	.02111	.03295	
		50.0 TO 100.0	.10353	.14173	.05167	.06884	
112	HMAC	4.0 TO 10.0	.01220	.01899	.01310	.02054	4.19
		10.0 TO 25.0	.02420	.04613	.01747	.03353	
		25.0 TO 50.0	.04528	.07656	.02703	.04076	
		50.0 TO 100.0	.11976	.17799	.06037	.08868	

NOTE: 1 foot = .3048 meters
1 inch = 2.540 centimeters

APPENDIX 4

APPROACHES FOR DEVELOPING A SINGLE SI REGRESSION MODEL WHICH IS USABLE FOR SENSITIVITY ANALYSIS

APPENDIX 4. APPROACHES FOR DEVELOPING A SINGLE SI REGRESSION MODEL WHICH IS USABLE FOR SENSITIVITY ANALYSIS

In this appendix statistical methods are discussed for developing an SI model which describes the overall roughness of a road and which can be used to study the sensitivity of the SI value to the various types of roughness. This analysis would be performed by first computing the SI value and then varying the values of the roughness terms one at a time. This approach might be extremely useful in prescribing maintenance, since it would reveal the type or types of roughness whose correction would yield the greatest improvement in SI.

A difficulty which must be recognized at the outset is the fact that different types of roughness are correlated because they tend to progress simultaneously (although probably not at exactly the same rate). This effect is evidenced by the presentation in Table 4.2 of the high correlations between terms describing the roughness of different wavelengths. Naturally, there are some exceptions to the general trend; a swelling subgrade could cause the rapid development of roughness with a narrow range of wavelengths.

Nevertheless, if a model were to be used to study the sensitivity of SI to individual roughness types, then that model should have been developed from a sample which allows such distinctions to be made; no two types of roughness should be completely confounded in the sample.

When either standard multiple regression or stepwise regression is used to develop an SI model using a set of roughness measures with strong correlations, the interdependence among the coefficients is such that no physical meaning can be associated with them; some coefficients even have the opposite sign from the correlation between PSR and the term to which they apply. This effect, which is treated in Ref 11, is also discussed in Chapters 2 and 4 of this report.

When these sign reversals exist, the model obviously cannot be used for sensitivity analysis of the type discussed above. Furthermore, it is disconcerting to know that a roughness term has a positive coefficient, since

this seems to indicate that SI increases as some types of roughness become worse. In light of the arguments given in Chapter 2, however, the second point certainly does not invalidate such an SI model for the purpose of PSR prediction.

Nevertheless, it is of interest to know whether a model can be developed which has coefficients which, when taken individually, are realistic. Two approaches to this problem, both of which had considerable intuitive appeal a priori and neither of which was fully successful, were tried. The two approaches are summarized below for possible benefit to other researchers who will study this problem in the future.

Principal Component Approach

As discussed above, it is generally not possible to associate meaning with the regression coefficients if there are a large number of predictor variables with high correlations. In these cases, it is usually necessary to select a subset of the variables for inclusion in the model. Thus, a predictor variable x may have a high correlation with PSR, but it may be excluded from the model because other variables, with which x is highly correlated, explain whatever variations in PSR x would have explained. Furthermore, the coefficients of the terms which are included are not generally interpretable.

For these reasons, applying a multivariate statistical approach to simplify the vector of predictor variables seemed natural. Principal component analysis (Ref 1, 6, and 14) is a method which can be used to linearly transform a set of correlated random variables into a set of uncorrelated ones called the principal components. If a dependent variable is regressed on the principal components of a set of predictor variables, then the exclusion of all but one of several predictor variables, which are highly correlated with each other and with the dependent variable, cannot occur, since the principal components are mutually uncorrelated. Whatever variation in the dependent variable is explainable as a linear function of one of the principal components cannot also be explained by the other components, since the principal components are linearly independent.

Moreover, each principal component is a linear combination of all the predictor variables; thus, a model involving one or more principal components involves all of the original predictor variables.

The principal components are computed in order of decreasing variance[1]; frequently, a subset of the principal components will retain a large portion of the variance of the original larger set of variables. For the sample of 50 flexible pavements, for example, the first four principal components retain 94 percent and the first eight components retain 99 percent of the variance of the original 16 roughness measures used in this study. Regression of PSR on the first four and the first eight principal components yielded correlations of .79 and .85, respectively. These correlations are somewhat lower than the .91 value obtained by regressing PSR on the roughness measures directly.

More importantly, when the inverse transformation was performed to express the models in terms of the original roughness measures, the signs of the coefficients did not always agree with the signs of the corresponding correlations between the roughness measures and PSR. Thus, principal component analysis did not solve the basic problem.

Parameterized Coefficient Approach

A second approach was investigated in which the model was formulated so that the coefficients of the roughness measures (1) are all negative and (2) are monotonically related to the correlations with PSR. To allow selection of the best possible model with the desired properties, the form of the model was designed so that the coefficients had wide latitude while still satisfying conditions (1) and (2).

The following linear combination $L(\alpha)$ is, from the standpoint of model building, the only "roughness" term:

$$L(\alpha) = \sum_i (-\rho_i)^{\alpha} \left(\frac{x_i - m_i}{\sigma_i} \right)$$

[1] The ith principal component has the maximum variance, subject to a normalization constraint, of any linear combination of the original random variables which is uncorrelated with the first (i-1) principal components.

The terms in the expression are defined as follows:

ρ_i - correlation between the i^{th} roughness measure and PSR,

x_i - i^{th} roughness measure,

m_i - mean of x_i , and

σ_i - standard deviation of x_i .

Since the ρ_i are all negative, $(-\rho_i)^{\alpha}$ is a real number for all i . The indicated transformation, to insure that each term

$$\left(\frac{x_i - m_i}{\sigma_i} \right)$$

has mean zero and variance one, is performed so that the values of the coefficients will not be affected by the considerably different ranges of values of the different roughness measures; we are interested only in the strength of the relationships between the x_i and PSR.

The parameter α , then, should be chosen so as to maximize the correlation (call it $C(\alpha)$) between $L(\alpha)$ and PSR. $C(\alpha)$ has a single peak of -.762 at $\alpha = 11$; the peak is very broad, since $C(\alpha)$ is -.692 at $\alpha = .3$ and -.730 at $\alpha = 49$. When PSR was regressed on L(11) and the pavement type variable ST (see Appendix 1), a multiple correlation of only .77 was obtained. This should be compared to the correlation of .91 obtained for the unconstrained model.

It is important to remember that, as stated above, the coefficients have extremely wide latitude as α varies. Thus, no significant limitations except the stated constraints are placed on the model-building procress.

The conclusion which must be drawn is that the constraints which are required to insure that the coefficients are directly related to the correlations with PSR also limit the development of a model which agrees with the data on which it is based. The basic test of a predictive model should be whether the model is capable of predicting accurately. If not, any use of the model, including sensitivity analysis, is suspect.

For the reasons stated above, it is suggested that the loss in predictive accuracy does not justify whatever benefits might be associated with a constrained model such as the one discussed above.

APPENDIX 5

AN INVESTIGATION OF SIGNAL PROCESSING TECHNIQUES FOR THE PURPOSE OF CHARACTERIZING ROAD ROUGHNESS

APPENDIX 5. AN INVESTIGATION OF SIGNAL PROCESSING TECHNIQUES FOR THE PURPOSE OF CHARACTERIZING ROAD ROUGHNESS

INTRODUCTION

The General Motors Surface Dynamics Profilometer is a special purpose van equipped with mechanical and electronic hardware necessary to measure a road profile, i.e., surface elevation vs. distance along the road. The profile is measured in both the right and left wheelpaths.

Measurement of a profile involves recording the vertical motion of a special purpose measuring wheel relative to the body of the truck and the vertical motion of an accelerometer, mounted in the truck above the measuring wheel, in an earth-fixed coordinate system. Then the two recordings are used to compute the vertical position of the wheel in an earth-fixed coordinate system. The vertical position of the wheel vs. distance is then the measured profile.

Reference 22 is a detailed description and analysis of the profile measuring system. Reference 16 includes a somewhat briefer description of the system (pp 5-16).

The subject of this appendix is the characterization of road roughness given the right and left profiles measured by an instrument such as the profilometer. The techniques to be discussed are by no means limited to analysis of data from a particular measuring system; it is anticipated that the methods will be used in the future in conjunction with more sophisticated systems, such as a system using either radar or sonar instead of a road-following wheel to measure the distance from the body of the truck to the road surface.

The road profiles themselves characterize road roughness in the sense that they contain information from which one can infer the nature and extent of the roughness. However, the two road profiles in the form of surface elevation tabulated at, say, every 2 inches (5.08 centimeters) for a road

section of 1200 feet (365.8 meters) are not conveniently usable except for visual inspection of plots.

Thus, it is desirable to have a method for reducing the road profiles to a set of quantities which

(1) is small in number and

(2) is meaningful from the standpoint of riding quality.

An investigation of various signal processing techniques for the purpose of profile characterization is discussed in the following sections.

It is emphasized that the objective here is not only to present a discussion of signal-processing techniques, but to discuss the adequacy of the techniques specifically for analyzing road profiles.

For this purpose, it is felt that certain mathematical background is required if this work is to be of maximum benefit to other researchers. Thus, for example, the mathematical concept of the frequency response function of a digital filter is developed in an early section. In later sections, the concept is used to discuss the capabilities of various filters for isolating certain types of information in a road profile.

Mathematical concepts which are considered to be of only minor relevance are discussed briefly, and references are given for readers who want to study the theory more deeply.

There is much potential for the application of sophisticated profile analysis tools. An assessment of the amount of surface deformation is an important part of the evaluation of the condition of a road. The breadth of the practical need for such evaluations is discussed in Chapter 1. The following are examples of the areas in which road evaluations are needed.

(1) The acceptance or rejection of new highway constructions must be made on a basis which is both consistent and relevant to the ability of the road to serve the public.

(2) Existing pavements must be evaluated in order to prescribe maintenance. The assessment of the need for maintenance will be a necessary function of the highway engineer as long as paved roads are in use.

(3) The improvement of pavement design, construction, and maintenance practices is dependent on experimental research studies. The success of such a research program often requires having a method which is consistent over a period of time, perhaps several years, for evaluating road conditions. The evaluation at successive points in time is necessary to analyze various types of pavement deterioration.

POWER SPECTRUM

Reference 21 documents a method for characterizing roughness in terms of the power spectra of the right and left profiles and of the cross power spectrum. The development of a regression model to predict pavement serviceability in terms of amplitudes and cross amplitudes computed from the spectra is also discussed.

The signal processing involves the following:

(1) low-pass filtering (filtering techniques are discussed later in this appendix) the raw profiles to reduce the aliasing error introduced in step 2 (discussions of aliasing error are given in Ref 2, pp 228-231, and Ref 3, p 46),

(2) decimating (subsampling) the profiles so that the sampling rate is reduced from 5.92 data per foot (19.42 data per meter) to one-fourth of that, i.e., the sampling interval is increased from about 2 inches (5.08 centimeters) to about 8 inches (20.32 centimeters),

(3) removing any possible linear trends from either profile,

(4) applying a cosine taper window to reduce the distortion (side lobes) introduced in step 5,

(5) performing a fast Fourier transform (FFT) on both profiles,

(6) averaging the power spectral values over several bands - the number of frequency points obtained from the FFT is more than is needed, and

(7) computing approximate root-mean-square (r.m.s.) amplitudes and cross-amplitudes corresponding to a discrete set of center frequencies. This is done for each frequency band by computing the r.m.s. amplitude of the steady sine wave at the center frequency which has the power spectral density value actually computed.

The method is discussed in some detail in Ref 21. An excellent overview of the FFT and its properties, including pitfalls, is given in Ref 3. The FFT is also discussed in Refs 2, 8, and 13.

A regression model was developed using rating panel serviceability data as the response variable and the amplitudes and cross-amplitudes plus a dummy variable, $T = 1$ for concrete pavements and $T = 0$ for asphalt pavements, as the independent variables. Collection of the rating panel data is discussed in Ref 16.

The regression model had a squared multiple correlation coefficient of .89 and a residual standard error of .33. Thus, 89 percent of the

road-to-road variation in human serviceability ratings was explained in terms of the roughness amplitudes. It was established, therefore, that roughness characterization via profilometer data plus intelligent use of signal processing techniques does have a very strong correlation with human evaluations of roads.

The FFT approach gives a single roughness measure, r.m.s. amplitude, corresponding to each of a discrete set of frequencies. Thus, we do not know whether the roughness at a given frequency occurred as steady surface waves with moderate amplitude variations, as a single severe bump, etc. Some measure of within-section roughness variation would enhance the amplitude vs. frequency characterization.

Furthermore, there is not an adequate measure of right-left profile inconsistencies, which would cause an automobile to rotate slightly about a lengthwise axis (to roll). The amplitudes clearly do not characterize rolling. The cross amplitudes are computed from cross-power values, the latter being defined in Ref 21 as a constant times the sum over a discrete set of frequency bands of quantities of the form

$$\hat{x}_t \cdot \hat{y}_t^*$$

where

$\hat{x}_t$ is the t^{th} FFT value of the right profile

$\hat{y}_t^*$ is the complex conjugate of the t^{th} FFT value of the left profile.

The cross power, then, is a constant times the inner product of the left conjugate and right FFT values. Thus, the cross power increases in magnitude as the right and left roughness amplitudes increase, but tends to decrease as the right and left profiles become increasingly dissimilar. If the magnitude of the cross power were normalized by the square root of the product of the right and left power values to obtain the coherence, then the result would be a measure of right-left similarity which would be clear of the longitudinal roughness effect mentioned above. Still, a measure of extreme transverse roughness in a road section would be of interest along with an overall measure.

MOVING FOURIER TRANSFORM

An obvious way to obtain a within-section variance estimate would be to use a moving finite Fourier transform. This approach has a couple of very desirable features.

If the i^{th} through the $(i + k)^{th}$ data points are used in computing a local transform, the 1^{st} through $(i - 1)^{st}$ and $(i + k + 1)^{st}$ and subsequent data points can have no effect. For example, if the transform is taken over one cycle at the center frequency, then we have extremely fine resolution in the space domain (distance along the road) in the sense that we have a measure of the roughness over a very short distance.

High resolution in the domain of the independent variable would not be important if the input time series were the sum of a set of approximately steady sinusoids and background noise or if the random amplitude fluctuations were not of primary interest.

In the highway problem, however, the amplitudes typically change from half cycle to half cycle; a rise and fall in the pavement is not necessarily followed by a symmetric or even similar fall and rise. The within-section roughness variations are, moreover, of practical interest, since they relate to riding quality.

The second desirable point is that the local transform could be computed recursively, with a great saving in computer time. Since the finite transform is defined as

$$\hat{x}(j) = \frac{1}{N} \sum_{K=0}^{N-1} x(k)\, \bar{e}^{\, i2\pi jk/N}$$

two such transforms (for the same center frequency) centered at successive points in space differ in that at each step one term is discarded and one is added; thus, subtracting and adding the appropriate terms are sufficient to update the sum. The fact that the real and imaginary parts of the factor $\bar{e}^{\, i2\pi jk/n}$ at the first point of the local transform would not always have phase 0^{o} and 90^{o} is irrelevant as far as computing roughness measures is concerned.

If the series were a sine wave with frequency f and with varying amplitude, one could choose the distance T for each transform to be $T = 1/f$, i.e., T = one cycle at frequency f, and an excellent measure of local roughness would be obtained. The question, however, is, in what way do irregularities at other frequencies contribute to the roughness measure at frequency f? We now investigate this problem.

Ideally, one would like any irregularity at frequency g to contribute proportionally to its amplitude if g were within a reasonably small band centered at f and not to contribute at all if g were not in the passband.

The problem with the moving transform is that high resolution in the space domain is achieved only at the expense of having very little resolution in the frequency domain. To study this in more detail, we examine the effect on the Fourier transform of using a finite data record (see Ref 13, pp 48-50).

Suppose $s(t)$ is a time series, defined for all real t, with Fourier transform $S(f)$. Then if only the part of $s(t)$ such that $|t| \leq T/2$ is used in computing a transform, i.e., if we compute the transform of

$$s_T(t) = s(t)\ w(t)$$

where

$$w(t) = 1, \quad |t| \leq T/2$$

$$= 0, \quad |t| > T/2$$

then the transform $S_T(f)$ of $s_T(t)$ is

$$S_T(f) = \int_{-\infty}^{\infty} S(g)W(f-g)dg$$

where

$$W(f) = T\ \frac{\sin(\pi fT)}{(\pi fT)}$$

Note that

$$\lim_{f \to 0} W(f) = \lim_{g \to f} W(f-g) = T$$

and that

$$\frac{1}{T} \left| S_T(f) \right|$$

could be used as the basis for a roughness measure for frequencies near f; if

$$s(t) = A \sin (2\pi f t + \phi)$$

where

ϕ is any angle,

then

$$S_T(f) = \int_{t=0}^{t=\frac{1}{f}} s(t)\, e^{-2\pi i f t} dt = \frac{TA \sin \phi}{2} + i \frac{TA \cos \phi}{2}$$

so

$$\left| S_T(f) \right| = \frac{TA}{2}$$

But the r.m.s. value of a sine wave with amplitude A is $A/\sqrt{2}$; therefore the r.m.s. value of $s_T(t)$ is

$$\frac{1}{T} \left| S_T(f) \right| \sqrt{2}$$

Although $s(t)$ is not in general a pure sine wave, the point is that there is justification for using $\frac{1}{T} \mid S_T(f) \mid \sqrt{2}$ as a roughness amplitude measure.

The function

$$\frac{W(f-g)}{T} \quad \text{vs.} \quad f \ ,$$

which is the relative contribution of irregularities at frequency g to the roughness measure centered at f, is plotted in Fig A5.1 for the case in which $T = 1/f$ and the center frequency is .1 cycles per foot (.3281 cycles per meter). The wavelength in unit length/cycle is simply the reciprocal of the frequency in cycles/unit length.

The side lobes at high frequencies are not a serious defect, since it is well-known that the amplitudes of road roughness generally drop off rapidly as frequency increases; a very sharp cutoff at the high frequency edge of the passband is not necessary.

For the same reason, however, the gradual cutoff at the low frequency end means that the contribution of irregularities with frequencies less than $f/2$ will in general obscure the contributions near f; in other words, the amplitude measure fails to measure roughness only near f.

It is clear from the form of W that the cutoff in the frequency domain can be made more sharp by increasing T, but then resolution in the space domain is lost in that several cycles of data are used to compute each "local" roughness measure.

Using a more sophisticated type of window, e.g., a Bartlett window (Ref 13, pp 239-243), would increase cutoff sharpness, but would necessitate a considerable amount of calculation, since the transforms must be taken at successive points along the road. The recursive scheme mentioned above for computing successive transforms could not be used.

The fact that the weighting function $W(f)/T$ is not approximately flat in the passband is undesirable in the sense that physical interpretation of the roughness measures is obscured to some extent.

Thus, although it has certain very desirable features, the moving Fourier transform is less than ideal.

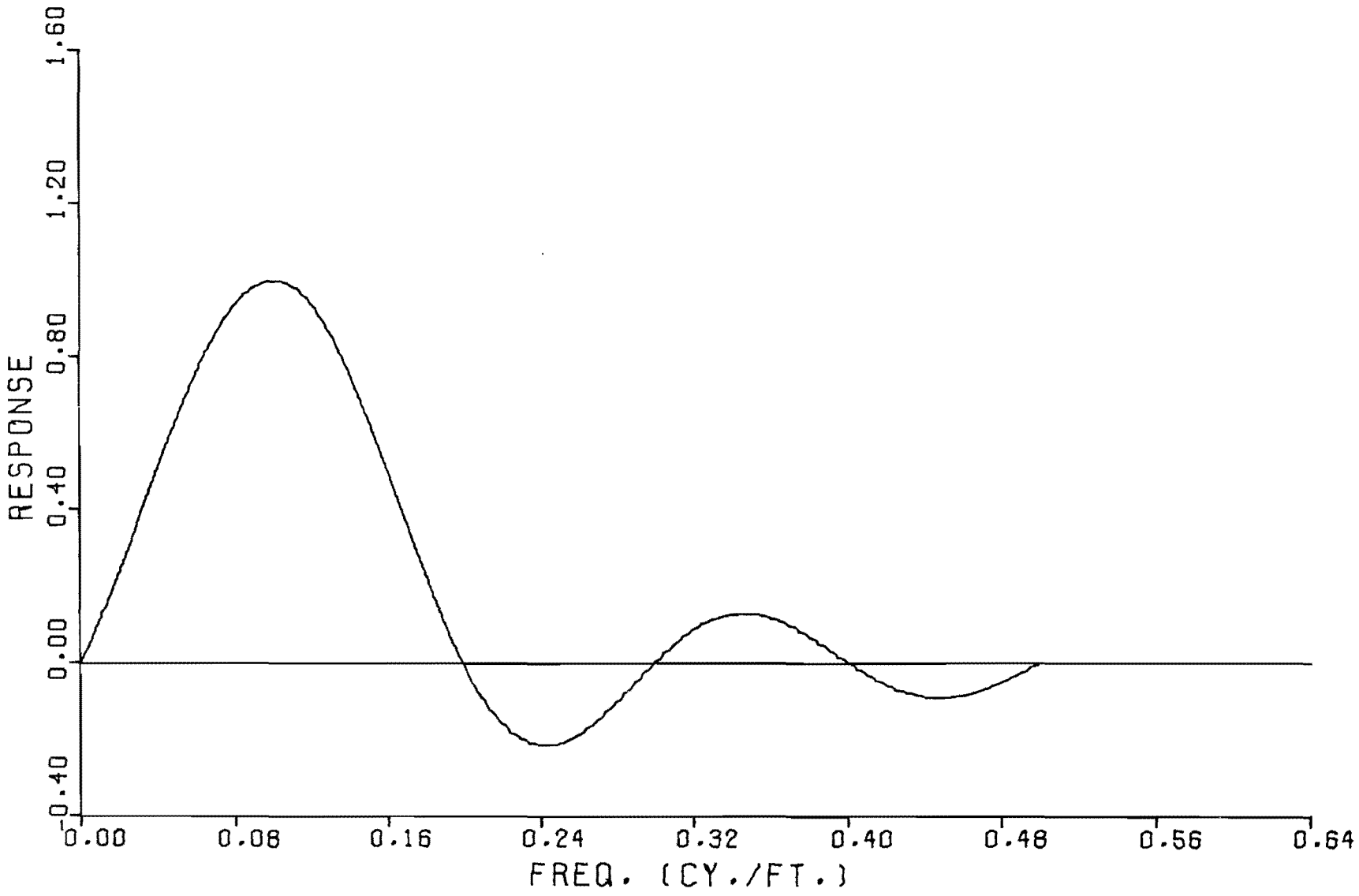

1 foot = .3048 meters

Fig A5.1. Frequency response of a finite Fourier transform. Transform taken over one cycle at center frequency, .1 cycle/ft.

In the following sections, the application of digital filtering techniques to the riding quality problem is explored.

DIGITAL FILTERING TECHNIQUES AND ROAD PROFILES - GENERAL

Filtering has been mentioned in the literature, e.g., in Refs 4, 19, and 21, as a technique for isolating the components of road roughness by wavelength.

Reference 15 gives an excellent general discussion of digital filtering techniques. In this section, we will frequently draw on that reference in discussing the basic concept of digital filtering as it might apply to riding quality.

An m^{th}-order difference equation can be written

$$Y_n = \sum_{j=0}^{r} L_j X_{n-j} - \sum_{j=1}^{m} K_j Y_{n-j}$$

The process of using such a relationship to produce an output time series Y_n, $n = 1, 2, \ldots N$ given in input series X_i, $i = 1, 2, \ldots N$, is called digital filtering. The constants L_i and K_i are chosen according to the purpose to be achieved by filtering. We shall assume that the step size of the independent variable is constant.

A filter is called "recursive" if $K_j \neq 0$ for some $j > 0$, i.e., if each Y_n is a function of at least one previously computed filtered value, as well as of a set of unfiltered values. Otherwise, the filter is called nonrecursive. Generally, recursive filters are much more computationally efficient than nonrecursive filters.

Now, suppose we are interested in processing a road profile, where the X_i are road surface elevations measured at equidistant points along the road in order to isolate the roughness with wavelengths between 10 and 25 feet (3.048 and 7.620 meters) or, equivalently, frequencies between .04 and .1 cycles/foot (.1312 and .3281 cycles per meter). The Y_i, then, could be examined for local roughness patterns.

Thus, within-section roughness variations for each of a set of frequency bands could be studied; this eliminates one of the limitations stated earlier of a power spectral roughness characterization in which the entire section is processed in the Fourier transform.

The other stated objection is the lack of an adequate measure of right-left profile discrepancies, which would cause a rolling effect in a passing vehicle. If we formed a new time series by taking the pointwise difference between the right and left profiles, then we could process the new series directly to obtain a space-frequency decomposition of the elevation changes in one wheelpath relative to the other. Then, if filtering were used, a within-section variability measure could be computed for rolling as well as for longitudinal roughness.

It has been pointed out that if the right and left profiles had different vertical reference levels, then a spurious zero-frequency component would be present in the difference time series (see Ref 11, p 83). But, having no relationship to roughness, the zero-frequency component would be filtered out anyway. Similar comments apply to very long waves possibly introduced by drift in the vertical reference level.

Thus, we see that the potential of digital filtering in terms of detailed road roughness characterization is great. We now discuss the basic concept of filtering from a mathematical viewpoint.

The Z-transform is a basic tool used in analyzing digital filters. The transform $X(Z)$ of the time series X_i, $i = 0, 1, 2, \ldots$ is defined as follows:

$$X(Z) = \sum_{n=0}^{\infty} X_n Z^{-n}$$

Now rewrite the difference equation

$$\sum_{j=0}^{m} K_j Y_{n-j} = \sum_{j=0}^{r} L_j X_{n-j}$$

where

$$K_o = 1 .$$

Then we use Z-transforms to develop the system function $H(Z)$, which is used extensively in characterizing filters.

$$\sum_{j=o}^{m} K_j Y_{n-j} Z^{-n} = \sum_{j=0}^{r} L_j X_{n-j} Z^{-n}$$

Now, for convenience, we define $X_j = Y_j = 0$ if $j<0$. Then

$$\sum_{n=0}^{\infty} \sum_{j=0}^{m} K_j Y_{n-j} Z^{-n} = \sum_{n=0}^{\infty} \sum_{j=0}^{r} L_j X_{n-j} Z^{-n}$$

$$\sum_{j=0}^{m} K_j Z^{-j} \sum_{n=0}^{\infty} Y_{n-j} Z^{-n+j} = \sum_{j=0}^{r} L_j Z^{-j} \sum_{n=0}^{\infty} X_{n-j} Z^{-n+j}$$

But, since $Y_{m-j} = X_{m-j} = 0$ if $m-j<0$, we have

$$\sum_{j=0}^{m} K_j Z^{-j} \sum_{n=j}^{\infty} Y_{n-j} Z^{-n+j} = \sum_{j=0}^{r} L_j Z^{-j} \sum_{n=j}^{\infty} X_{n-j} Z^{-n+j}$$

or

$$\sum_{j=0}^{m} K_j Z^{-j} \sum_{n=0}^{\infty} Y_n Z^{-n} = \sum_{j=0}^{r} L_j Z^{-j} \sum_{n=0}^{\infty} X_n Z^{-n}$$

$$\sum_{j=0}^{m} K_j Z^{-j} Y(Z) = \sum_{j=0}^{r} L_j Z^{-j} X(Z)$$

Then $H(Z)$ is defined as

$$H(Z) = \frac{Y(Z)}{X(Z)} = \frac{\sum_{j=0}^{r} L_j Z^{-j}}{\sum_{j=0}^{m} K_j Z^{-j}}$$

Now, $H(Z)$ is called the system function or frequency response function, the motivation for which will become apparent shortly.

Suppose $X_n = e^{in\omega\Delta t}$; X_n is a complex sinusoid with frequency ω. The step size of the independent variable is Δt. If we determine the response of the filter to such an input, where ω is an arbitrary frequency, then we will have determined the frequency response of the filter. Because of the linearity of the class of filters we are dealing with, we do not have to worry about interaction effects of sinusoids of different frequencies.

The linearity property is easily proved by induction as follows.

Suppose

$$d_n = c_1 a_n + c_2 b_n \text{ , } n \geq 0 \text{ , where } c_1 \text{ and } c_2 \text{ are constants.}$$

We will denote the filtered outputs of the d, a, and b arrays by $\hat{d}$, $\hat{a}$, and $\hat{b}$ respectively. We wish to show

$$\hat{d}_n = c_1 \hat{a}_n + c_2 \hat{b}_n$$

Now,

$$\hat{d}_n = \sum_{j=0}^{r} L_j d_{n-j} - \sum_{j=1}^{m} K_j \hat{d}_{n-j}$$

Thus,

$$\hat{d}_1 = L_0 d_1 = c_1[L_0 a_1] + c_2[L_0 b_1] = c_1 \hat{a}_1 + c_2 \hat{b}_1$$

and linearity follows for $n=1$.

Suppose the result is true for $K = 1, 2, \ldots n-1$.

Then

$$\hat{a}_n = \sum_{j=0}^{r} L_j d_{n-j} - \sum_{j=1}^{m} K_j (c_1 \hat{a}_{n-j} + c_2 \hat{b}_{n-j}) =$$

$$c_1 \left[\sum_{j=0}^{r} L_j a_{n-j} - \sum_{j=1}^{m} K_j \hat{a}_{n-j} \right] + c_2 \left[\sum_{j=0}^{r} L_j b_{n-j} - \sum_{j=1}^{m} K_j \hat{b}_{n-j} \right] =$$

$$c_1 \hat{a}_n + c_2 \hat{b}_n$$

This concludes the proof by induction.

Now, we assume the filtered output has the form

$$Y_n = F(e^{i\omega\Delta t})\, e^{in\omega\Delta t}$$

where F is a function to be determined.

By assuming that the factor F is a function of ω only, and not of n, we shall obtain the steady state solution; there are transient effects near the first of the data record where the amplitude of x changes from zero to one.

Then, substituting the expressions for X_n and Y_n into the difference equation,

$$\sum_{j=0}^{m} K_j F(e^{i\omega\Delta t})\, e^{i(n-j)\omega\Delta t} = \sum_{j=0}^{r} L_j e^{i(n-j)\omega\Delta t}$$

$$F(e^{i\omega\Delta t})\, e^{in\omega\Delta t} \sum_{j=0}^{m} K_j e^{-ij\omega\Delta t} = e^{in\omega\Delta t} \sum_{j=0}^{r} L_j e^{-ij\omega\Delta t}$$

$$F(e^{i\omega\Delta t}) = \frac{\sum_{j=0}^{r} L_j e^{-ij\omega\Delta t}}{\sum_{j=0}^{m} K_j e^{-ij\omega\Delta t}} = H(e^{i\omega\Delta t})$$

Now, suppose

$$H(e^{i\omega\Delta t}) = R(\omega)\, e^{i\Theta(\omega)}$$

Then $R(\omega)$, being the factor by which the amplitude of an input complex sinusoid at frequency ω is multiplied (effectively) in the filtering process, is called the "gain."

$\Theta(\omega)$, being the angular shift imposed on an input signal of frequency ω , is called the "phase shift."

In the highway problem, we are interested in processing time series in which amplitudes typically vary from half cycle to half cycle. The problem of choosing a filter for such time series and of defining physically meaningful roughness measures in terms of the filtered output is treated in the following sections.

It should be noted that the phase shift is, in our problem, a frequency-dependent spatial translation of the surface irregularities. Such an effect must be considered a distortion introduced by the filter.

In Ref 17, p 41, a scheme is mentioned which reduces the phase shift to zero at all frequencies. Simply (1) filter the input time series forward, continuing the filtering past the last data point to allow transients to die out, and (2) filter the output time series backwards. Then the double filter has zero phase shift.

Now, we have seen that $H(Z)$ is interpretable as the frequency response if Z is evaluated on the unit circle, i.e., if $Z = e^{i\omega\Delta t}$.

Since it is a rational polynomial, we can describe $H(Z)$ uniquely except for a constant multiplier in terms of its poles (values of Z for which the denominator of $H(Z)$ is zero) and zeroes (values of Z for which the numerator is zero). Thus, the gain is expressible as

$$\left| H(e^{i\omega\Delta t}) \right| = c\, \frac{\prod R_j}{\prod P_j}$$

where the R_j and the P_j are distances from $e^{i\omega\Delta t}$ to the zeroes and poles, respectively, and c is a frequency-independent factor. (See Ref 15, p 152).

It is clear that if a pole is near one in magnitude and has angular polar coordinate $\omega\Delta t$, the effect is to make the gain relatively large at frequency ω. Similarly, if a zero is near one in magnitude and has angle $\omega\Delta t$, the effect is to make the gain small for frequency $\omega\Delta t$.

Thus, the poles and zeroes play a vital role in digital filter design.

If each pole (zero) is real or its complex conjugate is a pole (zero) also, then we are guaranteed that the coefficients will be real. This is clear from the equations

$$H(Z) = \frac{\sum_{j=0}^{r} L_j Z^{-j}}{\sum_{j=1}^{m} K_j Z^{-j}} =$$

$$C \frac{\prod_{j=1}^{r} (Z^{-1} - A_j^{-1})}{\prod_{j=1}^{m} (Z^{-1} - B_j^{-1})} ,$$

where the A_j and B_j are the zeroes and poles, respectively, and C is a real constant.

Now, according to Ref 17, p 34, if the filter is stable, a condition which is satisfied if and only if all the poles have magnitudes less than one, we can use long division to express $H(Z)$ as a power series in Z^{-1}:

$$H(Z) = \frac{\sum_{j=0}^{r} L_j Z^{-j}}{\sum_{j=0}^{\infty} K_j Z^{-j}} = \sum_{j=0}^{\infty} f_j Z^{-j}$$

If the filter is stable, then $H(Z)$ can be approximated as a polynomial in Z^{-1} ; i.e., a stable recursive filter can be approximated as a nonrecursive filter. If many terms are required for the approximating nonrecursive filter, then an event near X_k has effects on the Y_{k+j} for large values of j ; thus the filtering operation tends to smooth the half-cycle to half-cycle amplitudes, causing local transient effects. This phenomenon is examined in the following sections as it affects the characterization of road profiles.

DIGITAL RESONATOR

The digital resonator, one of the simplest digital filters, has poles $re^{\pm i\omega_o \Delta t}$ and one zero at q . Then, from Ref 15, p 155,

$$\left| H(e^{i\omega\Delta t}) \right| =$$

$$\left[\frac{1 + q^2 - 2q \cos \omega\Delta t}{[1 + r^2 - 2r \cos \left((\omega-\omega_o)\Delta t\right)] \, [1 + r^2 - 2r \cos \left((\omega+\omega_o)\Delta t\right)]} \right]^{\frac{1}{2}}$$

Note that as $\omega \to \omega_o$, the first factor in the denominator, approaches $1 + r^2 - 2r$, which is very small if r is near one. Thus, the gain reaches a maximum near $\omega = \omega_o$, and the closer r is to one, the sharper the peak is in the gain vs. frequency function. The squared gain vs. frequency functions are plotted in Figs A5.2 and A5.3 for two cases discussed below. Although the maximum gain for the digital resonator is generally greater than one, the output can be scaled to achieve a gain of unity at, say, ω_o .

The digital resonator is desirable if very sharp cutoff is necessary and if only frequencies in a narrow band are of interest.

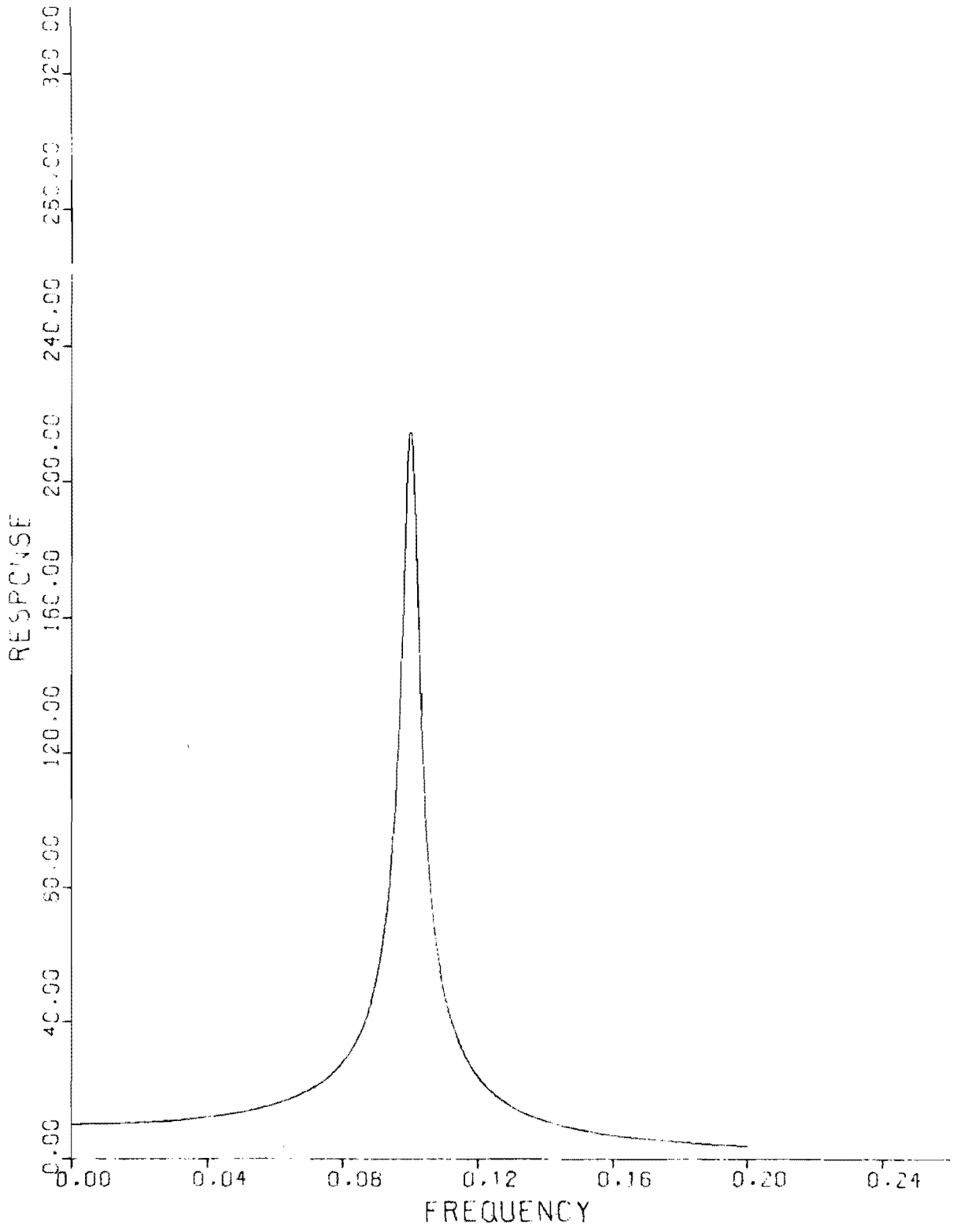

1 foot = .3048 centimeters

Fig A5.2. Squared gain vs. frequency for the digital resonator. ω_o = .1 cycle/ft., $\Delta\omega$ = .01, 20 data points per cycle at ω_o.

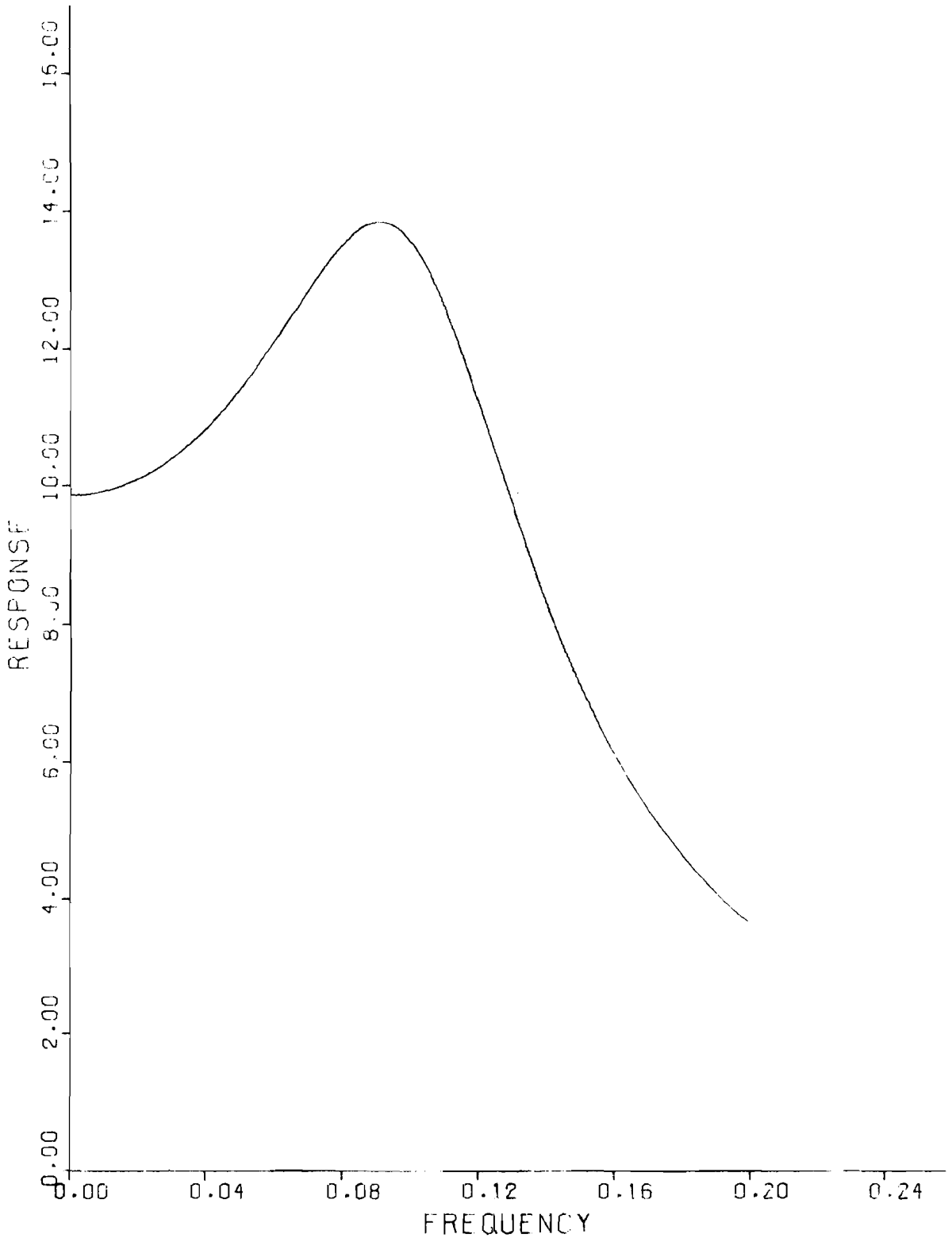

1 foot = .3048 meters

Fig A5.3. Squared gain vs. frequency for the digital resonator. ω_o = .1 cycle/ft., $\Delta\omega$ = .05, 20 data points per cycle at ω_o .

A computer program was written which

(1) computes the coefficients for a digital resonator with gain less than A for frequencies differing from ω_o by more than $\Delta\omega$, where A, ω_o, and $\Delta\omega$ are inputs, and

(2) performs forward and backward filtering as mentioned in the previous section to achieve zero phase shift at all frequencies.

We choose $q=0$, i.e., we will use a filter with no zeroes. The filter, then, has the form

$$Y_n = c_1 Y_{n-1} + c_2 Y_{n-2} + X_n$$

where

Y_n is the n^{th} filtered values

X_n is the n^{th} unfiltered value .

The usual convention, $X_n = Y_n = 0$ if $n \leq 0$, is adopted to allow calculation of Y_1 and Y_2.

Several test cases with artificial data were used to study the behavior of the filter when, as in a road profile, there are severe amplitude changes.

It is interesting that the same tradeoffs come into play in designing a digital filter as in choosing the number of points per transform to use in a moving Fourier transform. High resolution in either the frequency or spatial domain results in unacceptably low resolution in the other.

The digital resonator tends to smooth amplitudes over several half cycles; the narrower the bandwidth, the greater this tendency is. If the amplitude smoothing were great, then any "local" roughness measure computed from the filtered output would be a measure of the roughness over a long distance along the road. Thus, the point of computing a local roughness measure would be at least partially defeated.

The smoothing can be virtually eliminated by making the passband very wide. In this case, however, the gain decrease as the frequency moves away from the resonant frequency is very slow. (See Fig A5.3.) Thus, by the same

reasoning used in the case of the moving Fourier transform, the roughness measures would not be adequate.

The following is one of the test cases used to study the behavior of the filter when there are sharp amplitude changes in the signal:

(1) input time series: 100 zeroes followed by one cycle of a sine wave, including 20 data points, followed by 100 zeroes,

(2) ω_o = frequency of the sine wave,

(3) A = .707 , and

(4) various values of $\Delta\omega$, chosen to study the effect of varying the the width of the passband.

The filtered and unfiltered time series for the case, $\Delta\omega$ = 50 percent of the signal's frequency, are plotted in Fig A5.4. Since artificial data are being used, physical units are not indicated on the plot for the road elevation or distance along the road (data point number).

Because of the transient effect, the filtered output has amplitude less than one over the cycle of the original sine wave, and nonzero amplitude where the input signal was identically zero. The amplitude of the output series descreases as we move in either direction from the interval of the original sine wave. The tails, where the filtered output is near zero and the unfiltered time series is identically zero, are not shown.

Notice that the largest errors are at the main peaks, at the first spurious peaks on either side of the original sine wave, and near the first and last points of the original sine wave, where the derivative of the input time series is discontinuous. The last may be unrealistically conducive to filter-induced distortion, since traffic would tend gradually to remove discontinuous derivatives, if they were present. Thus, discrepancies at the discontinuous points are not cause for alarm.

A measure of the smoothing tendency is the absolute value of the filtered ordinate at either point where the original peaks occurred. If there were no amplitude smoothing at all, this measure would be one. The greater the effect of nearby points on filtered values within the abscissa interval that contained the original sine wave, the smaller the measure will be.

Table A5.1 contains a set of smoothing or distortion measures for a set of values of $\Delta\omega$.

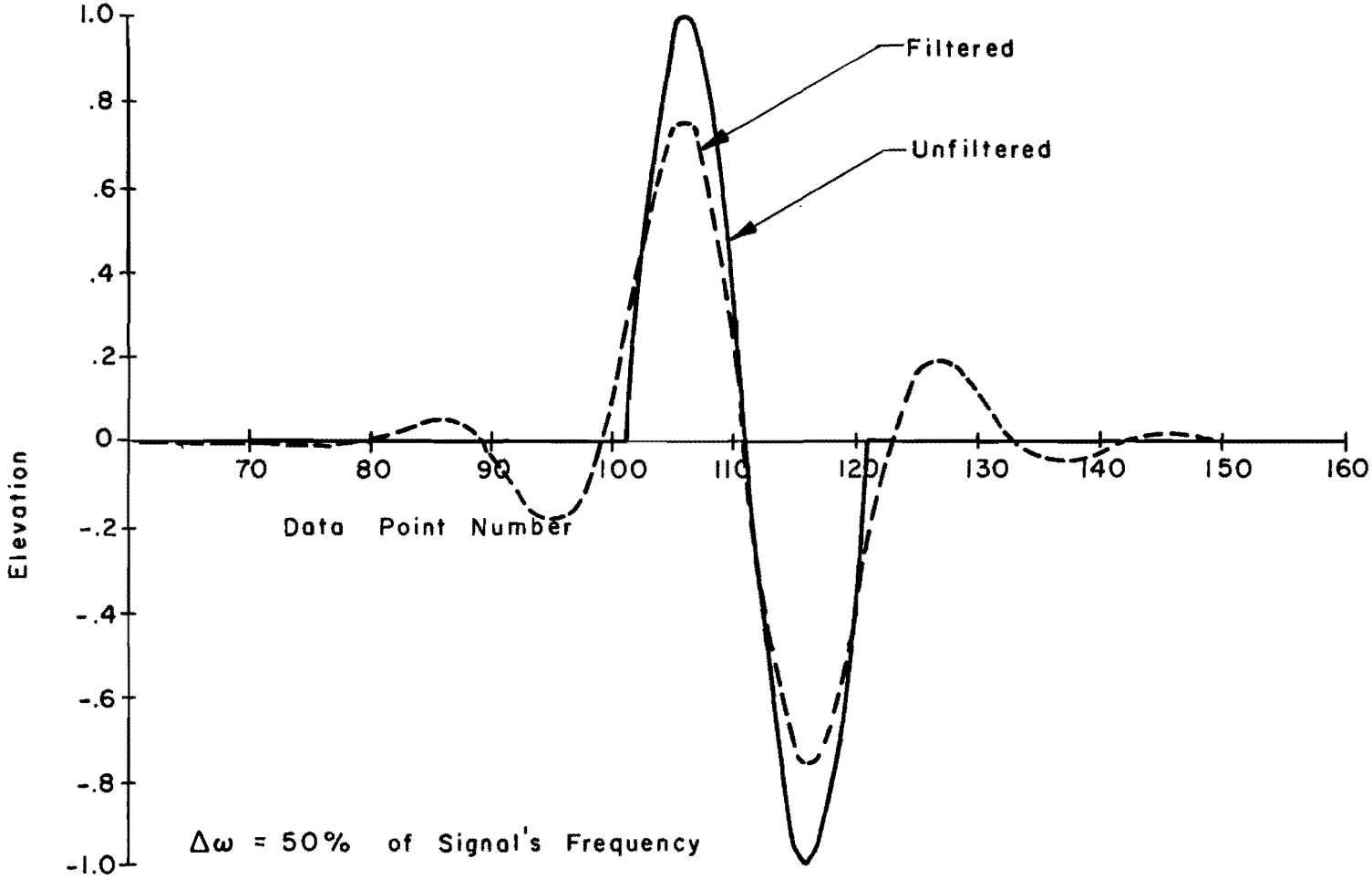

Fig A5.4. Illustration of the effects of the digital resonator.

TABLE A5.1. DISTORTION MEASURES FOR VARIOUS VALUES OF $\Delta\omega$

$\Delta\omega$, % of Frequency of Signal	Amplitude of Filtered Peak Where Original Peaks Occurred
10	.072
25	.167
33	.656
50	.745

Thus, we see that very wide passbands are required to avoid extreme distortion of the signal. Whereas reasonably wide passbands per se might not be undesirable, a slow cutoff at the low frequency end is unacceptable, for reasons discussed previously.[1] Thus, an approximately flat-topped wide-band filter with steep skirts would be preferable to the curve-topped resonator.

NONRECURSIVE FILTERS

It is mentioned in the general discussion of digital filters that nonrecursive filters differ from recursive ones in that each filtered value is a function only of unfiltered values, not of previously computer filtered values.

Thus a nonrecursive filter has the form

$$y_n = \sum_{j=r}^{s} L_j \; x_{n-j}$$

where

y_n is the n^{th} filtered value and

x_j is the j^{th} unfiltered value.

A method for computing local amplitude and phase is discussed in Refs 6 and 9. We will draw mainly on Ref 6 in our discussion, and we are interested primarily in the local amplitude calculation.

Suppose we have an input signal x_n, $n = 0, 1, \ldots N$.

---

[1] The cutoff at the low-frequency end of the passband would be improved somewhat if a zero at frequency zero were added, but the cutoff for a wide-band filter would still be slow compared to that of the filters discussed in the following sections.

A pair of nonrecursive filters are used:

$$y_k^{(1)} = \sum_{j=-m}^{m} b_j x_{k+j} \qquad \text{(filter 1)}$$

$$y_k^{(2)} = \sum_{j=-m}^{m} a_j x_{k+j} \qquad \text{(filter 2)}$$

Then local phase ϕ_k and amplitude R_k are defined by

$$R_k e^{i\phi k} = y_k^{(1)} + i y_k^{(2)}$$

The means of choosing the filters is discussed in Ref 9, p 440. Filters 1 and 2 are, respectively, in-phase and in-quadrature filters; the phase shifts within the passbands of the two filters are approximately 0^o and 90^o, respectively, and the gain of each filter is approximately unity within the passband.

Thus if the signal is $x(t) = A \sin \omega t$, and ω is in the passbands of the two filters, then the outputs 0_1 and 0_2 are approximately

$$0_1 = A \sin \omega t \quad \text{and} \quad 0_2 = A \sin(\omega t + 90°) = A \cos \omega t.$$

Thus,

$$| 0_1 + 0_2 | \cong A$$

is a local amplitude estimate.

If amplitude only, and not phase, were of interest, then an in-phase filter plus a moving r.m.s. calculation could be used to compute local amplitudes.

The relationship between the width of the frequency interval over which the gain is approximately unity and the number of points required to be used in the (in-phase or in-quadrature) filter is of interest. The frequency

interval of the attainable filter with $2m + 1$ points and trapezoidal gain vs. frequency function is

$$f_o \pm \frac{1}{m\Delta t}$$

where

Δt = step size of the independent variable.

(See Figs 5-8, p. 441, Ref 6.)

Thus, if we wanted to pass irregularities in the range $f_o \pm \frac{f_o}{2}$, we would require

$$\frac{1}{m\Delta t} = \frac{f_o}{2} \quad , \quad \text{or} \quad m = \frac{2}{f_o \Delta t}$$

Then the total interval in the independent variable space within which data are required for each filter evaluation has length

$$2m\Delta t = \frac{4}{f_o} = 4\lambda_o$$

where λ_o is the wavelength corresponding to frequency f_o.

If we wanted a narrower passband, say $f_o \pm \frac{f_o}{4}$, the interval length would increase to $8\lambda_o$.

Thus, we have the same tradeoff here as with the digital resonator and the moving Fourier transform. The finer the resolution we require in the frequency domain, the more points must be used in each local amplitude calculation, and, hence, the less spatial resolution we have.

The filters discussed in this section are preferable to the methods discussed in preceding sections, in that the gain vs. frequency here is

trapezoidal with fairly sharp cutoff. Nonrecursive filters, however, tend to require sizeable amounts of computation time. For example, if $f_o = .1$ cycles/foot (.3281 cycles/meter) ($\lambda_o = 10$ feet or 3.281 meters), we want to pass irregularities in the range $f_o \pm \frac{f_o}{2}$, i.e., 6.7 feet $< \lambda <$ 20 feet (2.045 meters $< \lambda <$ 6.096 meters), and if $\Delta t = 2$ inches (5.08 centimeters), then the total number of points used in each filter evaluation, $2m + 1$, is 241. Even if we used the coarser sampling step size $\Delta t = 6$ inches (14.24 centimeters), we would have $2m + 1 = 81$.

Thus, we are motivated to investigate the more efficient recursive filters.

It is emphasized that the preference for recursive filters over nonrecursive ones is strictly on the basis of computational efficiency. The two classes of filters have equally wide flexibility, and, in fact, there exist methods to design a filter of one type which approximates the performance of a given filter of the other type (see Ref 17).

RECURSIVE FILTERS

Reference 15 includes an excellent discussion of several methods for designing digital filters. Because of the sharp cutoff characteristics compared to other types, the filter designed from the tangent form of the squared magnitude approximating function was selected.

The n^{th} order low-pass filter is designed to have squared gain of

$$\left|H(e^{i\omega\Delta t})\right|^2 = \frac{1}{1 + \dfrac{\tan^{2n}\dfrac{\omega\Delta t}{2}}{\tan^{2n}\dfrac{\omega_c\Delta t}{2}}}$$

The squared gain vs. frequency of the low-pass filters of several orders is displayed in Table A5.2 and Fig A5.5. Since filtering forward and then filtering the output backwards is required to achieve zero phase shift at all frequencies, and since the gain of a double filter is the squared gain of a

TABLE A5.2. SQUARED GAINS OF FILTERS SPECIFIED BY THE TANGENT FORM OF THE SQUARED-MAGNITUDE APPROXIMATING FUNCTION

FREQUENCY (cy./ft.)	WAVELENGTH (ft.)	ORDER 2	ORDER 4	ORDER 6	ORDER 8	ORDER 10
0.	---	1.00000E+00	1.00000E+00	1.00000E+00	1.00000E+00	1.00000E+00
5.00000E-03	2.00000E+02	9.99994E-01	1.00000E+00	1.00000E+00	1.00000E+00	1.00000E+00
1.00000E-02	1.00000E+02	9.99976E-01	1.00000E+00	1.00000E+00	1.00000E+00	1.00000E+00
1.50000E-02	6.66667E+01	9.99496E-01	1.00000E+00	1.00000E+00	1.00000E+00	1.00000E+00
2.00000E-02	5.00000E+01	9.98408E-01	9.99997E-01	1.00000E+00	1.00000E+00	1.00000E+00
2.50000E-02	4.00000E+01	9.96122E-01	9.99985E-01	1.00000E+00	1.00000E+00	1.00000E+00
3.00000E-02	3.33333E+01	9.91992E-01	9.99935E-01	9.99999E-01	1.00000E+00	1.00000E+00
3.50000E-02	2.85714E+01	9.85262E-01	9.99776E-01	9.99997E-01	1.00000E+00	1.00000E+00
4.00000E-02	2.50000E+01	9.75114E-01	9.99349E-01	9.99983E-01	1.00000E+00	1.00000E+00
4.50000E-02	2.22222E+01	9.60719E-01	9.98331E-01	9.99932E-01	9.99997E-01	1.00000E+00
5.00000E-02	2.00000E+01	9.41328E-01	9.96130E-01	9.99758E-01	9.99985E-01	9.99999E-01
5.50000E-02	1.81818E+01	9.16361E-01	9.91738E-01	9.99240E-01	9.99931E-01	9.99994E-01
6.00000E-02	1.66667E+01	8.85507E-01	9.83557E-01	9.97843E-01	9.99721E-01	9.99964E-01
6.50000E-02	1.53846E+01	8.48803E-01	9.69246E-01	9.94380E-01	9.98994E-01	9.99821E-01
7.00000E-02	1.42857E+01	8.06678E-01	9.45686E-01	9.86423E-01	9.96712E-01	9.99210E-01
7.50000E-02	1.33333E+01	7.59936E-01	9.09262E-01	9.69439E-01	9.90140E-01	9.96864E-01
8.00000E-02	1.25000E+01	7.09693E-01	8.56655E-01	9.35937E-01	9.72763E-01	9.88676E-01
8.50000E-02	1.17647E+01	6.57256E-01	7.86202E-01	8.75803E-01	9.31142E-01	9.62869E-01
9.00000E-02	1.11111E+01	6.03995E-01	6.99365E-01	7.80128E-01	8.44033E-01	8.91938E-01
9.50000E-02	1.05263E+01	5.51202E-01	6.01342E-01	6.49443E-01	6.94686E-01	7.36460E-01
1.00000E-01	1.00000E+01	5.00000E-01	5.00000E-01	5.00000E-01	5.00000E-01	5.00000E-01
1.05000E-01	9.52381E+00	4.51271E-01	4.03459E-01	3.57414E-01	3.13858E-01	2.73353E-01
1.10000E-01	9.09091E+00	4.05642E-01	3.17774E-01	2.41215E-01	1.78281E-01	1.28976E-01
1.15000E-01	8.69565E+00	3.63495E-01	2.45927E-01	1.57005E-01	9.61361E-02	5.72625E-02
1.20000E-01	8.33333E+00	3.24998E-01	1.88193E-01	1.00409E-01	5.09997E-02	2.52222E-02
1.25000E-01	8.00000E+00	2.90155E-01	1.43163E-01	6.39300E-02	2.71584E-02	1.12824E-02
1.30000E-01	7.69231E+00	2.58844E-01	1.08712E-01	4.08574E-02	1.46590E-02	5.16887E-03
1.35000E-01	7.40741E+00	2.30856E-01	8.26510E-02	2.63319E-02	8.05223E-03	2.43068E-03
1.40000E-01	7.14286E+00	2.05968E-01	6.30436E-02	1.71541E-02	4.50694E-03	1.17299E-03
1.45000E-01	6.89655E+00	1.83878E-01	4.83107E-02	1.13079E-02	2.57027E-03	5.80255E-04
1.50000E-01	6.66667E+00	1.64319E-01	3.72236E-02	7.54484E-03	1.49258E-03	2.93836E-04

NOTE: 1 foot = .3048 meters

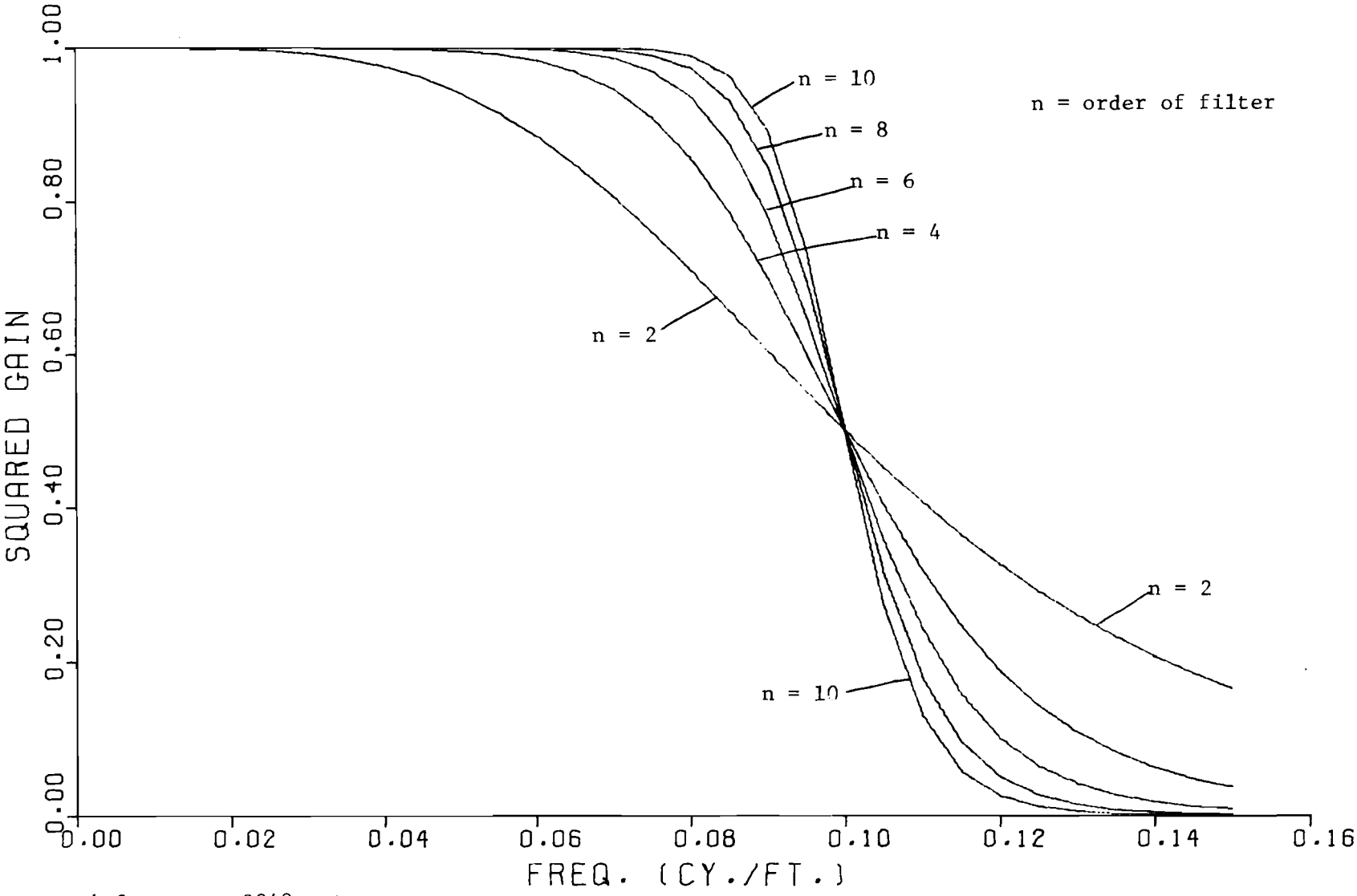

1 foot = .3048 meters

Fig A5.5. Squared gains of filters specified by the tangent form of the squared-magnitude approximating function.

single filter, Table A5.2 and Fig A5.5 also give the gain of the zero-phase double filter.

Design of the filter depends on the fact that

$$\tan^2 \frac{\omega \Delta t}{2} = \frac{-(Z-1)^2}{(Z+1)^2} ,$$

where

$$Z = e^{i\omega \Delta t} .$$

(See Reference 15, p 169.)

Thus, the squared magnitude function can be expressed as a rational polynomial in Z :

$$|H(Z)|^2 = \frac{\tan^{2n} \left(\frac{\omega_c \Delta t}{2}\right)}{\tan^{2n} \frac{\omega_c \Delta t}{2} + (-1)^n \left(\frac{Z-1}{Z+1}\right)^{2n}}$$

$Z = -1$ is obviously a zero of order $2n$.

The poles are derived in Reference 15, pp 159-160. The transformation $p = \frac{Z-1}{Z+1}$ is made, which allows derivation of the poles in terms of p .

Then we obtain the poles in terms of Z by the inverse transformation, $Z = \frac{1+p}{1-p}$.

Now, our rational polynomial is

$$|H(Z)|^2 = \frac{(Z+1)^{2n} \tan^{2n} \left(\frac{\omega_c \Delta t}{2}\right)}{(Z+1)^{2n} \tan^{2n} \frac{\left(\frac{\omega_c \Delta t}{2}\right)}{2} + (-1)^n (Z-1)^{2n}}$$

Note that the denominator (call it $D(Z)$) is a mirror image polynomial; that is, it is of the form $a_o + a_1 Z + \ldots + a_1 Z^{L-1} + a_o Z^L$. Thus, $D(Z) = Z^L D(Z^{-1})$ for all $Z \neq 0$, and the zeroes of $D(Z)$, which are the poles of $|H(Z)|^2$ and which are all nonzero, occur in reciprocal pairs. This is true because if $Z \neq 0$ and $D(Z) = 0$, then $D(Z^{-1}) = Z^{-L} D(Z) = 0$.

Thus, we must address the problem of filter stability, since half of the poles have magnitudes greater than unity.

It is proved on p 170, Ref 15, that the ratio of the distances from $re^{i\theta}$ and $1/re^{i\theta}$ to a point on the unit circle is a constant; i.e.,

$$\frac{|re^{i\theta} - e^{i\phi}|}{|1/re^{i\theta} - e^{i\phi}|} = C$$

Thus, for any Z on the unit circle,

$$|H(Z)|^2 = \frac{|1+Z|^{2n}}{\prod_{j=1}^{n} C_j D_j^2} K$$

where D_j and $C_j D_j$ denote the distance from the j^{th} reciprocal pair of poles with magnitudes less than one and greater than one, respectively, to the point Z , and K is a constant.

Following Ref 15, then, we discard n of the zeroes and n of the poles; from each reciprocal pair, the pole with magnitude greater than 1 is discarded.

Thus, we are left with

$$\frac{|1+Z|^n}{\prod_{j=1}^{n} D_j} = \sqrt{\frac{\left(\prod_{j=1}^{n} C_j\right)|H(Z)|^2}{K}} = |H(Z)| \; K_1$$

where K_1 is a constant.

Then, if n is even, we set

$$H(Z) = \frac{(Z+1)^n}{\prod_{j=1}^{n/2} (Z-P_j)\,(Z-P_j^*)} \; K_2$$

where (P_j , P_j^*) is the j^{th} pair of retained poles; the poles occur in complex conjugate pairs. If n is odd, one of the poles is real, and the others occur in complex conjugate pairs.

Note that we chose the poles to discard so as, effectively, to perform a square-root transformation on the squared-magnitude function. Then we defined $H(Z)$, not $[H(Z)]^2$, to equal the resulting rational polynomial in Z, thereby recovering the originally desired form of $|H(Z)|^2$.

We choose K_2 so that the gain at $\omega = 0$ is one:

$$|H(e^{i\omega\Delta t})|_{\omega=0} = |H(1)| = 1$$

If we multiply numerator and denominator of $H(Z)$ by Z^{-n}, the numerator and denominator both become n^{th} degree polynomials in Z^{-1}, and we can read the filter coefficients directly.

Now, similar techniques can be used to design a flat-topped bandpass filter. We would specify

$$\left|H(e^{i\omega\Delta t})\right|^2 = \frac{1}{1 + \dfrac{\tan^{2n}\dfrac{\omega\Delta t}{2}}{\tan^{2n}\dfrac{\omega_1\Delta t}{2}}} - \frac{1}{1 + \dfrac{\tan^{2n}\dfrac{\omega\Delta t}{2}}{\tan^{2n}\dfrac{\omega_2\Delta t}{2}}} ,$$

where the frequency interval (ω_2 , ω_1) is the passband.

Then upon combining the two terms into a rational polynomial with a common denominator, we would discover that both numerator and denominator were $(4n)^{th}$, not $(2n)^{th}$, degree polynomials in Z. Thus, the bandpass filter would involve about twice as many terms as a low-pass filter with comparably sharp cutoff (actually, $2n + 1$ vs. $4n + 1$ terms per filter evaluation).

If we were interested in a single passband, then, the difference in computational efficiency between using a bandpass filter or the difference between two low-pass filtered outputs would be trivial.

For the purposes of road profile analysis, however, we are in general interested in a set of contiguous passbands which cover a frequency interval of interest. It is more efficient, then, by almost a factor of 2 to use a set of low-pass filters, since filtering with passbands (f_1 , f_2), (f_2 , f_3), . . . (f_n , ∞) requires either low-pass filters with cutoff frequencies f_i, $i = 1 , \ldots n$, or $n - 1$ bandpass filters and a high-pass filter.

ARTIFICIAL TEST CASES WITH VARYING AMPLITUDES

In the preceding section, we discussed the design of the low-pass filter specified by the tangent form of the squared-magnitude function. We also argued the case for using differences between low-pass filtered outputs instead of bandpass filters to isolate roughness in contiguous frequency intervals.

The low-pass filter is acceptable from the standpoints of sharpness of cutoff and computational efficiency. We now turn our attention to local transient effects, which have been investigated for other signal-processing techniques.

As discussed in the general treatment of filtering techniques, it is possible to derive in closed form the steady-state response of a filter to a sinusoidal input. If, however, the amplitude of the input signal has large changes from half-cycle to half-cycle, as in a road profile, the steady-state solution may not be applicable. Thus, to study local transient effects, the following two types of artificial cases were used:

(1) 120 zeroes followed by one half-cycle of a sine wave with amplitude one followed by 120 zeroes.

(2) 120 zeroes followed by four cycles of a sine wave with amplitudes .333, .333, .667, .333, .333, 1.0, and .333 at the successive half-cycles, followed by 120 zeroes.

In each case, the step size of the independent variable was assumed to be two inches (5.08 centimeters), and the gain (of the zero phase, double filter) at frequency .1 cycles/foot (.3281 cycles/meter), i.e., at wavelength 10 feet (3.048 meters), was selected to be .5 .

The frequency of the sine wave was varied to study the relationship between transient distortion and proximity of the frequency to the edge of the passband.

Because of the linearity of filters of the type we are discussing, there is no need to consider interactions between different frequencies present in the same time series. The linearity property is proved in an earlier section.

Note that case (1) is the worst case in the sense that an amplitude change from 0 to a finite value to 0 in successive half-cycles is the greatest possible relative half-cycle to half-cycle amplitude variation - 100 percent of the maximum amplitude.

Figures A5.6, A5.7, and A5.8 display the filtered and unfiltered profiles for the 11.33 , 14.00 , and 20.00-foot (3.453, 4.267, and 6.048-meter)-wavelength signals. Again, since we are using artificial data, physical units are not indicated on the axes. The signal is identified by its wavelength in feet for convenience and illustration.

Tables A5.3 - A5.5 summarize the results for five signals, with wavelengths 11.33 , 12.67 , 14.00 , 16.67 , and 20.00 feet (3.453, 3.862, 4.267, 5.081, and 6.048 meters), all within the filter passband. The fourth, sixth, and tenth-order filters of the type discussed in the preceding section were used.

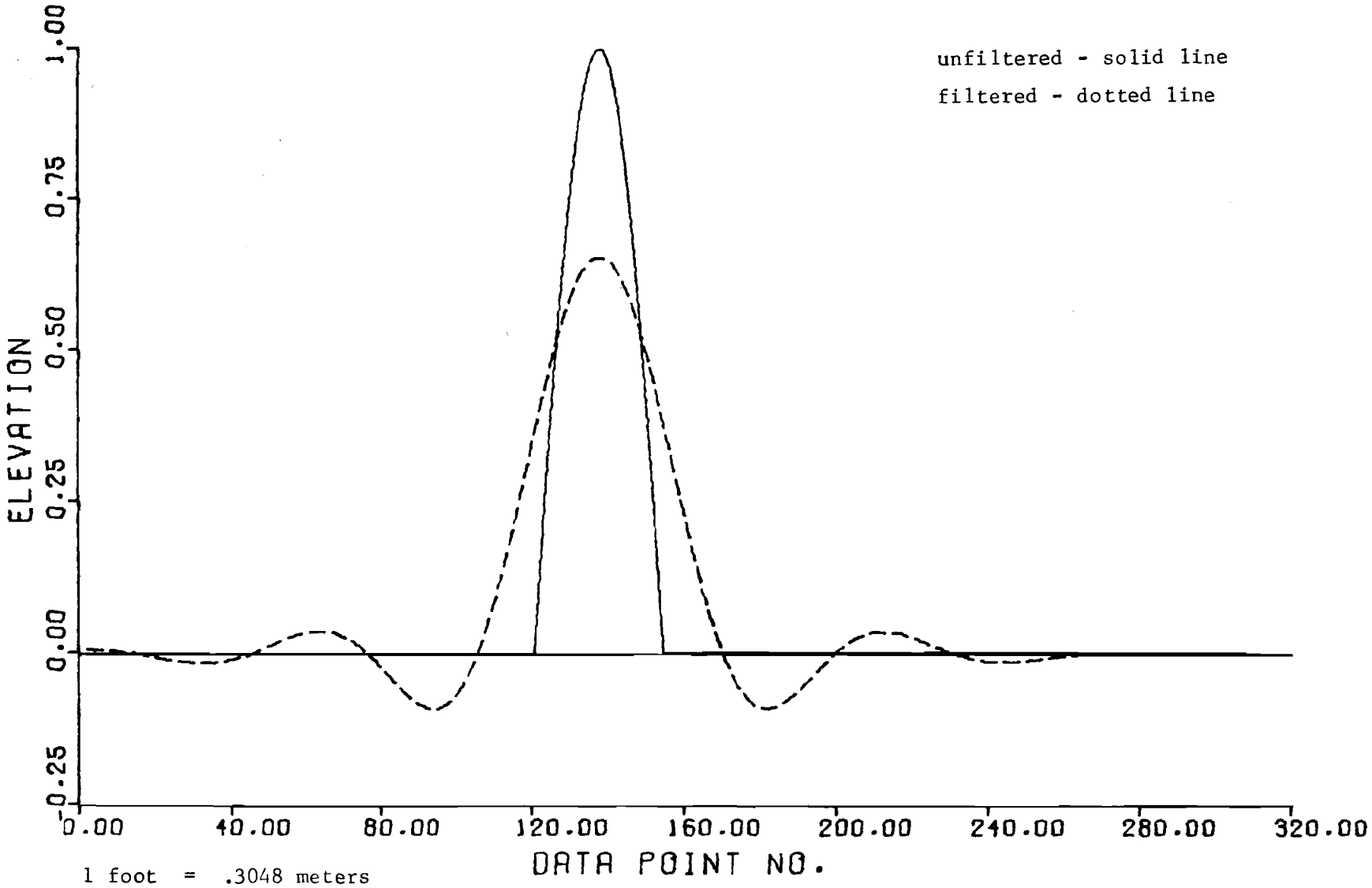

1 foot = .3048 meters

Fig A5.6. Filtered and unfiltered profiles for Case (1), 11.33-ft wavelength signal, sixth-order filter.

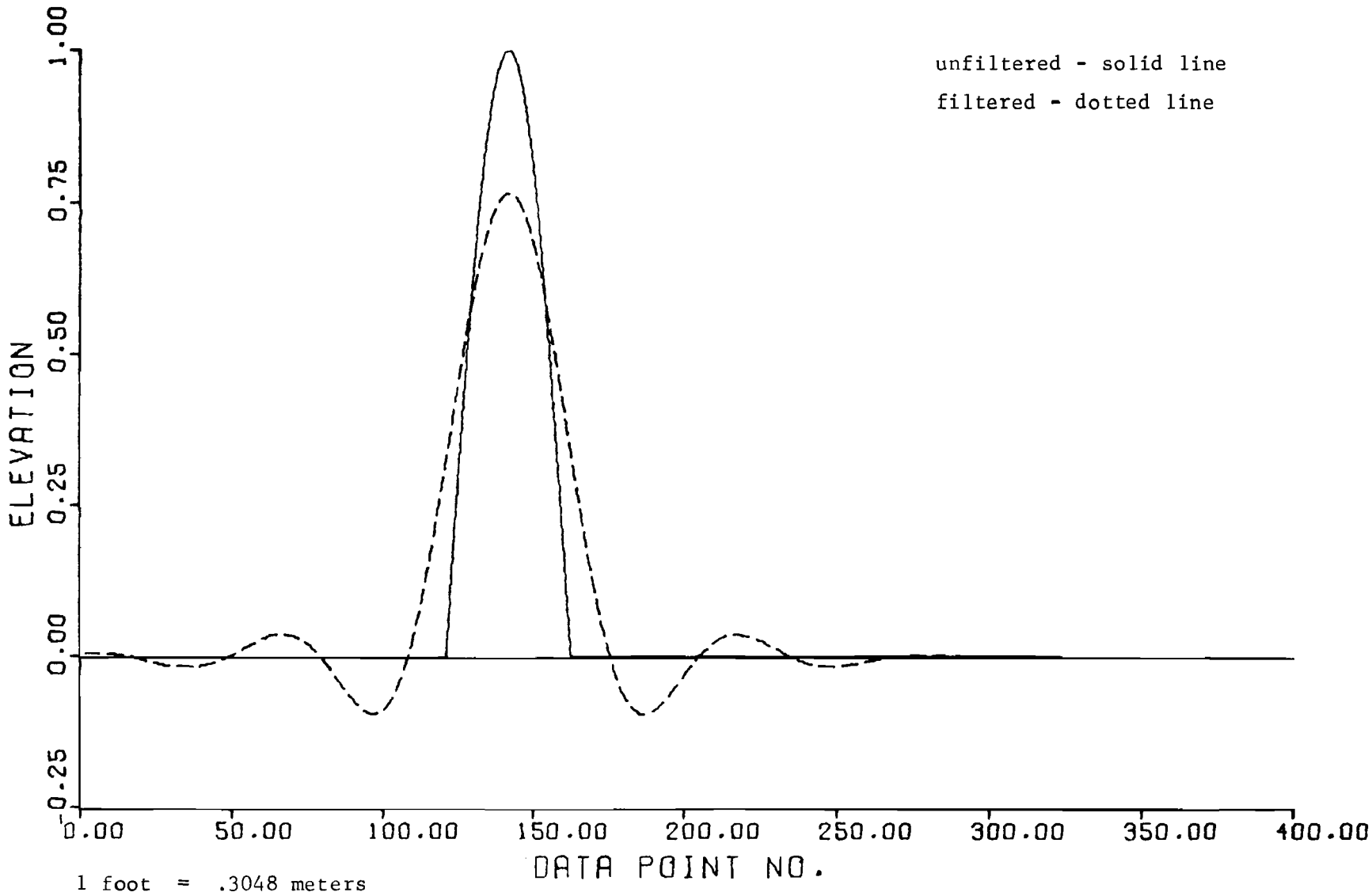

1 foot = .3048 meters

Fig A5.7. Filtered and unfiltered profiles for Case (1), 14-ft wavelength signal, sixth-order filter.

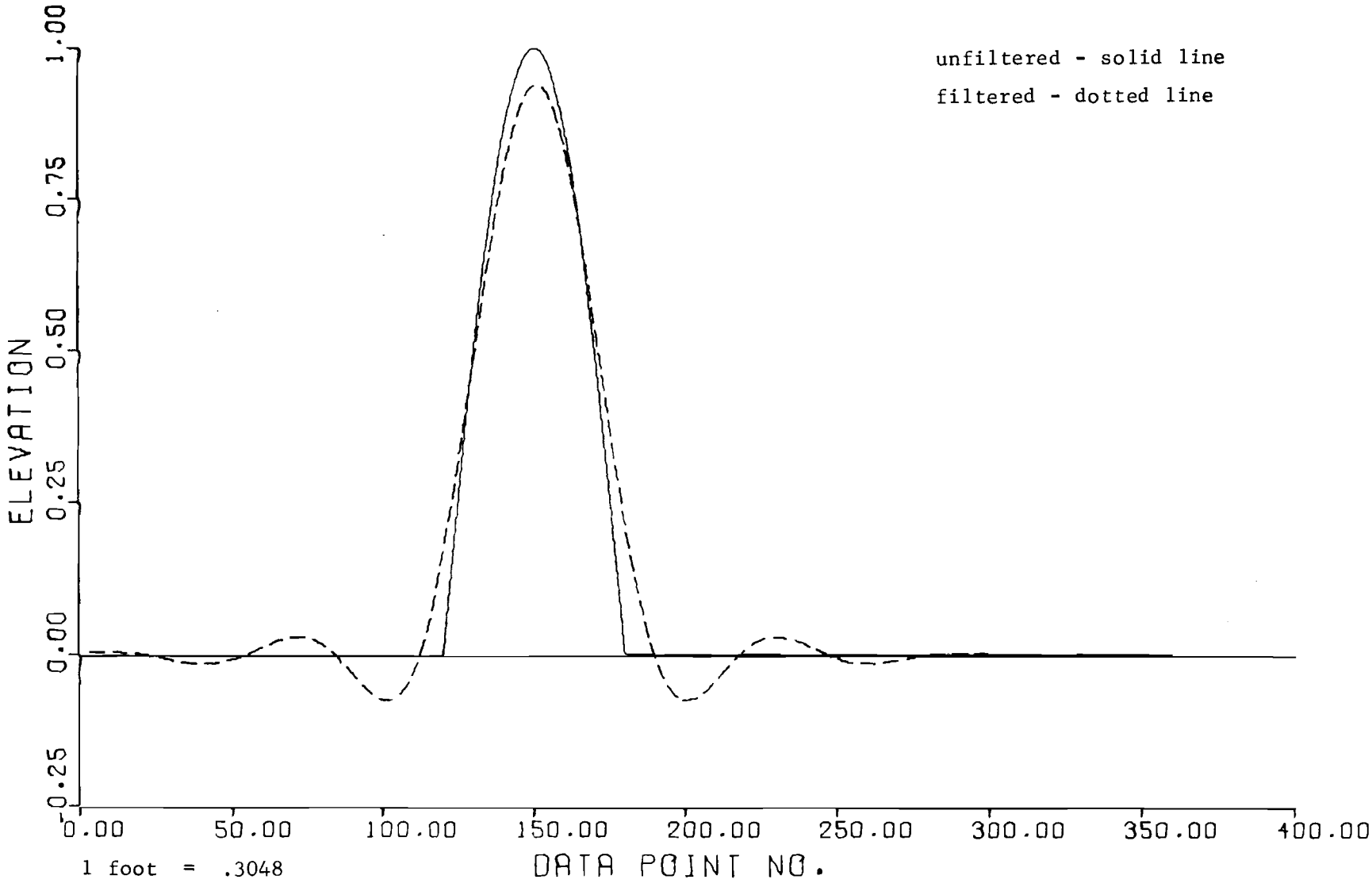

Fig A5.8. Filtered and unfiltered profiles for Case (1), 20-ft wavelength signal, sixth-order filter.

TABLE A5.3. TEST CASE: ZEROES FOLLOWED BY 1/2 CYCLE OF A SINE WAVE FOLLOWED BY ZEROES. FOURTH-ORDER FILTER.

			Unfiltered		Filtered			
Freq. (cy./ft.)	Wavelength (ft.)	Pts./ Cycle	Value At Peak	R.M.S. Value At Peak	Value At Peak	R.M.S.* Value At Peak	Magnitude, Filtered Value 1/2 Cycle Past Peak	Gain At Freq. of Signal
.088	11.33	68	1	.5	.657	.415	.170	.732
.079	12.67	76	1	.5	.714	.431	.050	.869
.071	14.00	84	1	.5	.765	.445	.044	.937
.060	16.67	100	1	.5	.852	.466	.068	.984
.050	20.00	120	1	.5	.930	.482	.037	.996

*The R.M.S. value was taken over one cycle at the wavelength of the signal.

NOTE: 1 foot = .3048 meters

TABLE A5.4. TEST CASE: ZEROES FOLLOWED BY 1/2 CYCLE OF A SINE WAVE FOLLOWED BY ZEROES. SIXTH-ORDER FILTER.

			Unfiltered		Filtered			
Freq. (cy./ft.)	Wavelength (ft.)	Pts./ Cycle	Value At Peak	R.M.S. Value At Peak	Value At Peak	R.M.S. Value At Peak	Magnitude, Filtered Value 1/2 Cycle Past Peak	Gain At Freq. of Signal
.088	11.33	68	1	.5	.655	.419	.027	.818
.079	12.67	76	1	.5	.714	.435	.066	.945
.071	14.00	84	1	.5	.767	.449	.088	.983
.060	16.67	100	1	.5	.857	.471	.083	.998
.050	20.00	120	1	.5	.940	.486	.036	1.000

NOTE: 1 foot = .3048 meters

TABLE A5.5. TEST CASE: ZEROES FOLLOWED BY 1/2 CYCLE OF A SINE WAVE FOLLOWED BY ZEROES. TENTH-ORDER FILTER.

			Unfiltered		Filtered			
Freq. (cy./ft.)	Wavelength (ft.)	Pts./ Cycle	Value At Peak	R.M.S. Value At Peak	Value At Peak	R.M.S. Value At Peak	Magnitude, Filtered Value 1/2 Cycle Past Peak	Gain At Freq. of Signal
.088	11.33	68	1	.5	.641	.414	.186	.925
.079	12.67	76	1	.5	.701	.431	.069	.991
.071	14.00	84	1	.5	.755	.446	.097	.999
.060	16.67	100	1	.5	.847	.467	.092	1.000
.050	20.00	120	1	.5	.932	.482	.032	1.000

NOTE: 1 foot = .3048 meters

As with the digital resonator, there are discrepancies at the first and last points of the input sine wave, where the input has discontinuous derivatives. As discussed previously, this effect may be unrealistically conducive to filter-induced distortion, since traffic would tend gradually to remove discontinuous derivatives if they were present. Thus, the importance of the discrepancies at the discontinuous points should not be overemphasized.

The r.m.s. value at the peak, which is given in the tables, is defined to be

$$\sqrt{\frac{1}{u - L + 1} \sum_{j=j_o-L}^{j_o+u} x_{j_o+j}^2}$$

where X_{jo} is the filtered elevation where the peak occurred in the input time series, and u and L are chosen so that the sum is taken over one cycle at the wavelength of the input signal.

It is interesting to compare the filtered and unfiltered values; ideally they should be the same if the signal is in the passband. Realistically, we know that any signal processing technique will introduce some distortion near the edge of the passband.

The following points are of interest.

(1) As expected, the distortion (the difference between the filtered and unfiltered values) decreases as we move away from the edge of the passband.

(2) The filtered values at the peak are <u>smaller</u> in all cases than the gain at the frequency of the signal. This is the local transient effect caused by the very sharp amplitude change.

(3) The local r.m.s. value taken over one cycle at the wavelength of the signal at the peak is less distorted than the filtered value at the peak. This was expected, because the amplitudes of 0 , 1 , and 0 at successive half cycles are smoothed somewhat by the filtering process.

(4) Except for the 11.33-foot (3.453-meter) case, the amplitude 1/2 cycle past the peak, i.e., at the peak of the first spurious half cycle introduced by the filter, is relatively small.

There are two types of distortion near the edge of the passband. The first type is due to the fact that the gain decreases gradually from one to

zero; it is impossible to design a filter with a rectangular gain vs. frequency function. The second is the local transient effect.

The first type can be made arbitrarily small by making the order of the filter large.

As can be seen from Tables A5.3 - A5.5, however, the transient effect, which can be thought of as the difference between the gain and the filtered value at the peak, increases as the order increases.

The tables indicate that the filtered values vary only in the third decimal place from order to order. Thus, for this test case, a decrease in one type of distortion is achieved only at the expense of an increase in the other type of distortion.

Table A5.6 summarizes the results of the test case discussed above for five wavelengths, 2, 4, 6, 8, and 10 feet (.6096, 1.219, 1.829, and 2.438 meters), all not in the passband. The main point here is that the filter cutoff is not as sharp as the gain vs. frequency curve would indicate in this test case with rapidly changing amplitudes.

It must be remembered that the test was chosen because of its extreme characteristics of the type conducive to filtering distortion.

Test case (2) described above also employs a signal with rapidly changing amplitude, but case (2) is not as conducive to distortion as case (1) is. The results from the case (2) experiments are given in Tables A5.7 - A5.9. Generally, the same types of effects are observed as in case (1), but the distortion is somewhat less.

Figures A5.9 - A5.11 display the filtered and unfiltered profiles for case (2) for 11.33 , 14.00 , and 20.00-foot (3.453, 4.267, and 6.048-meter)-wavelength signals.

Note that, for wavelengths of 14 feet (4.267 meters) or larger, the maximum and r.m.s. errors of the moving r.m.s. values are .059 and .029 or less for all three filters. The errors are somewhat smaller for the sixth and tenth order filters - .047 and .023 or less for the maximum and r.m.s. errors, respectively. The maximum errors, which occur near the largest peak of the input time series, should be compared to the local r.m.s. value of .50 centered at that peak.

Table A5.10 gives the filtered values at the peak in case (1) and at the sixth peak in case (2) for the sixth order filter. Thus, we can compare the

TABLE A5.6. TEST CASE: ZEROES FOLLOWED BY 1/2 CYCLE OF A SINE WAVE FOLLOWED BY ZEROES. SINE WAVE IS ONE AT PEAK. SIXTH ORDER FILTER. SIGNAL OUT OF PASSBAND.

			Unfiltered		Filtered			
Freq. (cy./ft.)	Wavelength (ft.)	Pts./ Cycle	Value At Peak	R.M.S. Value At Peak	Value At Peak	R.M.S. Value At Peak	Magnitude, Filtered Value 1/2 Cycle Past Peak	Gain At Freq. of Signal
.500	2	12	1	.5	.125	.122	.116	3.13×10^{-9}
.250	4	24	1	.5	.252	.231	.187	1.58×10^{-5}
.167	6	36	1	.5	.374	.310	.183	.0021
.125	8	48	1	.5	.487	.363	.117	.0639
.100	10	60	1	.5	.591	.400	.027	.5000

NOTE: 1 foot = .3048 meters

TABLE A5.7. TEST CASE: ZEROES FOLLOWED BY FOUR CYCLES OF A SINE WAVE WITH AMPLITUDE VARYING FROM HALF-CYCLE TO HALF-CYCLE. THE AMPLITUDES FOR THE EIGHT HALF CYCLES ARE GIVEN BELOW. FOURTH-ORDER LOW-PASS FILTER.

Freq. (cy./ft.)	Wavelength (ft.)	Pts./ Cycle	Magnitudes of Filtered Values at the Peaks							
			1	2	3	4	5	6	7	8
.088	11.33	68	.236	.244	.464	.257	.259	.681	.250	.240
.079	12.67	76	.271	.298	.529	.320	.329	.766	.314	.278
.071	14.00	84	.289	.329	.568	.346	.363	.823	.352	.294
.060	16.67	100	.305	.351	.611	.349	.372	.896	.374	.305
.050	20.00	120	.319	.345	.643	.341	.355	.953	.357	.318
Amplitude of Input Time Series			.333	.333	.667	.333	.333	1.0	.333	.333

R.M.S. Error* Moving R.M.S. Value**	Max Error Moving R.M.S. Value	Gain at Freq. of Sine Wave	Filtered Value ½ cycle Past last peak
.078	.132	.732	.015
.047	.088	.869	.029
.029	.059	.937	.029
.014	.029	.984	.021
.007	.014	.996	.011

* Points from 1/2 cycle before to 1/2 cycle after the sine waves were used in the r.m.s. error calculation.

** The r.m.s. values were each taken over one cycle at the wavelength of the signal.

NOTE: 1 foot = .3048 meters

TABLE A5.8. TEST CASE: ZEROES FOLLOWED BY FOUR CYCLES OF A SINE WAVE WITH AMPLITUDE VARYING FROM HALF-CYCLE TO HALF-CYCLE. THE AMPLITUDES FOR THE EIGHT HALF CYCLES ARE GIVEN BELOW. SIXTH-ORDER LOW-PASS FILTER.

Freq. (cy./ft.)	Wavelength (ft.)	Pts./ Cycle	Magnitudes of Filtered Values at the Peaks							
			1	2	3	4	5	6	7	8
.088	11.33	68	.257	.268	.492	.295	.294	.705	.274	.264
.079	12.67	76	.288	.321	.557	.363	.372	.791	.343	.301
.071	14.00	84	.299	.348	.584	.375	.396	.840	.378	.308
.060	16.67	100	.305	.365	.617	.352	.384	.904	.392	.302
.050	20.00	120	.321	.347	.648	.340	.354	.960	.359	.318
Amplitude of input time series			.333	.333	.667	.333	.333	1.000	.333	.333

R.M.S. Error** Moving R.M.S. Value*	Max Error Moving R.M.S. Value	Gain at Freq. of Sine Wave	Filtered Value ½ cycle Past last peak
.063	.114	.818	.036
.034	.071	.945	.045
.022	.046	.983	.034
.012	.025	.998	.021
.006	.013	1.000	.011

NOTE: 1 foot = .3048 meters

TABLE A5.9. TEST CASE: ZEROES FOLLOWED BY FOUR CYCLES OF A SINE WAVE WITH AMPLITUDE VARYING FROM HALF-CYCLE TO HALF-CYCLE. THE AMPLITUDES FOR THE EIGHT HALF CYCLES ARE GIVEN BELOW. TENTH-ORDER LOW-PASS FILTER

Freq. (cy./ft.)	Wavelength (ft.)	Pts./ Cycle	Magnitudes of Filtered Values at the Peaks							
			1	2	3	4	5	6	7	8
.088	11.33	68	.281	.293	.518	.327	.323	.721	.291	.280
.079	12.67	76	.295	.330	.574	.396	.403	.802	.353	.309
.071	14.00	84	.302	.350	.581	.388	.410	.837	.384	.311
.060	16.67	100	.296	.370	.608	.342	.381	.893	.400	.287
.050	20.00	120	.315	.336	.640	.330	.347	.949	.350	.312
Amplitude of input time series			.333	.333	.667	.333	.333	1.000	.333	.333

R.M.S. Error** Moving R.M.S. Value*	Max Error Moving R.M.S. Value	Gain at Freq. of Sine Wave	Filtered Value ½ cycle Past last peak
.054	.104	.925	.046
.030	.066	.991	.053
.023	.047	.999	.034
.014	.028	1.000	.018
.009	.017	1.000	.014

NOTE: 1 foot = .3048 meters

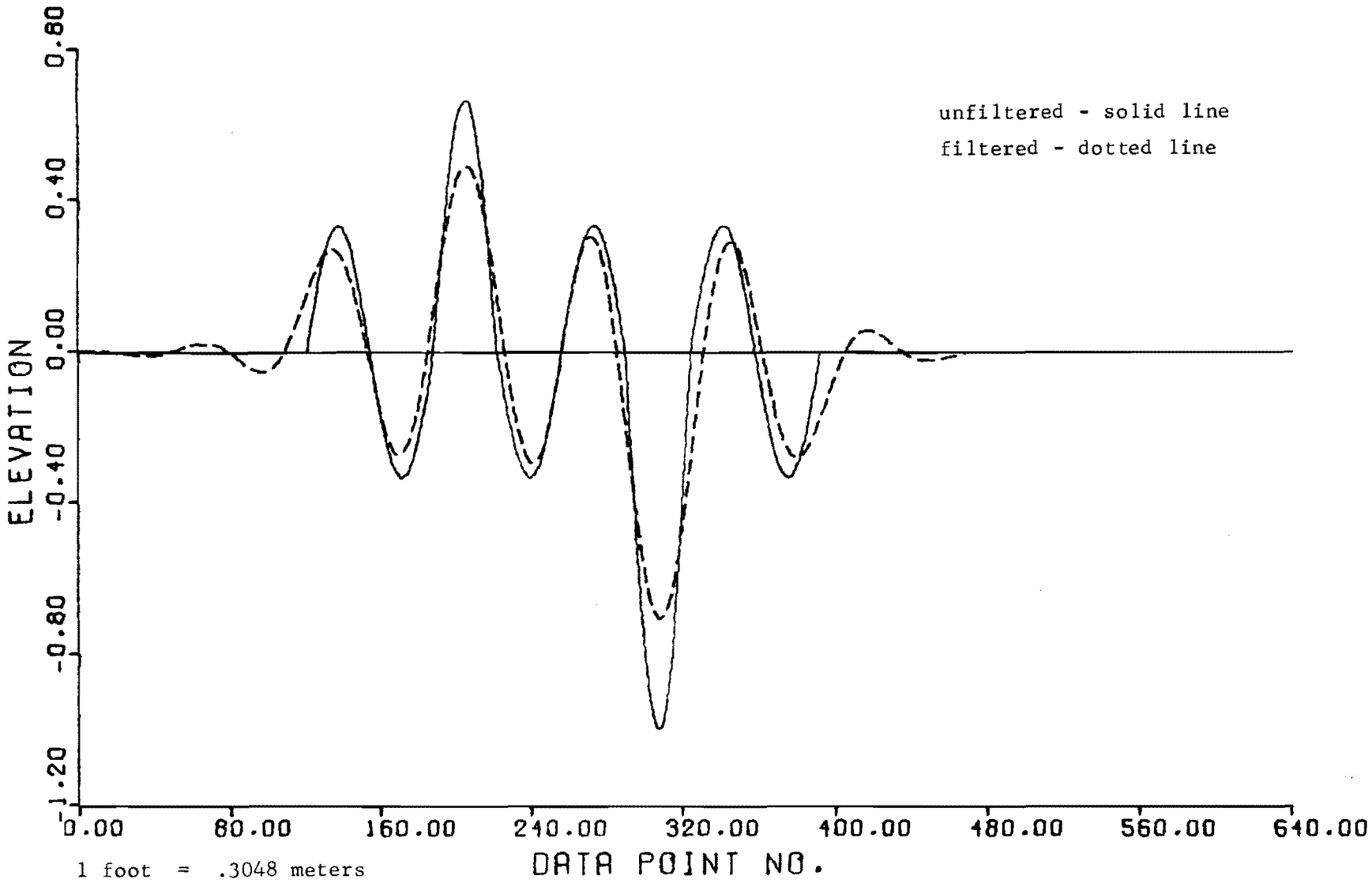

Fig A5.9. Filtered and unfiltered profiles for Case (2), 11.33-ft wavelength signal, sixth-order filter.

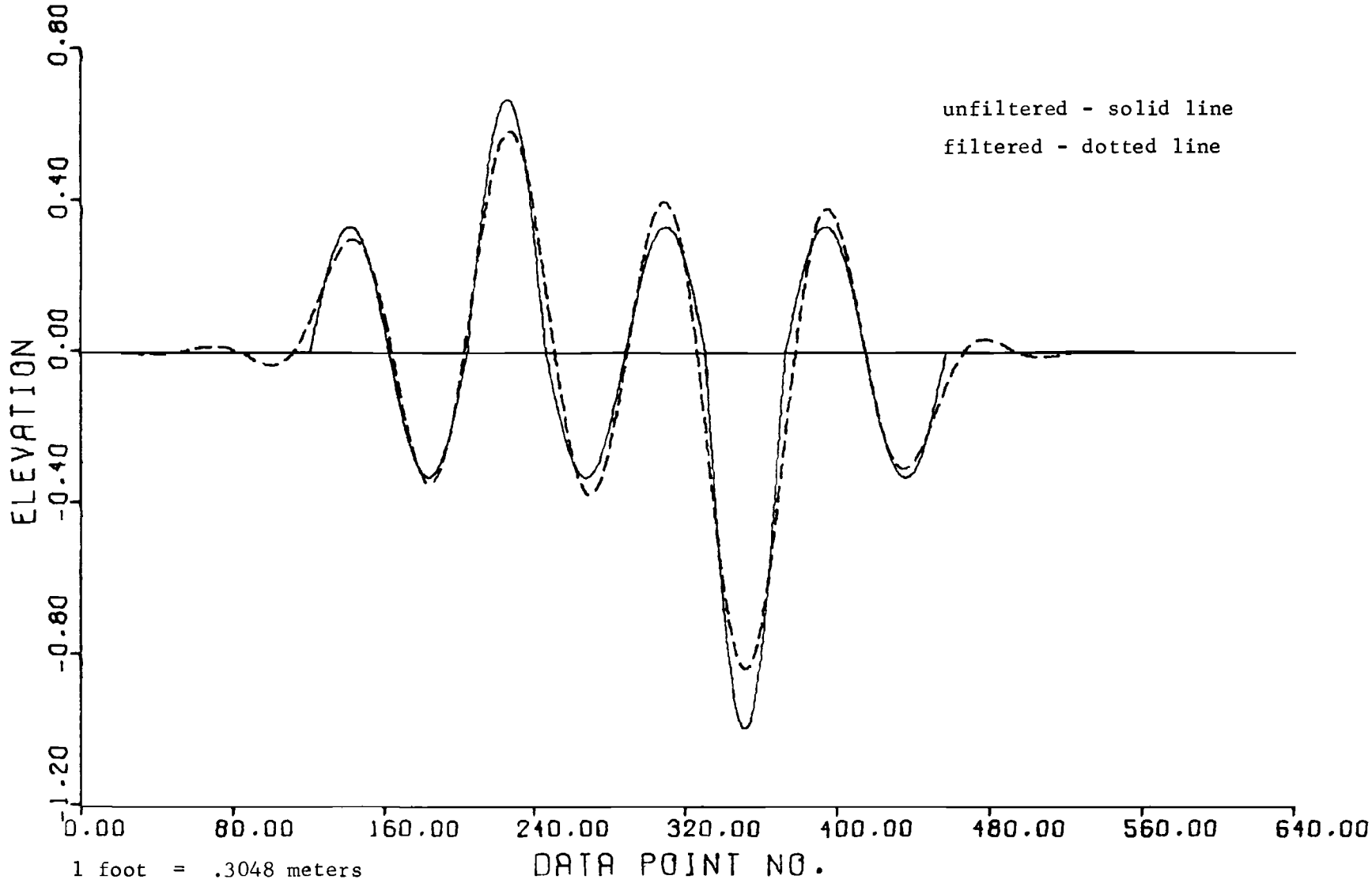

Fig A5.10. Filtered and unfiltered profiles for Case (2), 14-ft wavelength signal, sixth-order filter.

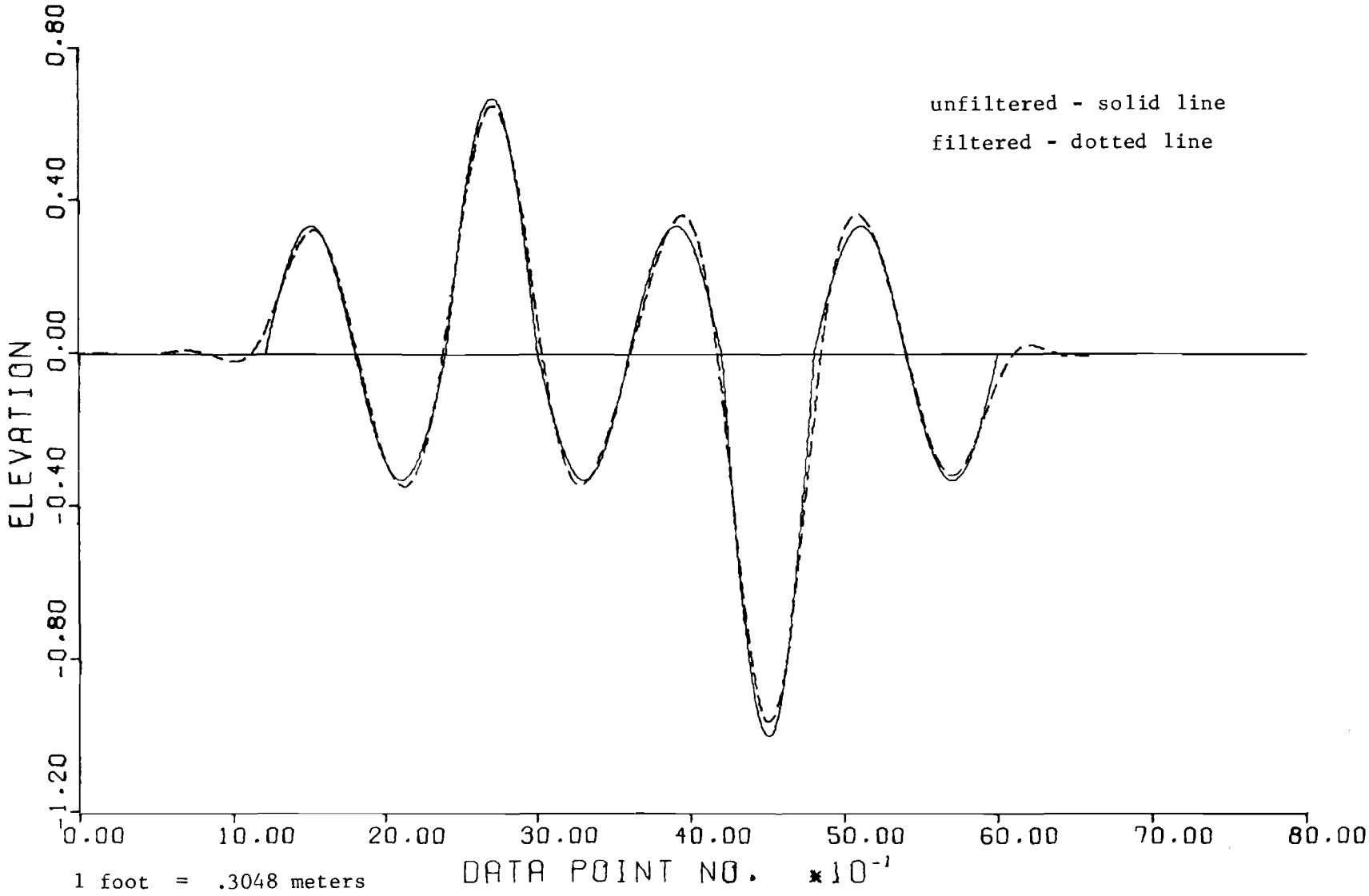

1 foot = .3048 meters

Fig A5.11. Filtered and unfiltered profiles for Case (2), 20-ft wavelength signal, sixth-order filter.

TABLE A5.10. LOCAL TRANSIENT COMPARISONS

Wavelength (ft.)	Filtered Values: At Peak, Case (1)	Filtered Values: At 6th Peak, Case (2)
11.33	.655	.705
12.67	.714	.791
14.00	.767	.840
16.67	.857	.904
20.00	.940	.960
Amplitude of input time series	1.000	1.000

NOTE: 1 foot = .3048 meters

TABLE A5.11. COMPARISON OF DISTORTION INTRODUCED BY DIGITAL RESONATOR AND LOW-PASS FILTER

Digital Resonator: $\Delta\omega$, % of Frequency of Signal	Digital Resonator: A	6th Order Low-Pass Filter: Wavelength (ft.)	6th Order Low-Pass Filter: A
10	.072	11.33	.682
25	.167	12.67	.780
33	.656	14.00	.855
50	.745	16.67	.941
		20.00	.976

A = Amplitude of filtered output at either of the two points where the original peaks with amplitude one occurred.

NOTE: 1 foot = .3048 meters

distortion when the amplitude changes from 0 to 1 to 0 with the distortion when the amplitude changes from 1/3 to 1 to 1/3 .

One might ask whether the results would differ greatly if the sampling rate were decreased or the cutoff frequency were changed; the two questions are really the same - does changing the number of points per cycle at the cutoff frequency change the results significantly.

Test case (1) was run for a 14-foot (4.267-meter) and a 20-foot (6.048-meter)-wavelength signal with a step size of 2 feet (.6048 meters) to study this question.

The r.m.s. values at the peak after filtering for the 2-inch (.0504-meter) and 2-foot (.6048-meter) cases are, respectively,

(1) .4492 and .4429 for the 14-foot (4.267-meter) signal and
(2) .4861 and .4825 for the 20-foot (6.048-meter) signal.

Thus, a decrease in the sampling rate by a factor of 12 increases the distortion only in the third decimal place. The differences are considered trivial, since they are less than the expected measurement errors.

For purposes of comparison of the low-pass filter discussed above with the digital resonator, results obtained using the "easier" test case of zeroes followed by one cycle of a sine wave with amplitude one followed by zeroes are presented in Table A5.11. This test case was used to illustrate the distortion and the frequency resolution of the digital resonator. Since the resonator was inadequate for this case, there was no point in testing it with the more difficult half-cycle case.

Note that except for the 11.33-foot (3.453-meter)-wavelength case, which is very near the edge of the passband, the low-pass filter induces less distortion than the digital resonator even when $\Delta w = 50\%$ of the frequency of the signal. (See also Table A5.1 and Fig A5.4.) The frequency of the signal was the resonant frequency of the simpler filter.

ILLUSTRATIVE EXAMPLES

Two asphalt surface-treated sections on the Old San Antonio Road near Bryan, Texas, were chosen to illustrate the type of information which can be obtained by filtering. The two-lane road is very rough, the SI (serviceability index) values being 1.7 and 2.4 for sections 2 and 3. Although swelling clay distress is present, there is severe roughness other than the relatively long waves typical of swelling clay.

The sixth-order low-pass filter[1] discussed in the preceding section was used successively to isolate the roughness in the set of passbands, 0 to 10, 10 to 30, 30 to 60, and 60 to 100-foot (0 to 3.048, 3.048 to 9.144, 9.144 to 18.29, and 18.29 to 30.48-meter) wavelength. This particular set was chosen for illustration; the number and widths of the passbands can be varied; an analysis of the same sections using a different set of passbands is presented in Chapter 3 for the purpose of demonstrating the SI models. Here we will emphasize physical characterization of roughness via digital filtering.

Central measures of roughness, the mean and fiftieth percentile points of the local r.m.s. values, are computed for both wheelpaths and for the point-wise difference between the road elevations in the two wheelpaths; the latter time series describes the vehicle rolling effect. The seventy-fifth, ninetieth, ninety-fifth, and ninety-ninth percentile points are measures of extreme roughness within the sections.

In each case, the local r.m.s. values are taken over the longest wavelength in the passband; e.g., for the 10 to 30-foot (3.048 to 9.144-meter) band, each r.m.s. calculation involves the data within a 30-foot (9.144-meter) interval along the road.

Tables A5.12 and A5.13 display the results. The following are points of interest.

(1) The results are consistent with the SI values in that the r.m.s. amplitudes are smaller for the section with the higher SI.

(2) As is true for most roads, which, like the Old San Antonio Road, have no curb or shoulder, the outside (right) wheelpath is rougher than the left. Except for the 0 to 10-foot (0 to 3.048-meter) passband for section 3, all the amplitudes are larger for the right wheelpath than for the left.

[1] Arguments for using low-pass filter differences as bandpass filters are given above.

TABLE A5.12. OLD SAN ANTONIO RD. - SEC. 2

SUMMARY STATISTICS FOR ROUGHNESS AMPLITUDES (IN.)

SI = 1.7

Series	Standard Deviation	Mean	Percentiles 50	75	90	95	99
		0.0 to 10.0 ft. Wavelengths					
Right	.02668	.05256	.04593	.05950	.08854	.11151	.15256
Left	.02450	.04246	.03659	.04421	.06382	.10024	.14565
Right-Left	.03921	.06936	.05633	.07773	.11270	.16134	.22288
		10.0 to 30.0 ft. Wavelengths					
Right	.05017	.09927	.08220	.11655	.18129	.21012	.23394
Left	.03129	.05318	.04166	.07254	.09295	.10984	.16423
Right-Left	.04872	.10708	.09296	.14974	.18510	.20042	.21208
		30.0 to 60.0 ft. Wavelengths					
Right	.11185	.18715	.16362	.19872	.32359	.47174	.54157
Left	.05700	.09540	.08753	.10931	.16569	.24435	.27728
Right-Left	.07752	.13327	.12425	.17655	.24604	.28023	.32190
		60.0 to 100.0 ft. Wavelengths					
Right	.09885	.22522	.19272	.32802	.37027	.37918	.39369
Left	.07989	.18539	.18143	.26710	.30136	.30787	.31551
Right-Left	.05588	.12506	.09674	.16329	.22186	.25268	.26333

NOTE: 1 foot = .3048 meters

1 inch = 2.540 centimeters

TABLE A5.13. OLD SAN ANTONIO RD. - SEC. 3

SUMMARY STATISTICS FOR ROUGHNESS AMPLITUDES (IN.)

SI = 2.4

Series	Standard Deviation	Mean	Percentiles 50	75	90	95	99
		0.0 to 10.0 ft. Wavelengths					
Right	.01025	.03768	.03647	.04313	.04996	.05699	.07336
Left	.01970	.04363	.04032	.05302	.07307	.08396	.10114
Right-Left	.01959	.05874	.05744	.06951	.08569	.09791	.10830
		10.0 to 30.0 ft. Wavelengths					
Right	.02427	.05863	.05103	.07724	.09579	.10253	.11527
Left	.02191	.03585	.03285	.04354	.05792	.08479	.11480
Right-Left	.02619	.06864	.06534	.08722	.09925	.11373	.14964
		30.0 to 60.0 ft. Wavelengths					
Right	.02531	.07356	.07266	.08911	.11245	.11889	.12472
Left	.01803	.03368	.02953	.05057	.05787	.06122	.06949
Right-Left	.02820	.06798	.06991	.09156	.10869	.11290	.11910
		60.0 to 100.0 ft. Wavelengths					
Right	.05674	.09764	.08035	.12287	.19765	.22199	.23173
Left	.03087	.06303	.05171	.07541	.12180	.13045	.13838
Right-Left	.03720	.09925	.09657	.12895	.15343	.16259	.17422

NOTE: 1 foot = .3048 meters

1 inch = 2.540 centimeters

(3) The right minus left amplitudes are larger than the right or left amplitudes for the 0 to 10-foot (0 to 3.048-meter) passband, but the right and left amplitudes increase relative to the difference amplitudes as the wavelength increases.

Figure A5.12 displays the left profile of section 2 and the filtered profile containing 0 to 10-foot (0 to 3.048-meter)-long waves. Due to the presence of roughness with wavelengths within a wide band in the unfiltered profile, it is difficult at times to spot what effects the filter should and should not respond to. Note, however, the identifiable short-wavelength roughness in the unfiltered profile near the right edge of Fig A5.12. The same roughness pattern, with the long-wavelength dip removed, is present in the filtered profile. Effects in the two profiles occur at very nearly the same position along the road; thus, as we have argued above, the filter does not introduce a phase shift. Recall that the zero-phase-shift characteristics are achieved by filtering the raw profile forward and then filtering the output backwards to obtain the final results.

The sharp dip at about 330 feet (100.6 meters) has wavelength near 10 feet (3.048 meters); thus, as expected, since it is near the edge of the filter passband, it is present in the filtered profile at reduced amplitude.[2] This dip contributes to the roughness measures for both the 0 to 10-foot (0 to 3.048-meter) and 10 to 30-foot (3.048 to 9.144-meter) passbands.

The filtered profile for 60 to 100-foot (18.29 to 30.48-meter) wavelengths is displayed along with the raw profile in Fig A5.13. It is even more difficult here to identify by eye what the filter should remove, since there are surface irregularities with both longer and shorter wavelengths which are not in the passband. Note, however, the identifiable waves in the passband in Fig A5.13, from about position 360 feet (109.7 meters) to 600 feet (182.9 meters). The almost unrealistically regular sinusoidal appearance of the filtered profile is due at least partly to the removal by the filter of the high-frequency waves. Even if the regular sinusoidal shape is partly due to filter-induced distortion, the amplitudes are very realistic, and, again, there appears to be no phase shift. Certainly, the filtered profile is adequate for computing local measures of roughness.

---

[2] Interpretation here is difficult. The "V" should probably be viewed as a longer wave with short waves superimposed - the filter responds only to the short waves composing the small v which appears in the filtered profile.

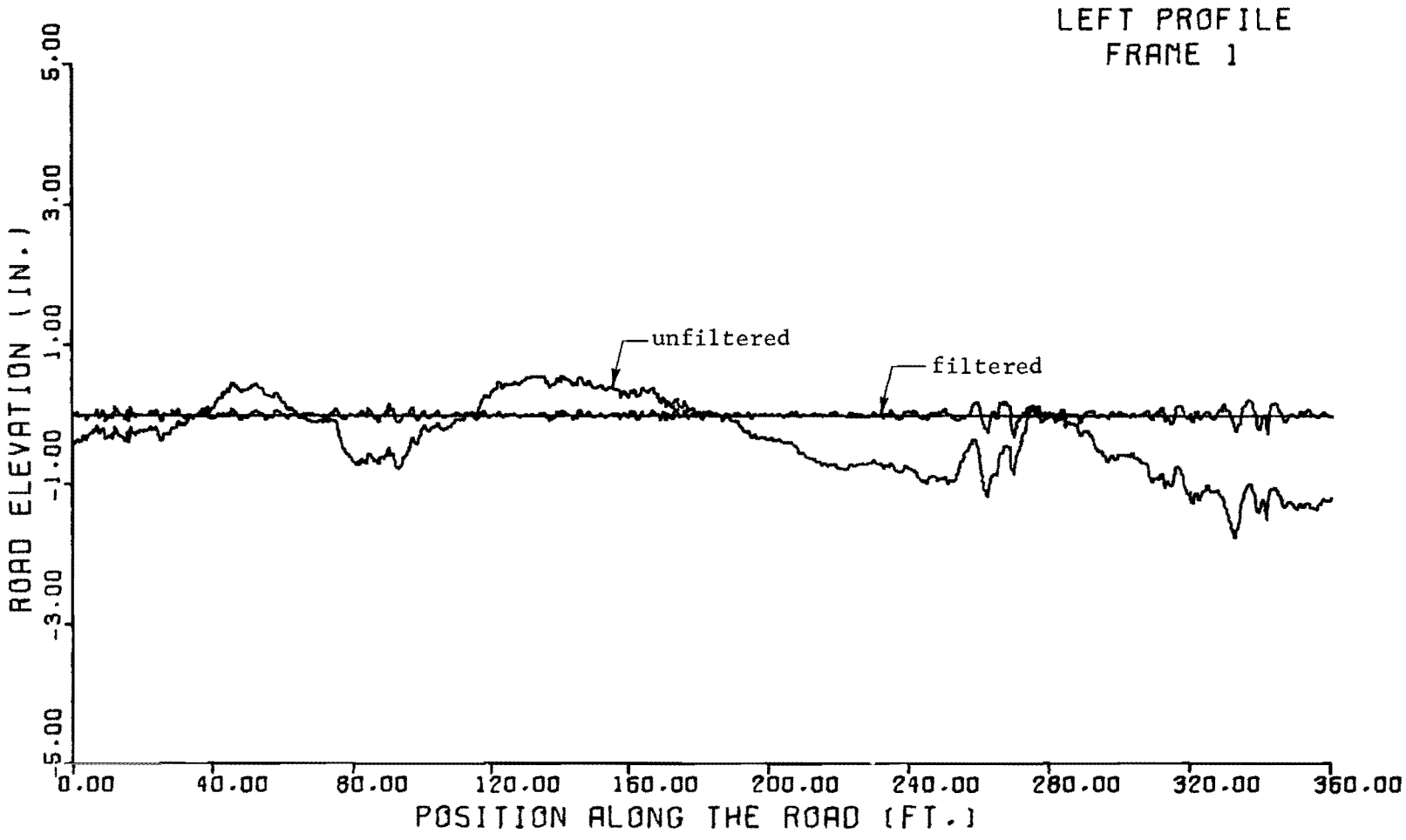

1 foot = .3048 meters
1 inch = 2.540 centimeters

Fig A5.12. Old San Antonio Road, Section 2: Filter Passband. (continued)
0 to 10 feet

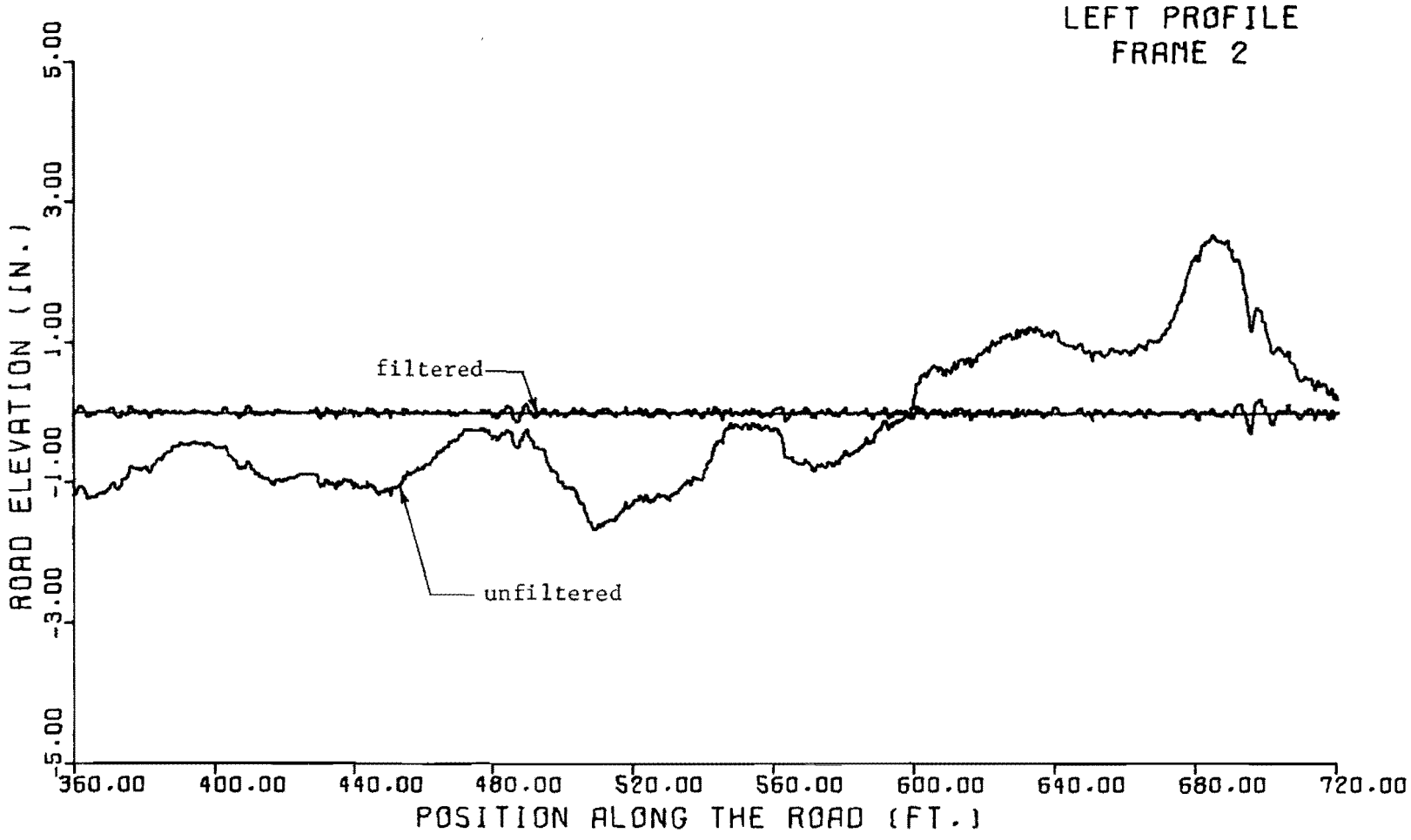

Fig A5.12. (continued)

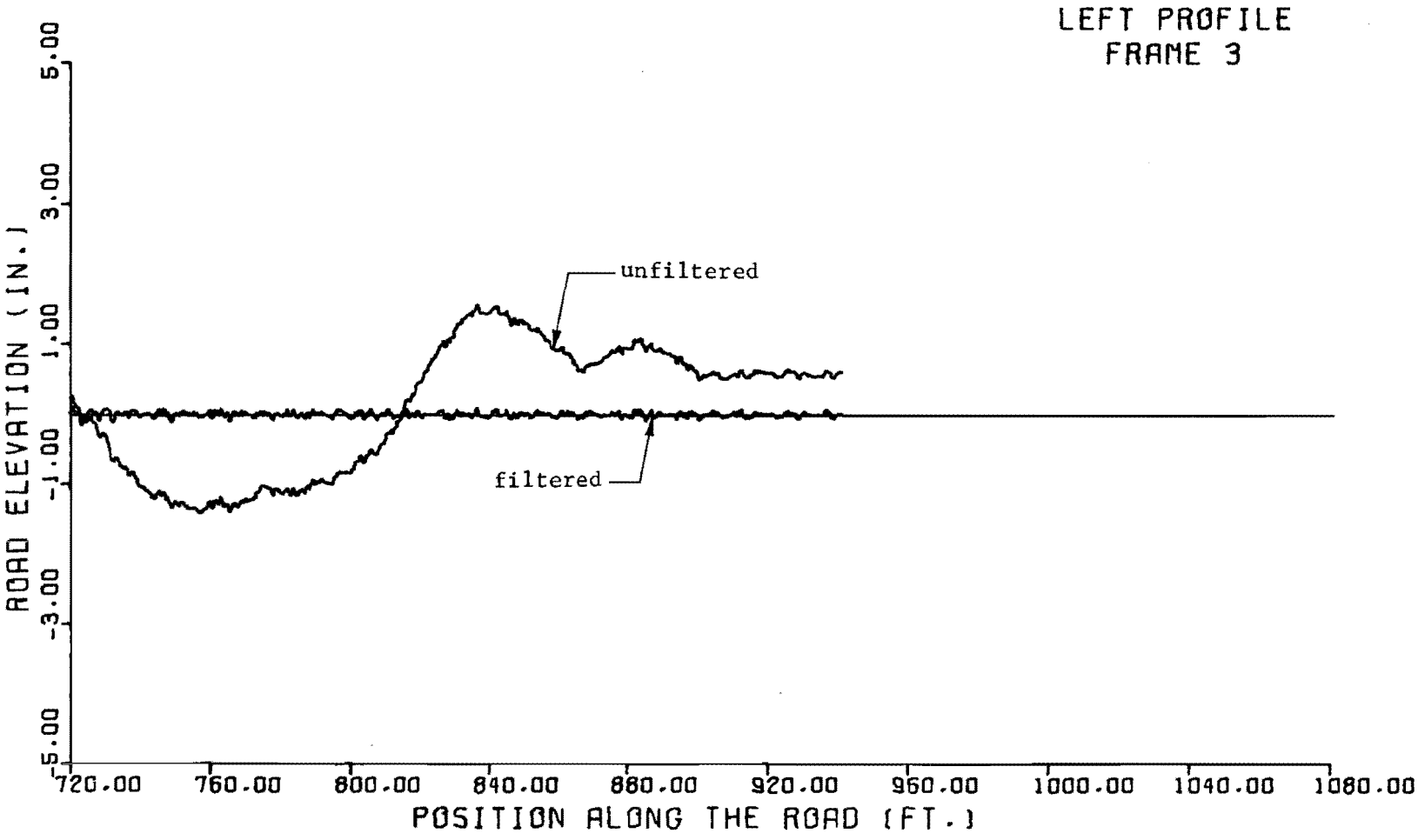

Fig A5.12. (continued)

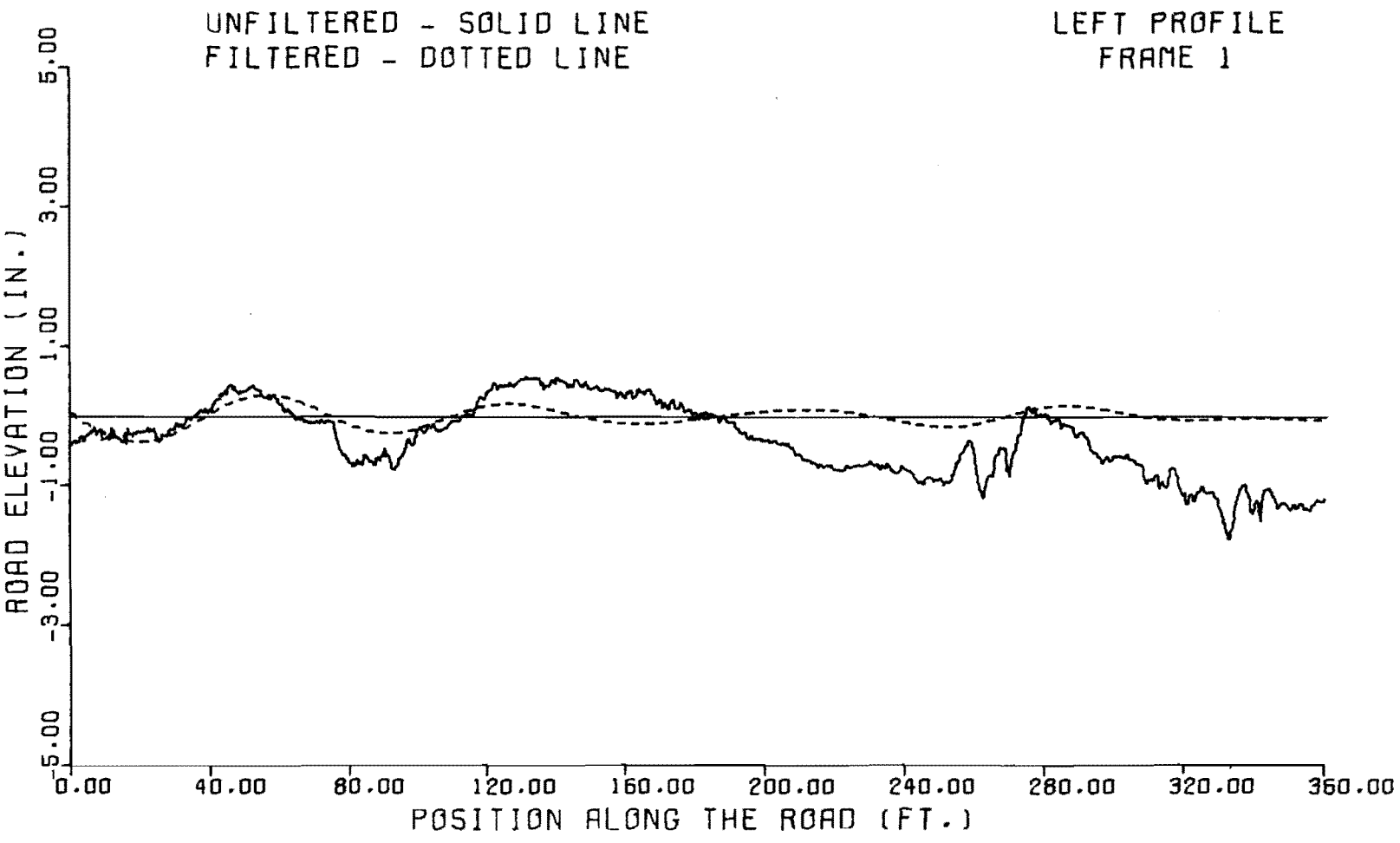

1 foot = .3048 meters
1 inch = 2.540 centimeters

Fig A5.13. Old San Antonio Road, Section 2: Filter Passband. 60 to 100 feet (continued)

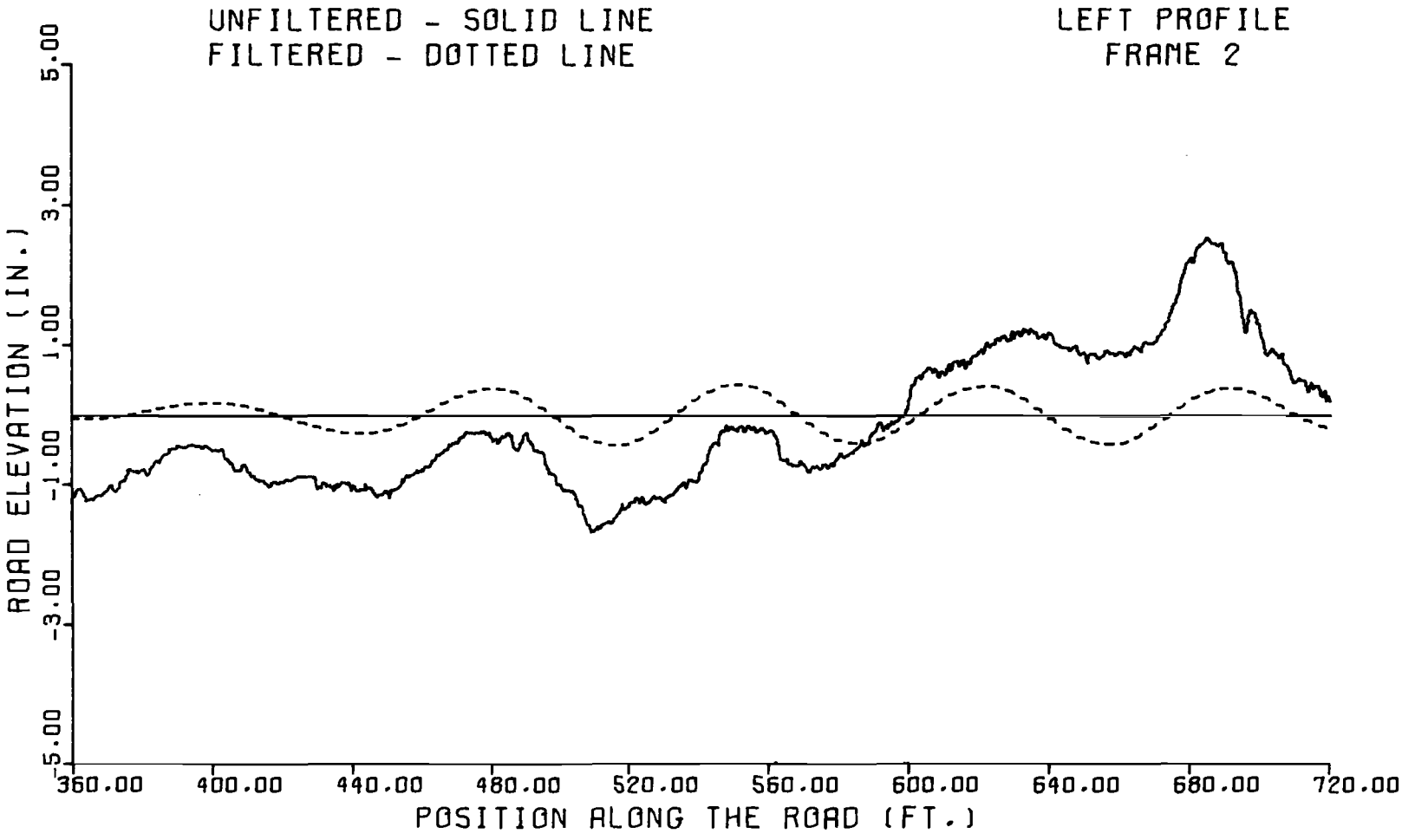

Fig A5.13. (continued)

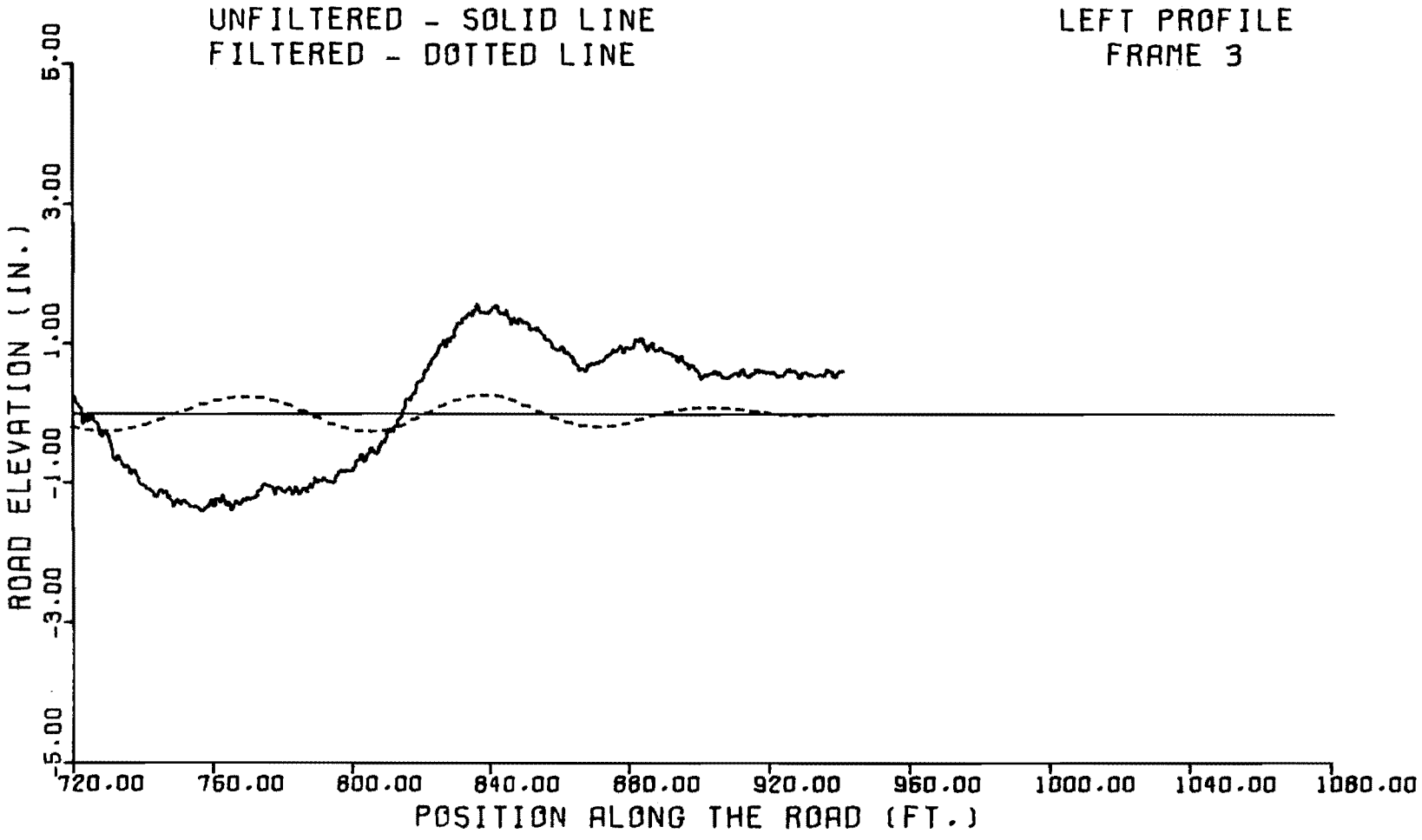

Fig A5.13. (continued)

Note the curious-looking effect near the left edge of Fig A5.13; the filtered profile reaches a peak while the unfiltered profile is near the minimum of a long dip. The large-amplitude dip, which extends from about 720 feet (219.5 meters) to 820 feet (249.9 meters), and thus has a wavelength of 200 feet (60.96 meters) (the dip is a half wave), is not in the passband, and thus is correctly absent from the filtered profile. The dip obscures the shorter-wavelength, smaller-amplitude peak shown in the filtered profile. The peak apparently corresponds to the slight bulge in the right center of the dip.

Notice also the absence of transient effects near the ends of data records. To perform the recursive filtering, it is necessary to make some sort of extension beyond the record; extension to the right and left of the terminal ordinates instead of zeroes was used to avoid discontinuities at the endpoints. The abrupt amplitude changes and discontinuous derivatives, however, still cause transients. Exclusion of one cycle at the longest wavelength of interest, 100 feet (30.40 meters) in this case, from either end of the data is the simplest solution. Then the spurious effects do not appear on the plots or influence the calculation of the roughness measures.

The comparable plots for the smoother section 3 are provided for comparison in Figs A5.14 and A5.15.

An interesting application, which is discussed briefly in the introduction, is the analysis of profiles before and after maintenance. Figures A5.16 through A5.19 display the profiles of a badly cracked hot-mix asphalt-concrete section on Interstate 20 between Odessa and Midland, Texas. Figures A5.16 and A5.18 are the profiles for the left and right wheelpaths before an overlay, respectively. Figures A5.17 and A5.19 are the corresponding profiles after the overlay. All plots show the unfiltered profiles and the filtered profiles containing 0 to 10-foot (0 to 3.048-meter)-wavelength irregularities.

Plots for the 4 to 10-foot (1.219 to 3.048-meter) wavelengths are given in Chapter 3; this is one of the passbands for which SI models were developed. The plots for the 0 to 10-foot (0 to 3.048-meter) wavelengths are included here to illustrate more clearly the capabilities of the filter; as mentioned above, it is easier to identify by eye what the filter should and should not respond to if either shorter or longer waves are removed by filtering, but not both.

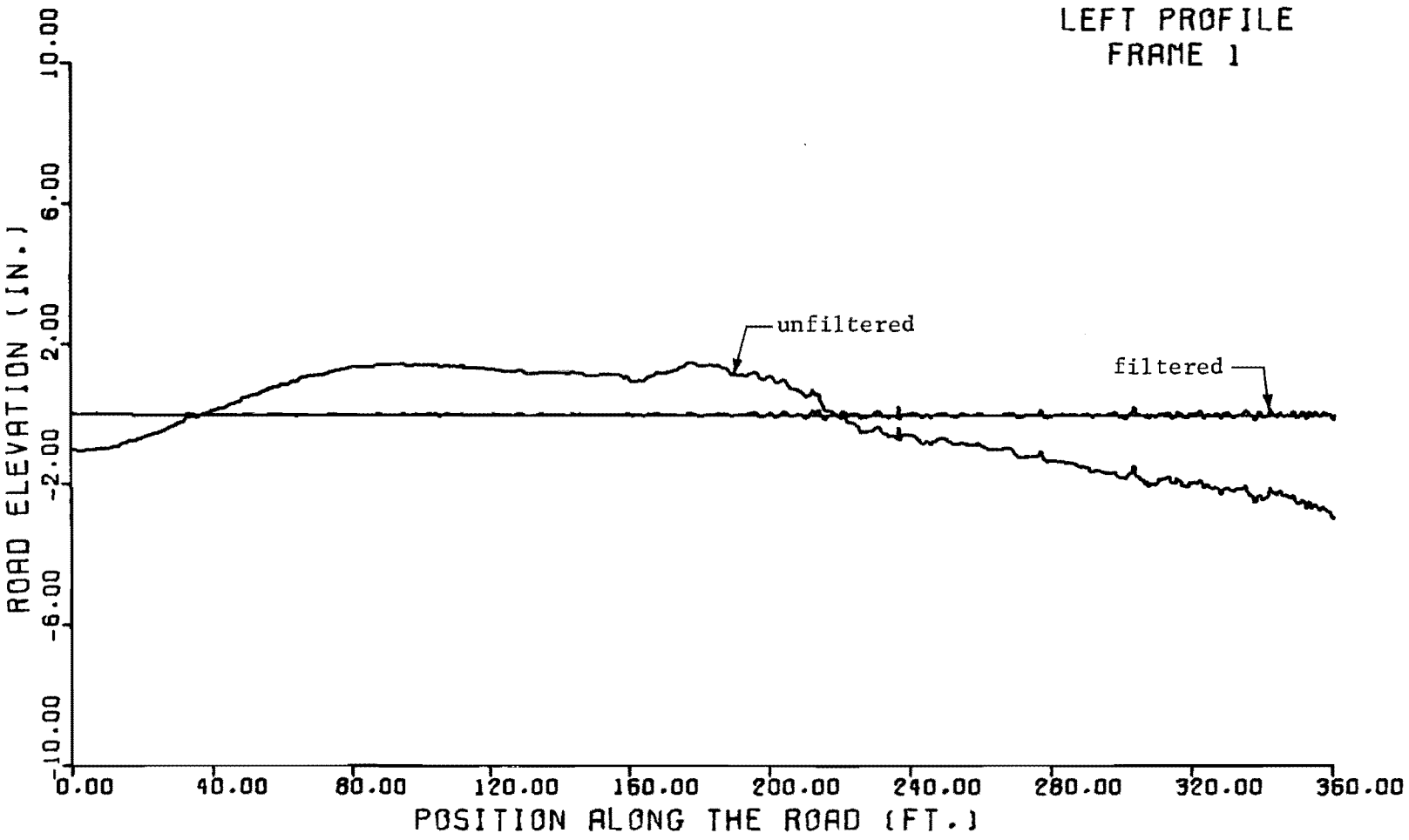

1 foot = .3048 meters
1 inch = 2.540 centimeters

Fig A5.14. Old San Antonio Road, Section 3: Filter Passband. 0 to 10 feet

(continued)

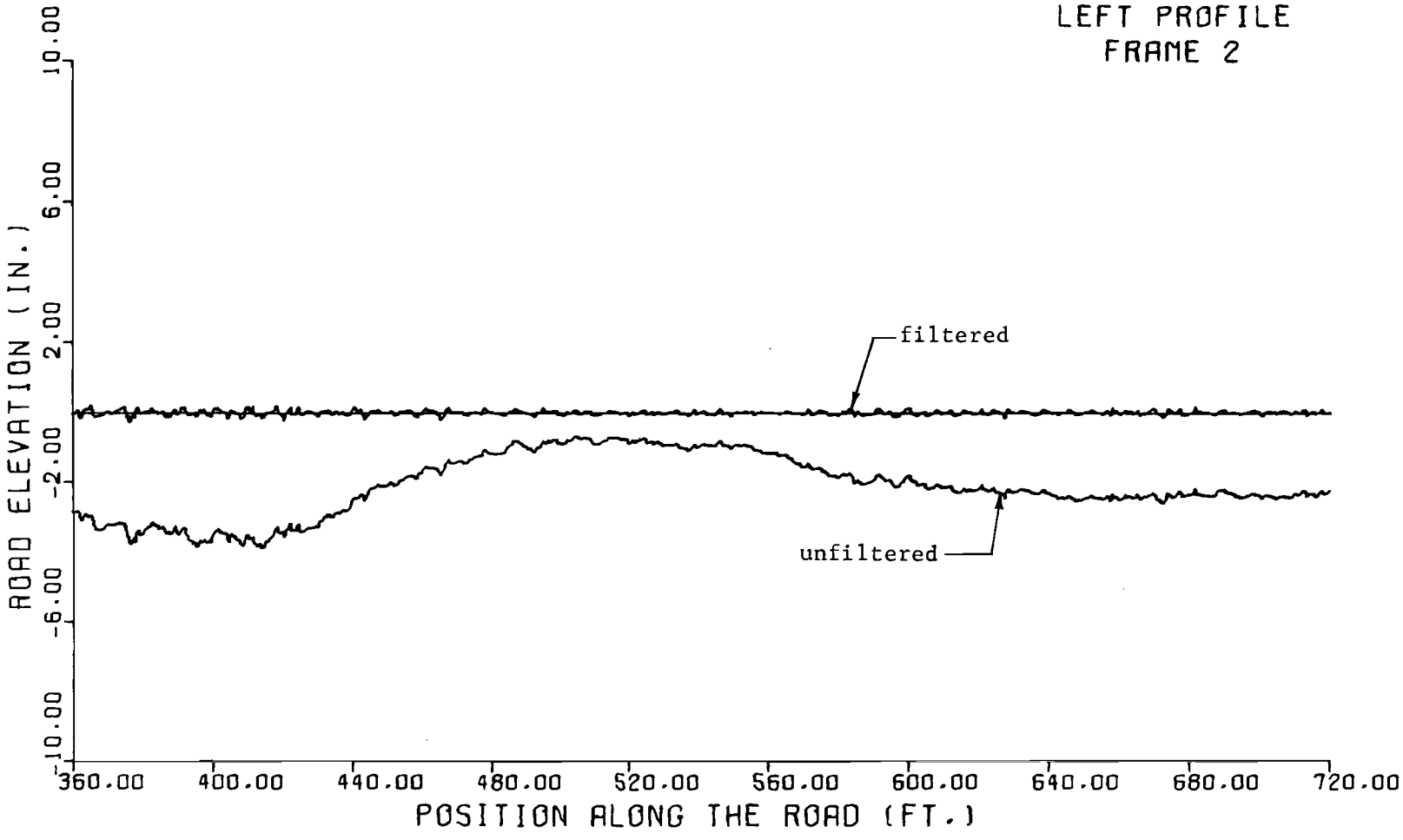

Fig A5.14. (continued)

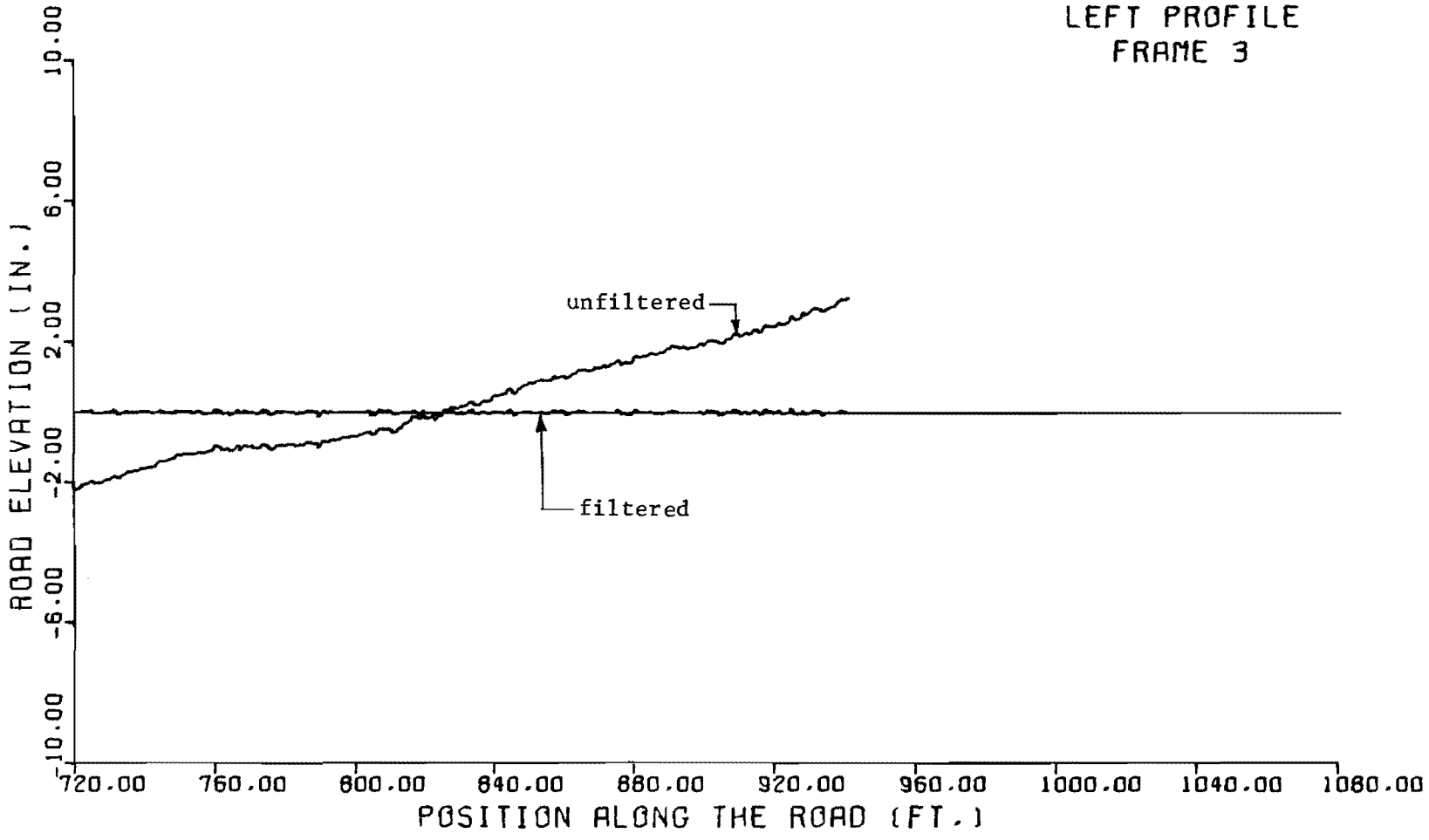

Fig A5.14. (continued)

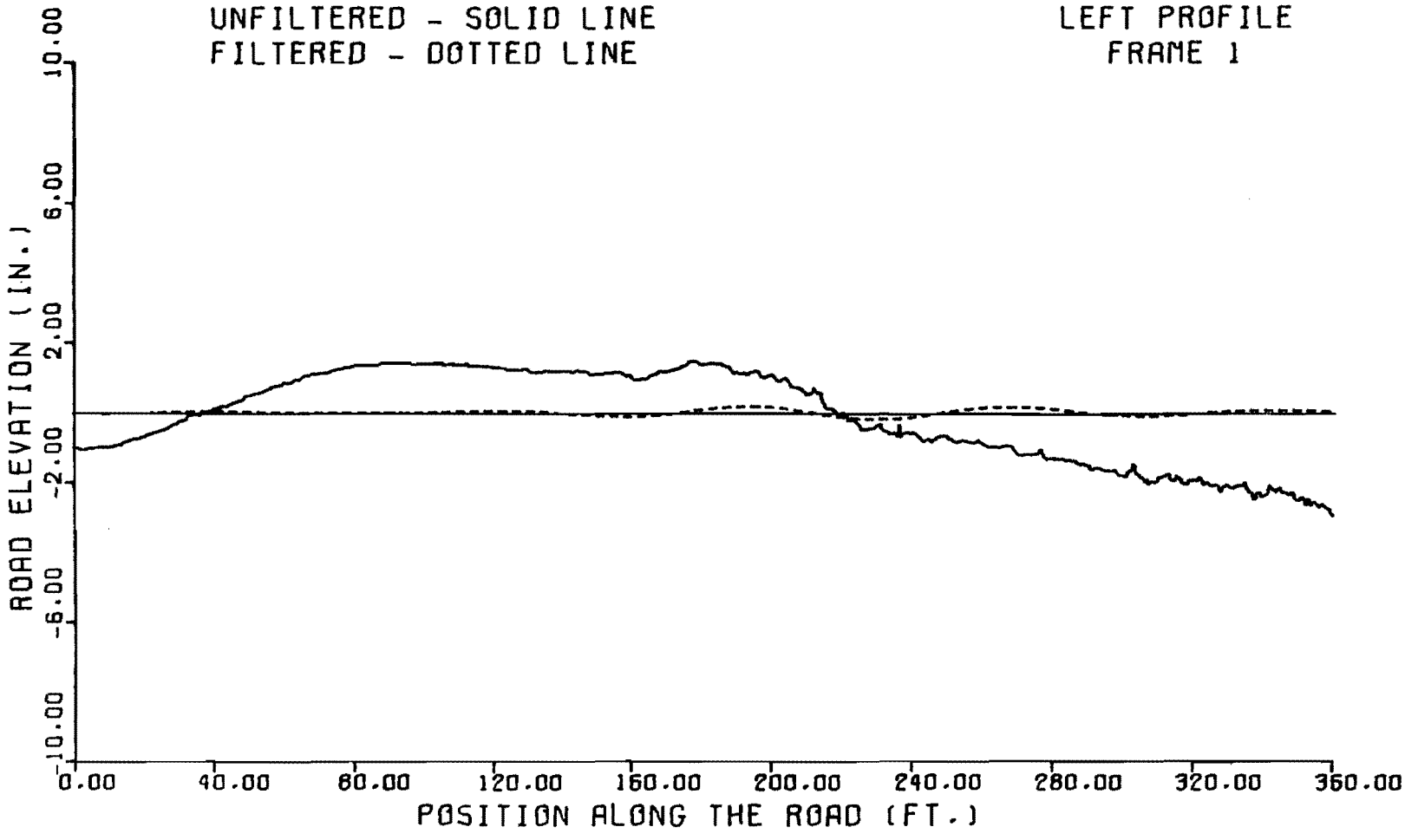

1 foot = .3048 meters
1 inch = 2.540 centimeters

Fig A5.15. Old San Antonio Road, Section 3: Filter Passband. 60 to 100 feet (continued)

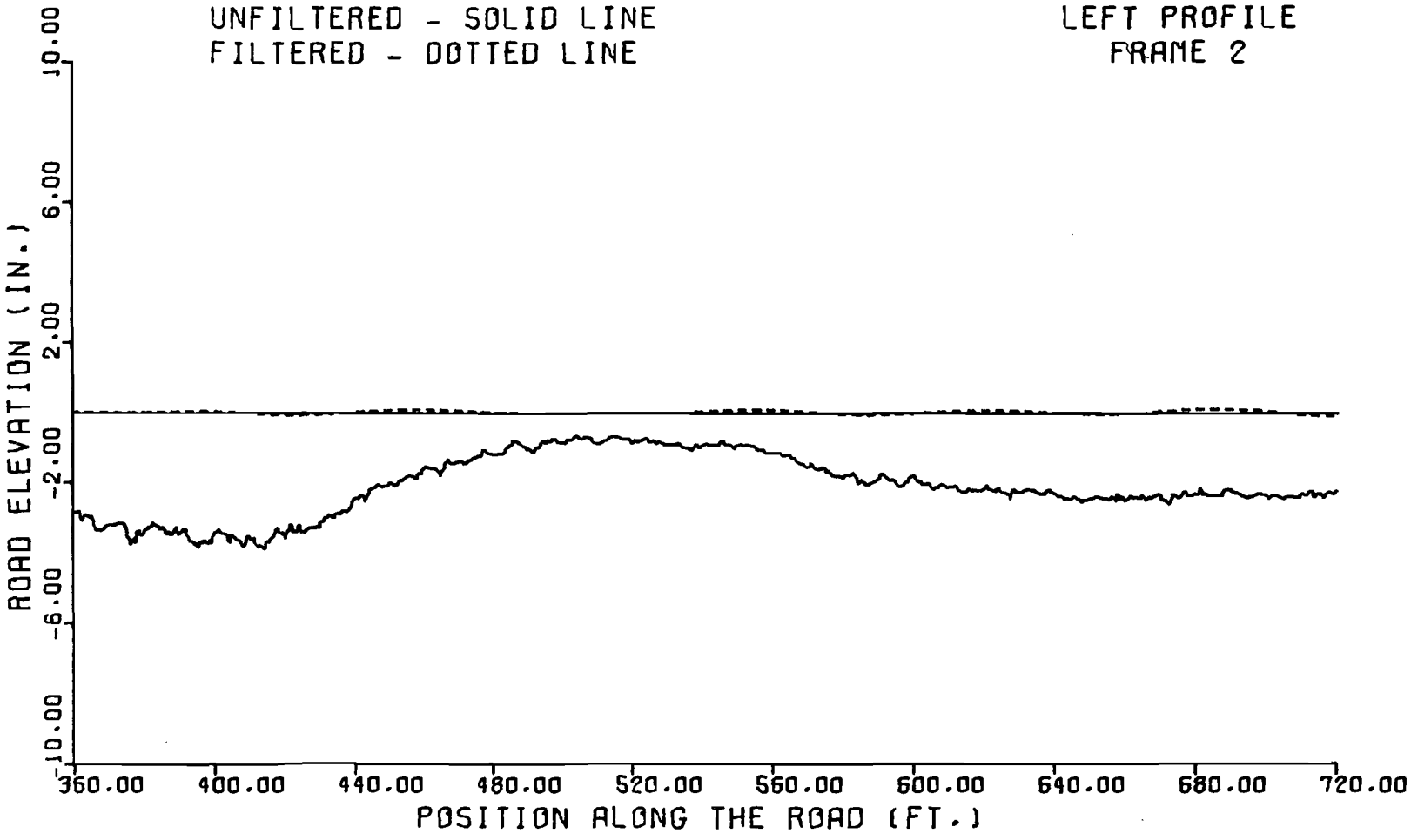

Fig A5.15. (continued)

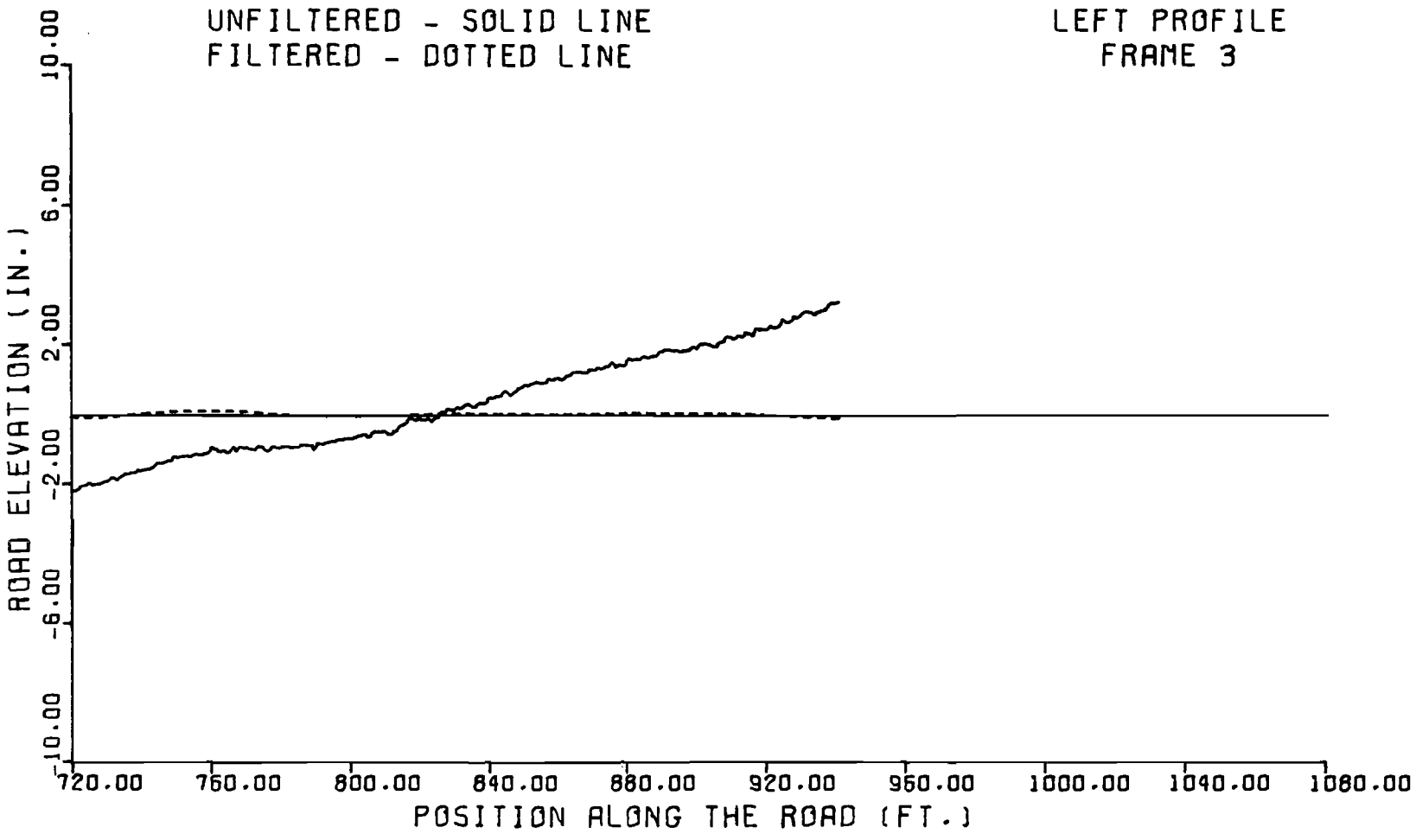

Fig A5.15. (continued)

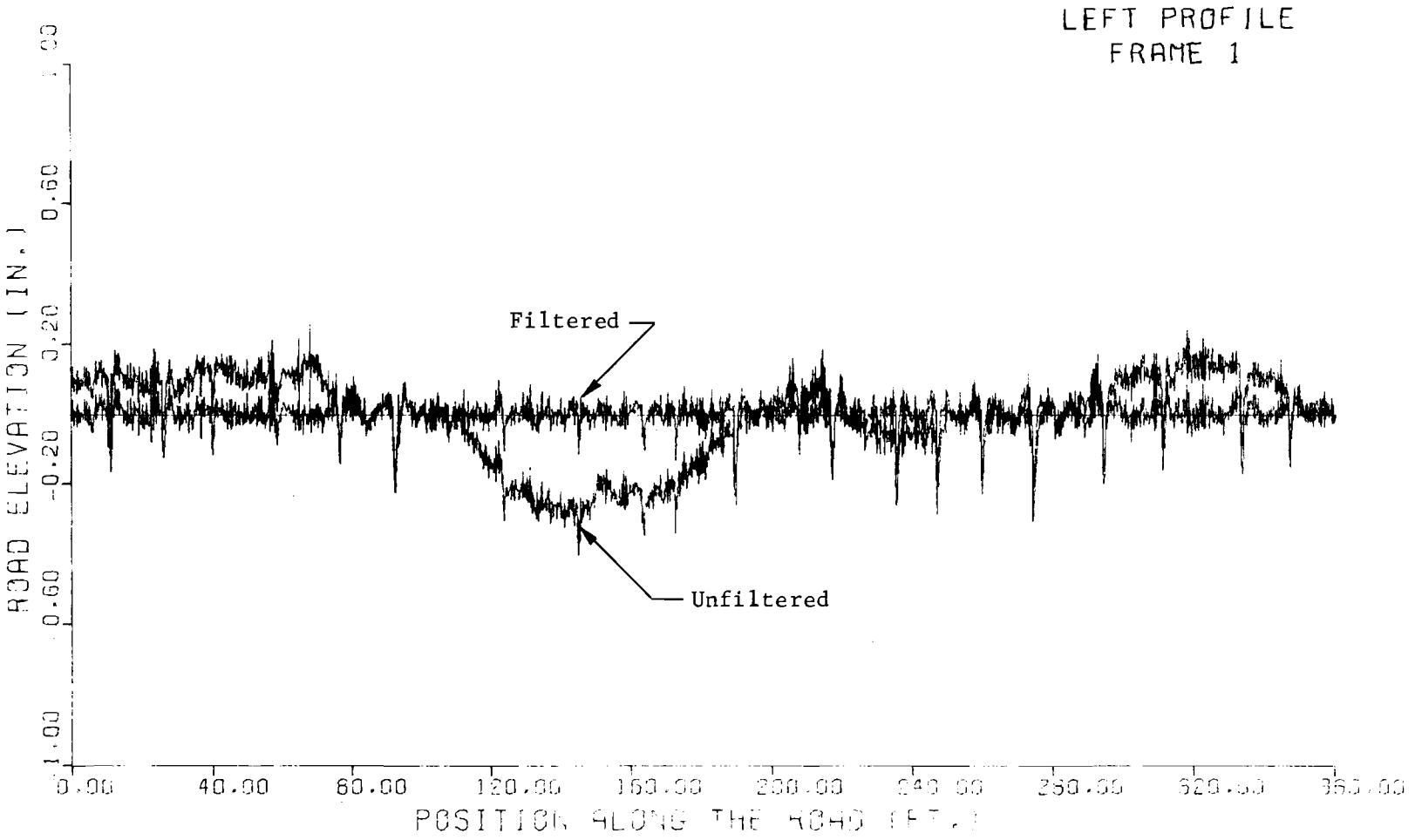

1 foot = .3048 meters
1 inch = 2.540 centimeters

Fig A5.16. Odessa Test Section, March, 1974: roughness with 0 to 10-foot wavelengths isolated by filter. Before overlay.

(continued)

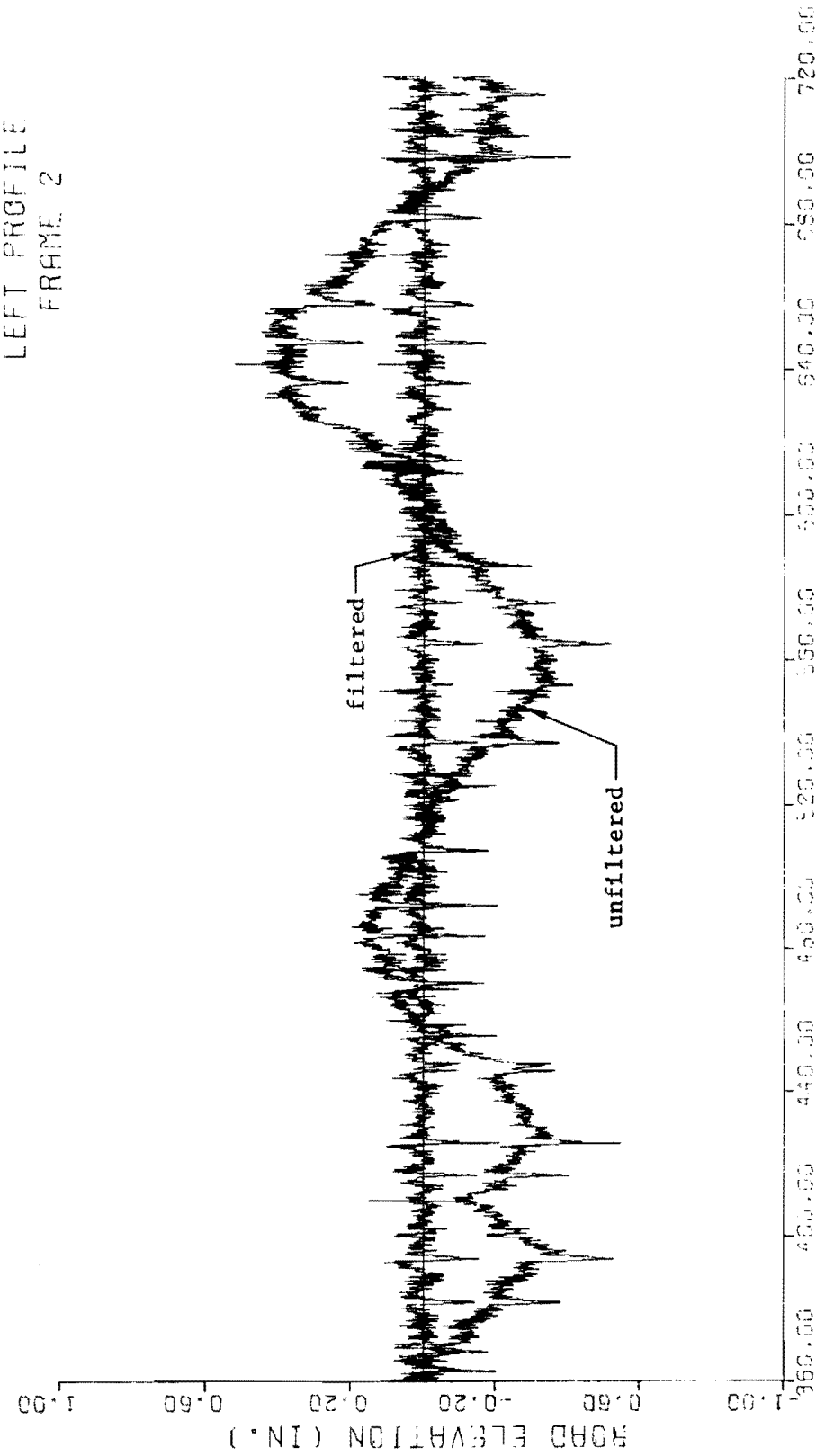

Fig A5.16. (continued)

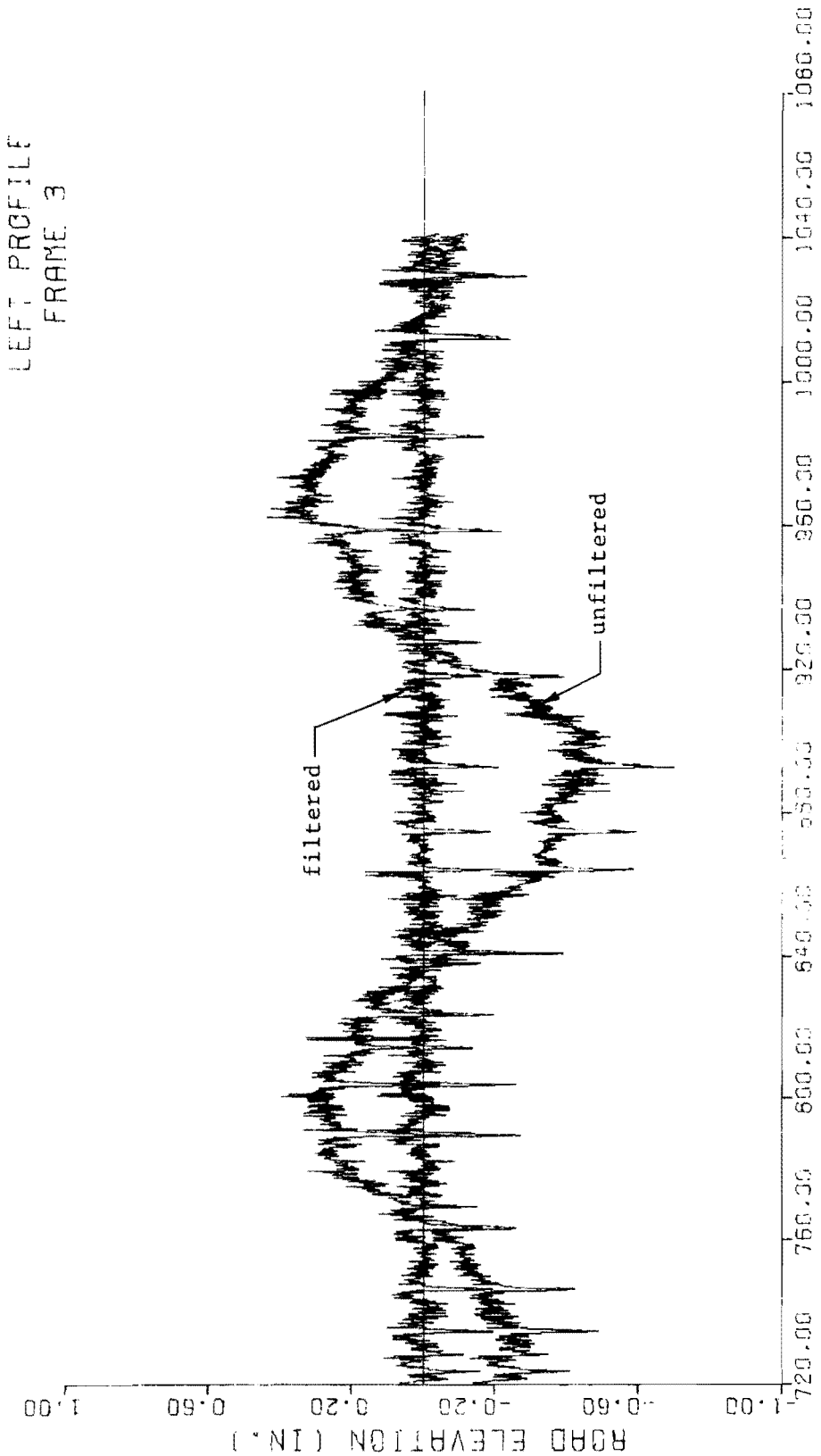

Fig A5.16. (continued)

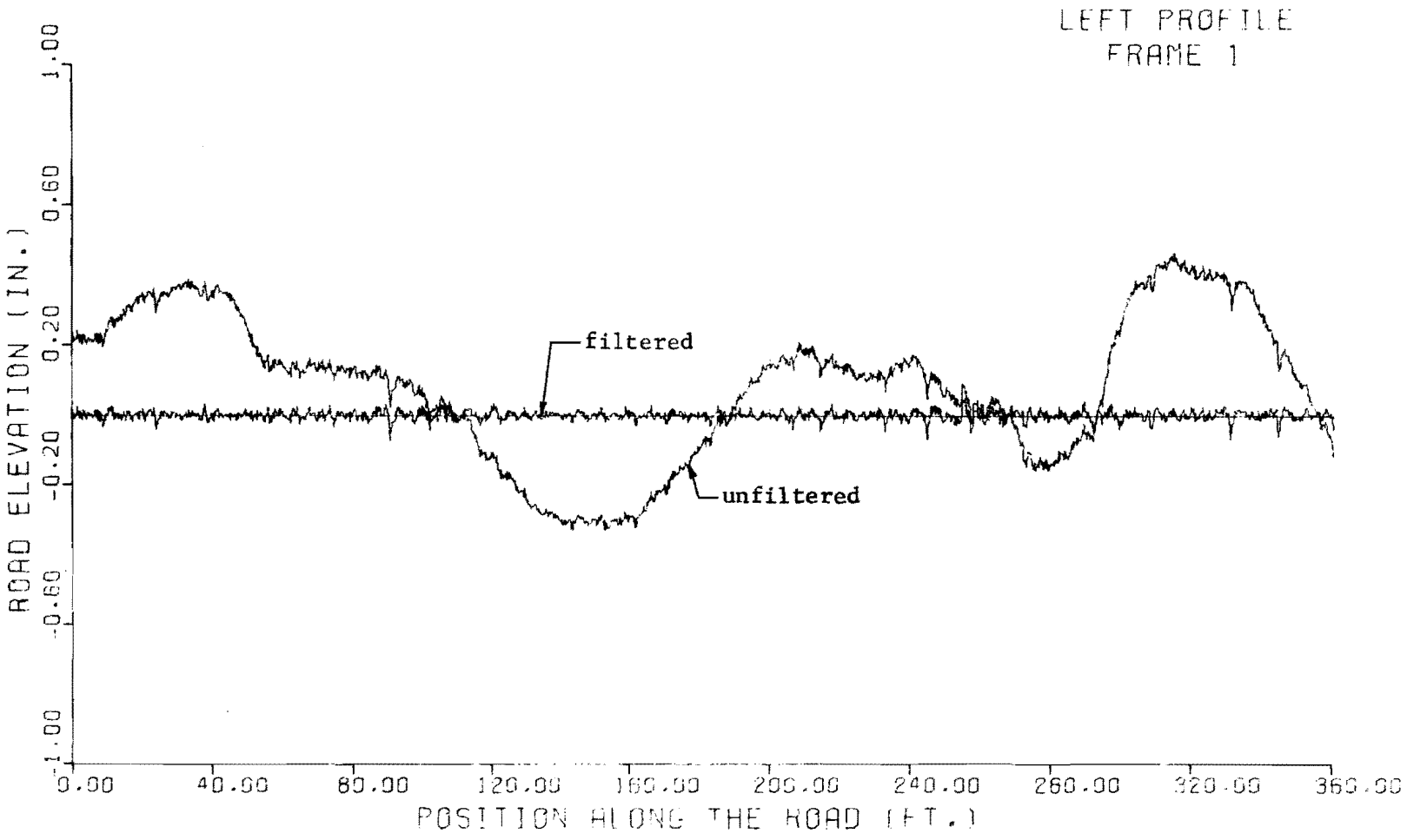

1 foot = .3048 meters
1 inch = 2.540 centimeters

Fig A5.17. Odessa Test Section, April, 1974: roughness with 0 to 10-foot wavelengths isolated by filter. After overlay.

(continued)

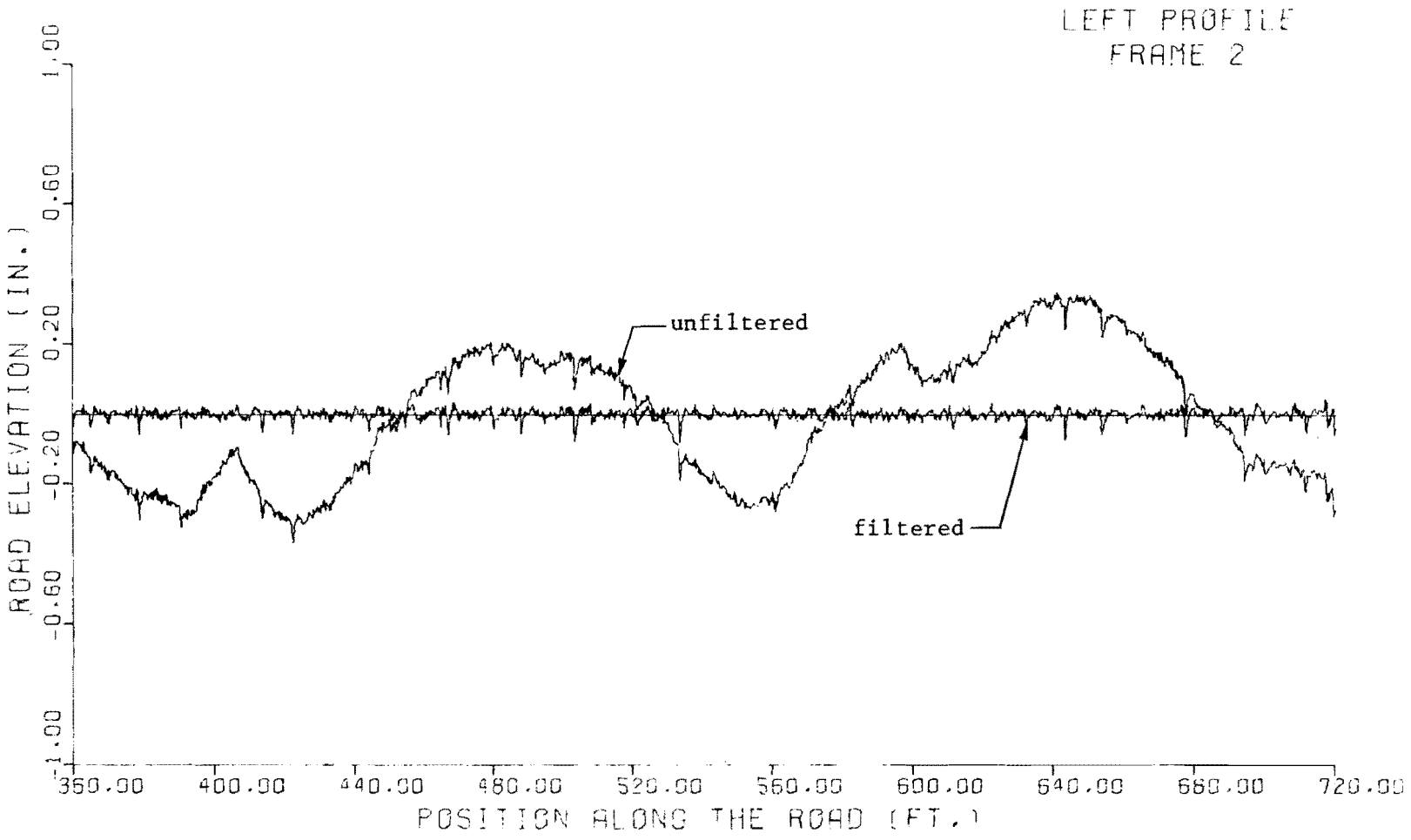

Fig A5.17. (continued)

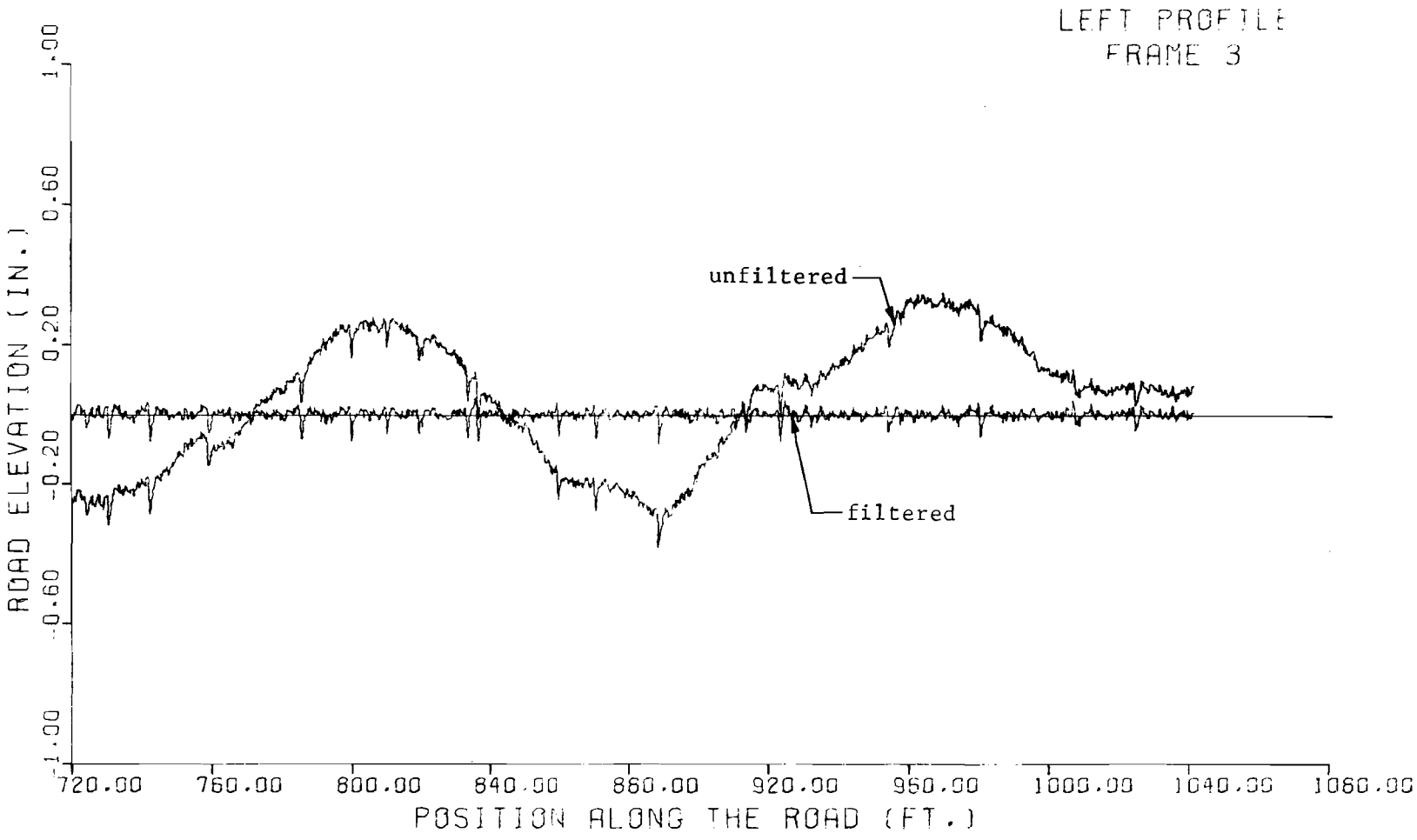

Fig A5.17. (continued)

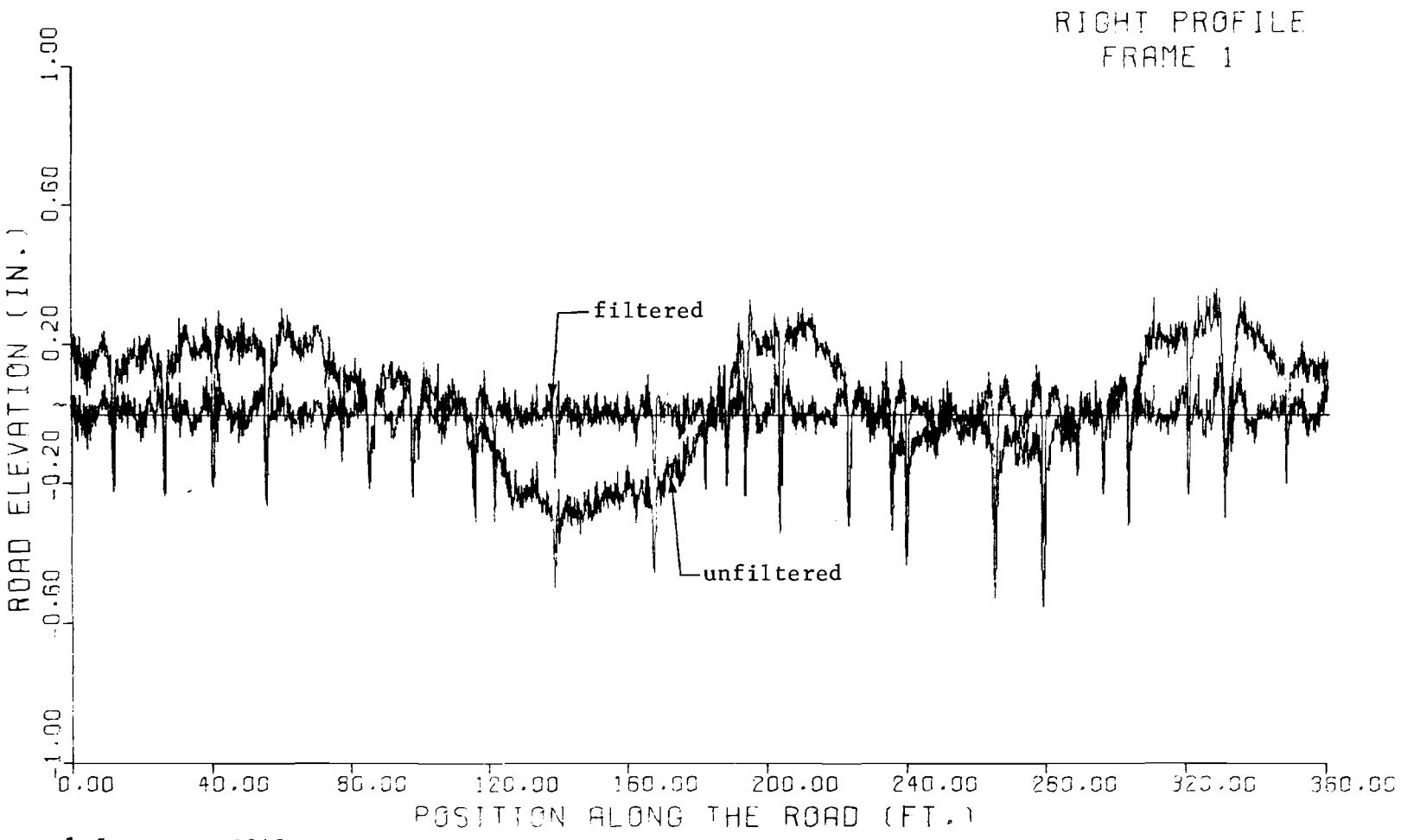

1 foot = .3048 meters
1 inch = 2.540 centimeters

Fig A5.18. Odessa Test Section, March, 1974: roughness with 0 to 10-foot wavelengths isolated by filter. Before overlay. (continued)

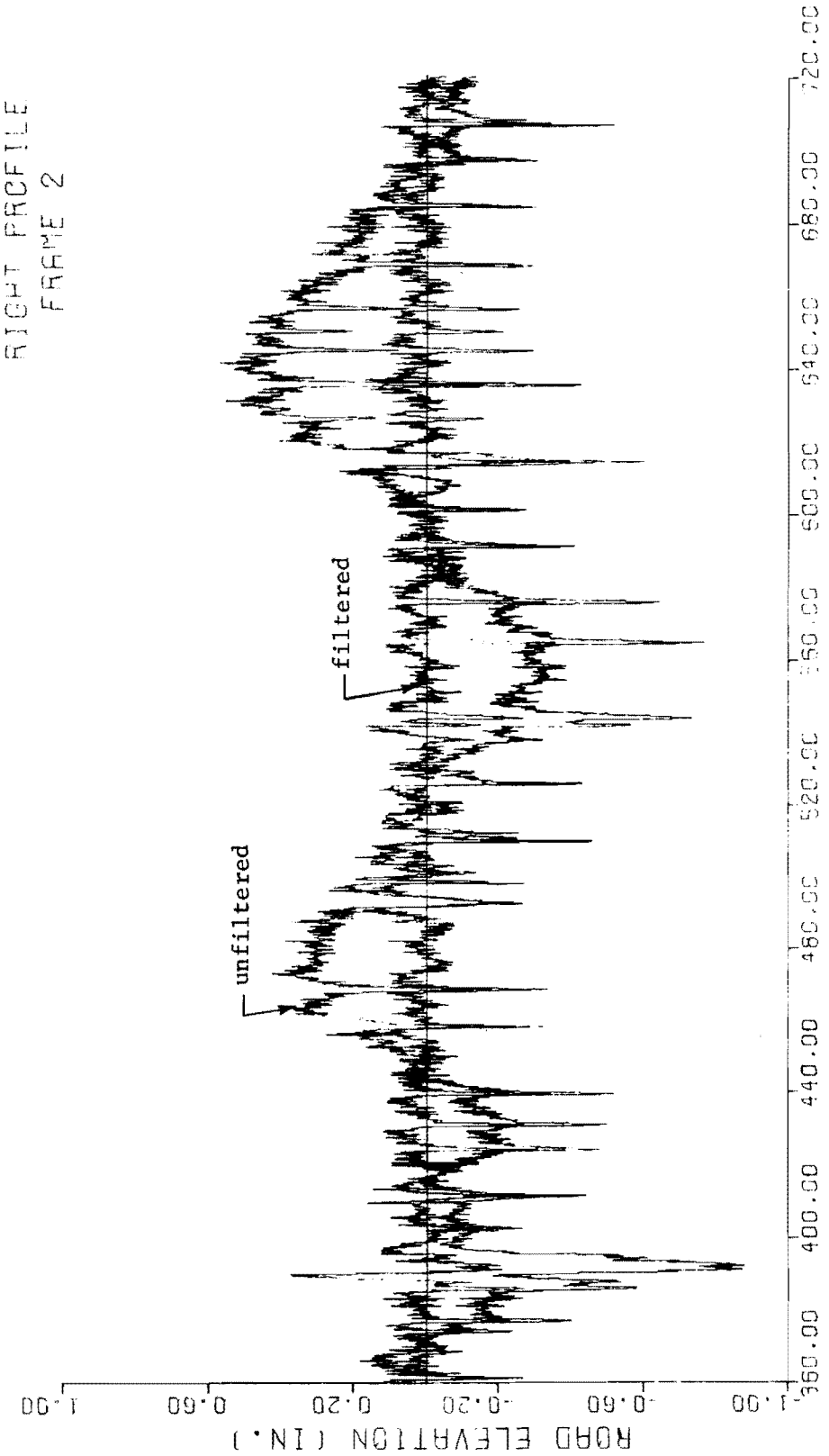

Fig A5.18. (continued)

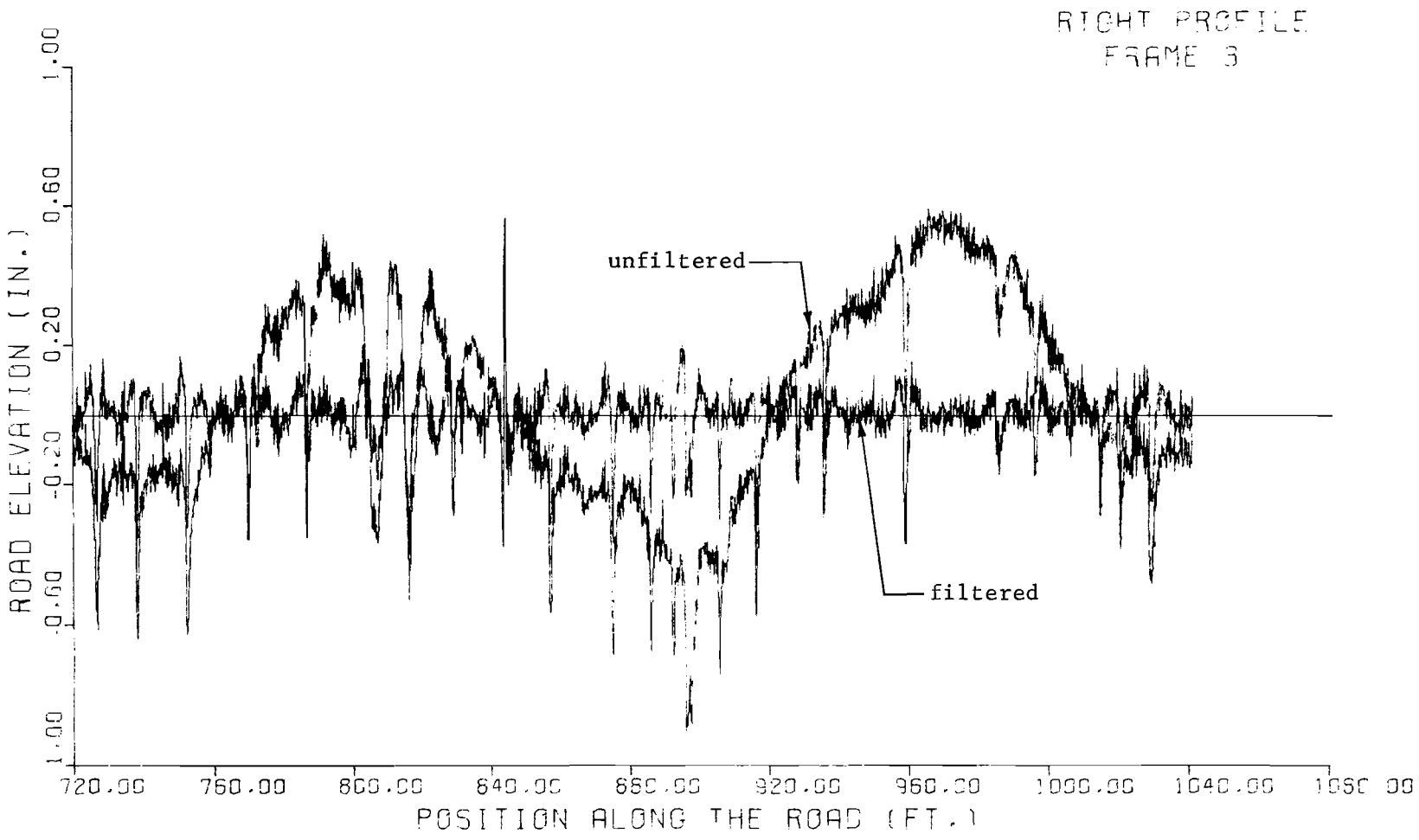

Fig A5.18. (continued)

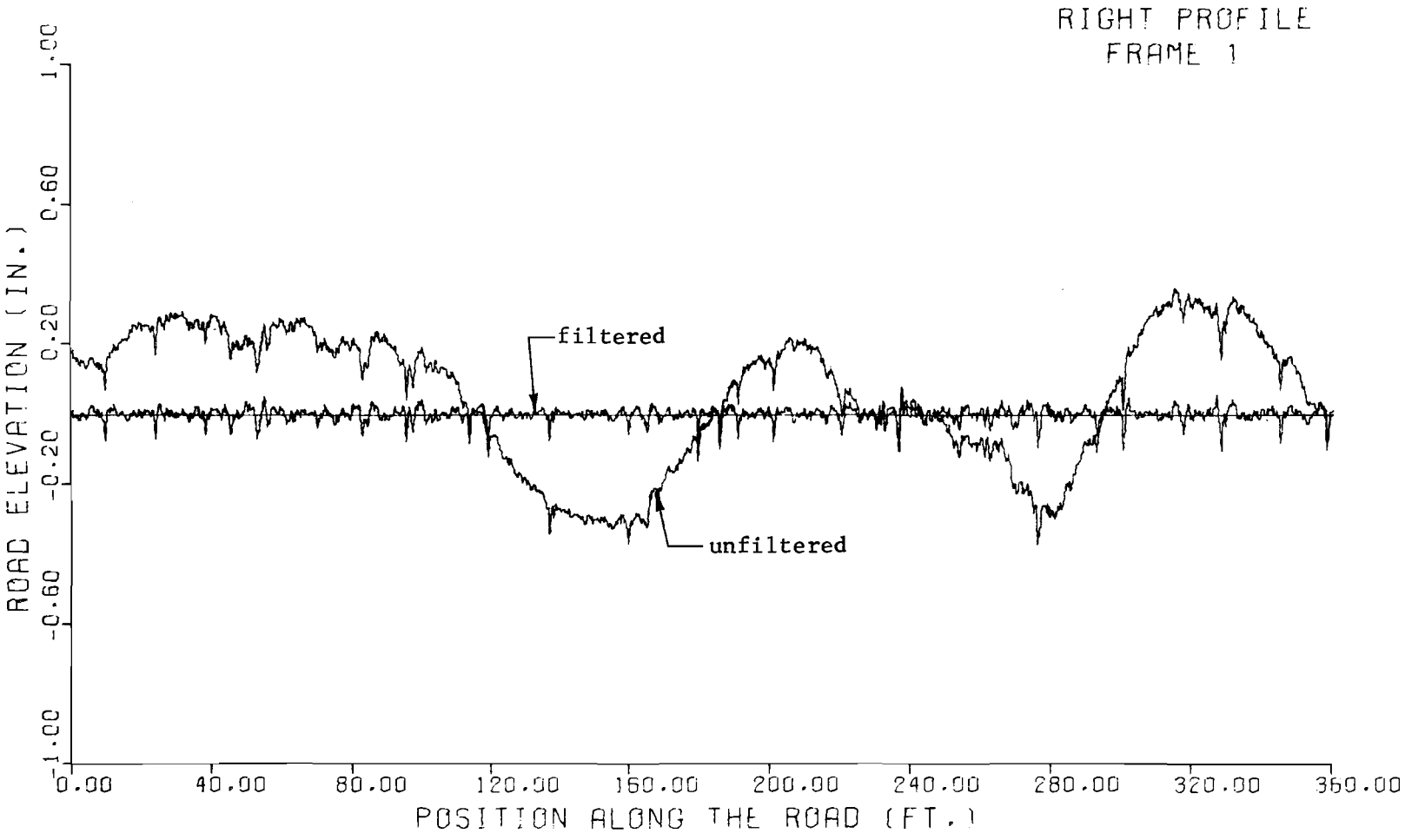

1 foot = .3048 meters
1 inch = 2.540 centimeters

Fig A5.19. Odessa Test Section, April, 1974: roughness with 0 to 10-foot wavelengths isolated by filter. After overlay.

(continued)

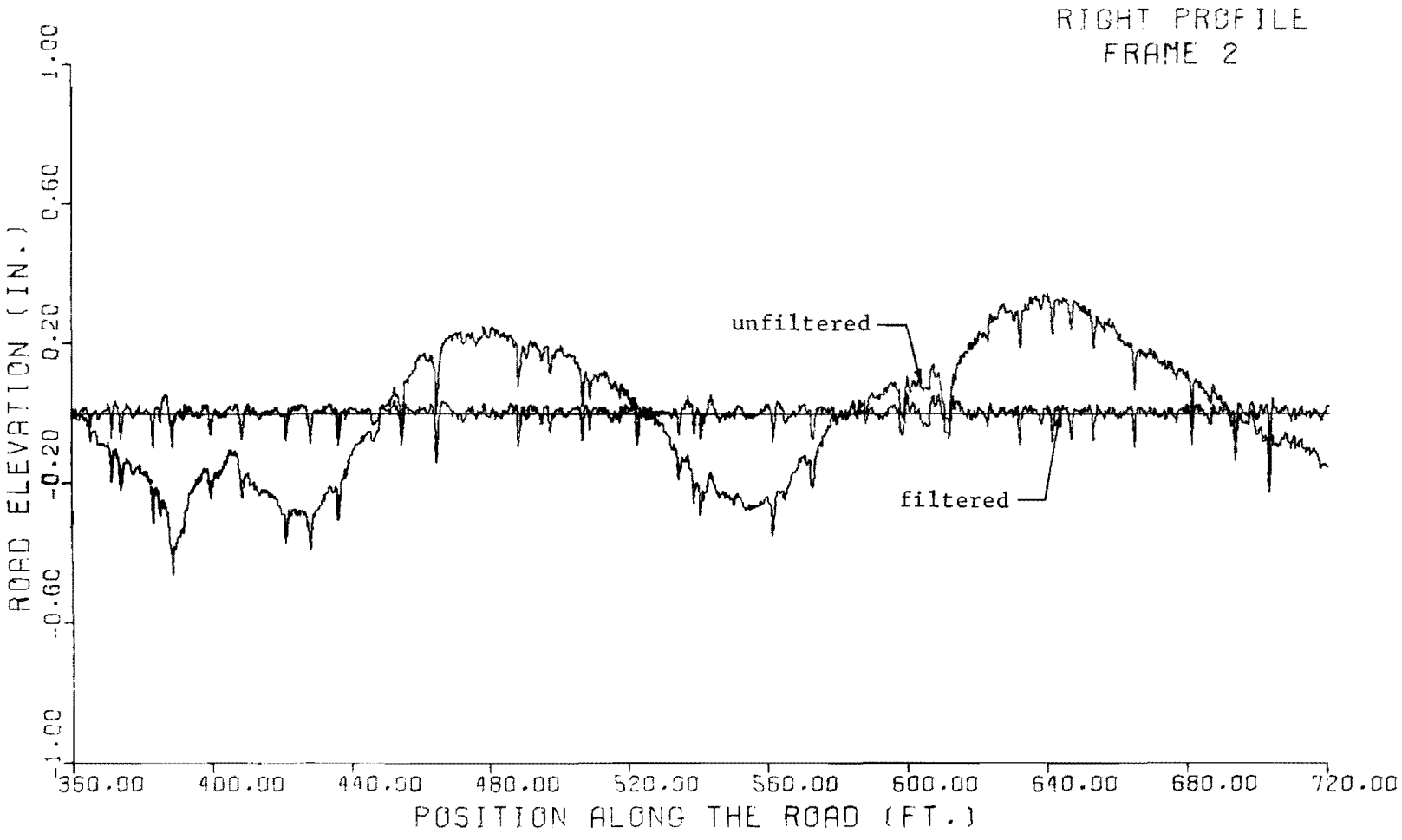

Fig A5.19. (continued)

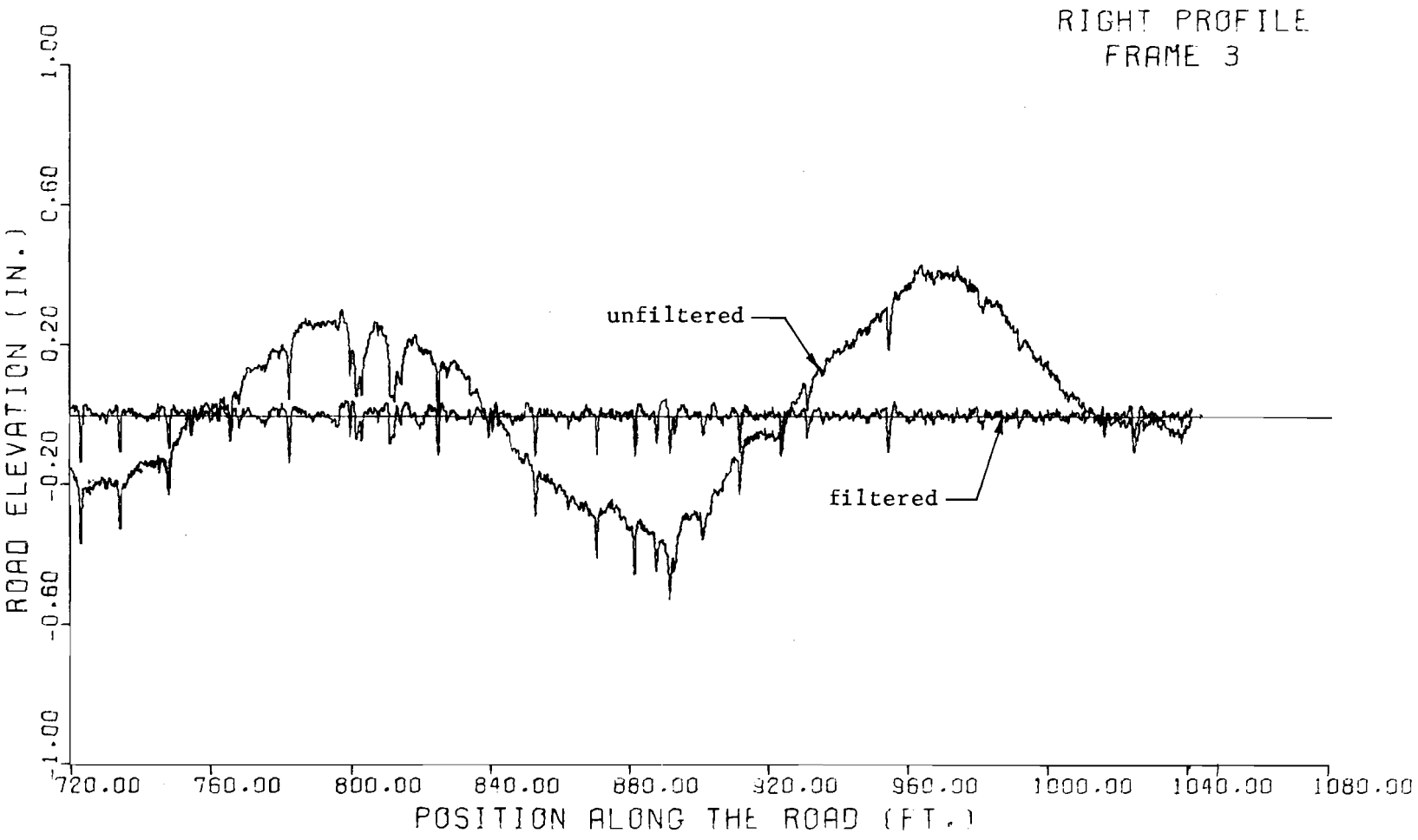

Fig A5.19. (continued)

The plots reveal a dramatic improvement in the high-frequency roughness, but much less change in the long waves after the overlay. Also, there is a marked difference between the right (outside) and left wheelpaths before the overlay; as expected, the outside wheelpath is much rougher; the road has a shoulder, but no curb. Although the differences between wheelpaths are decreased after the overlay, the outside wheelpath remains somewhat rougher. Notice especially the region from position 760 to 840 feet (231.6 to 256.0 meters) in Figs A5.17 and A5.19.

The plots indicate again that the high-frequency waves in the raw profile are accurately represented in the filtered profile. Even bumps which are so short they appear as vertical lines on the plot are represented.

Notice that when the long waves are occasionally absent, the raw and filtered profiles appear to be coincident, which indicates that the filter-induced distortion is very small. See, for example, position 90 to 110 feet (27.43 to 33.53 meters) in Fig A5.17.

CONCLUSIONS

The recursive filter designed by the tangent form of the squared-magnitude approximating function is recommended for use in analyzing road profiles.

There is little basis for determining which order is preferable on the basis of the artificial test cases chosen to study local transient effects. The sixth-order filter is recommended, however, as having acceptably sharp cutoff characteristics and as being computationally efficient.

The distortion introduced near the edges of the filter passband when the input road profile varies significantly in amplitude from half cycle to half cycle must be kept in mind. It is probably futile to expect to estimate with high accuracy the local amplitudes of the surface irregularities within a very narrow passband, e.g., 30 to 33 feet (9.144 to 10.06 meters) in wavelength.

It is felt, however, that the artificial test cases, which were chosen to be highly conducive to filter-induced distortion and to illustrate the types of transient effects to be expected, justify using digital filtering to compute measures of local amplitude vs. wavelength. Probably more important is the fact that the chosen sixth-order filter gave physically realistic results when applied to road profiles.

THE AUTHORS

Hugh J. Williamson is a Research Engineer with the Center for Highway Research at The University of Texas at Austin. He has had engineering experience in defense research with Tracor, Inc., and in pavement research with The University. He is the author of publications in sonar, computer science, and civil engineering, and he is presently concerned primarily with the development of statistical models for evaluating pavement properties.

W. Ronald Hudson is a Professor of Civil Engineering and Director of Research, Council for Advanced Transportation Studies at The University of Texas at Austin. He has had a wide variety of experience as a research engineer with the Texas Highway Department and the Center for Highway Research at The University of Texas at Austin and was Assistant Chief of the Rigid Pavement Research Branch of the AASHO Road Test. He is the author of numerous publications and was the recipient of the 1967 ASCE J. James R. Cross Medal. He is presently concerned with research in the areas of (1) analysis and design of pavement management systems, (2) measurement of pavement roughness performance, (3) slab analysis and design, and (4) tensile strength of stabilized subbase materials.

C. Dale Zinn is an Assistant Professor in the Operations Research Group in the Department of Mechanical Engineering at The University of Texas at Austin. He has a variety of experience in the use of mathematical models for solution of engineering problems. He is presently concerned with research in the areas of (1) analysis of alternative energy use policies, (2) bidding strategies for offshore oil leases, (3) optimal design of electrical transmission line systems, and (4) statistical models for evaluating pavement design and construction practices.